CHARACTERIZATION OF CHEMICALLY MODIFIED JUTE FIBER FOR POLYMER COMPOSITES

by

Sweety Shahinur

Roll-100711112

A Dissertation Submitted

In Partial Fulfillment of the Requirements for the Degree of

MASTER OF PHILOSOPHY IN MATERIAL AND METALLURGICAL ENGINEERING

DEPARTMENT OF MATERIAL AND METALLURGICAL ENGINEERING

BANGLEDESH UNIVERSITY OF ENGINEERING AND TECHNOLOGY

DHAKA-1000, BANGLADESH.

MARCH, 2011

The the sis title d "**Characterization of Chemically Modified Jute Fiber for Polymer Composites"** submitted by **Ms. Sweety Shahinur**, Student No. 100711112, Session-October 2007, ha s be en a ccepted a s s atisfactory i n pa rtial f ulfillment of t he r equirements f or t he degree o f M aster of P hilosophy i n M aterials a nd M etallurgical E ngineering on 16 A pril, 2011.

BOARD OF EXAMINERS

1.	Dr. Mahbub Hasan. Assistant Professor Department of Materials and Metallurgical Engineering BUET, Dhaka	Chairman (Supervisor)
2.	Dr. Md. Aminul Islam Professor and Head Department of Materials and Metallurgical Engineering BUET, Dhaka.	Member (Ex-officio)
3.	Dr. Kazi Md. Shorowordi Assistant Professor Department of Materials and Metallurgical Engineering BUET, Dhaka.	Member
4.	Dr. Latifa Binte Lutfar Operation Officer International Jute Study Group (IJSG) Dhaka.	Member (External)

Acknowledgement

All Praise is due to the almighty Allah; the most Gracious and the most Merciful.

First and foremost, I would like to express my utmost gratitude, profound regard and indebtedness toward my supervisor, Dr. Mahbub Hasan, Assistant Professor, Department of Materials and Metallurgical Engineering, Bangladesh University of Engineering and Technology (BUET), Dhaka, for his kindness and patience throughout the whole study. His thoughtful suggestion not only motivated me, but also encouraged at all stages of my research work finally made the successful thesis completion possible.

I would like to thank Dr. Qumrul Ahsan, Professor and all the teachers of MME Department, BUET, for their encouragement and guidance. I remember with gratefulness the kind help and inspiration of Dr. Dilip Kumar Saha, Chief Scientific Officer, Atomic Energy Centre, Dhaka and Mr. Sayed Farhad Khan, Scientific Officer, BCSIR, Dhaka.

I am grateful to the Director General, Director Technology, CSO, Textile Physics Division, Shamina Jafrin, SO of Pilot Plant Division and other colleagues of Bangladesh Jute Research Institute, Dhaka, for kind help, advice and permission to the use their lab facilities.

I am conveying my heartiest thanks to Mr. Shubhonkar Bishwas, M. Phil student, Md Rashnal Hasan, Ph.D student, Shikh Jamil Ahmed, student of the Department of Material and Metallurgical Engineering, for their valuable information and suggestions at every step of this project.

I acknowledge with appreciation the co-operation of Mr. Yusuf Khan, Md. Abdulla al Maksud, Mr. Ashiqur Rahman, Md. Harun-or-Rashid, and Md. Ahmed Ullah for their help at various stages of my research.

I am grateful to BUET for providing me financial support for conducting the research.

I would like to express my deep gratitude to the Department of Materials and Metallurgical Engineering Department for providing facilities throughout the work.

I am also grateful to the members of my family.

Sweety Shahinur
Dhaka, 2010.

Disclaimer

This is to certify that this research work has been carried out by the author under the supervision of Dr. Mahbub Hasan, Assistant Professor, Department of Materials and Metallurgical Engineering, BUET, Dhaka, and it is hereby declared that this thesis or any part of it has not been submitted elsewhere for the award of any degree or diploma.

Signature of the Candidate

( )

Sweety Shahinur

Dedicated to my

Family

& Teachers

CONTENTS

Chapter 4

Result and Discussion

List of Tables

List of Figures

List of Abbreviations

ATR	Attenuated Total Reflectance
FTIR	Fourier Transform Infrared Radiation
MAgPP	Meleic Anhydride Grafted Polypropylene
MMC	Metal Matrix Composites
PP	Polypropylene
SEM	Scanning Electron Microscope
DSC	Differential scanning Calorimetry
XRD	X-ray Diffractormeter
TGA	Thermal Gravimetric Analysis
AFM	Atomic Force Microscopy
Tg	Glass Transition Temperature
Tm	Melting Temperature
UTS	Ultimate Tensile Strength
TGA	Thermogravimetry Analysis
T_m	Melting Temperature
RR	Rot Retardant
FR	Fire Retardant
WR	Water Retardant
Arb	Arbitrary

List of Notations

V_f	Volume fraction of fiber
V_m	Volume fraction of matrix
E_m	Elastic modulus of matrix
E_f	Elastic modulus of fiber
σ_f	Fiber tensile stress
σ_m	Matrix tensile stress
σ_{Ltu}	Longitudinal ultimate tensile stress
σ_{fu}	Fiber ultimate tensile stress
V_{fc}	Critical fiber volume fraction
R	Rate of cross head motion
%	Percent
°C	Degree Celsius
ΔH_c	Heat of fusion
µ	Micron
cm^3	Cubic centimeter
g	Gram
GPa	Giga Pascal
MPa	Mega Pascal
J	Joule
kJ	Kilo Joule
m^2	Square meter
mg	Milligram
min	Minute
s	Second
mm	millimeter
mW	Milli Watt
wt	Weight
H_f	Heat of fusion of 100% crystalline material
X_c	Crystalinity
P	Load
b	Depth

d	Width
D	Elongation
z	Rate of staining of the outer fiber
L	Support span
m	Slope
tbs	Table spoon

ABSTRACT

Jute fiber reinforced composite as moderate structural materials have attracted the attention of material scientists all over the world because of their low cost, easy availability, light weight, renewability and biodegradability. In addition, low density and high specific strength of jute reinforced polymer composites make them the most suitable candidates for low load bearing applications. In this research work, control and chemically treated jute fibers were characterized by thermal, mechanical and structural testing. The effects of treatments on the physical, chemical and mechanical properties of the fiber have been studied. Reaction parameters such as time and temperature have been investigated for all chemical treatments. The control jute fibers were chemically treated to make the fiber rotretardant, fire retardant and water retardant. FTIR spectroscopy analyses were done for all retardant treatments and the results show the evidence of positive reaction. The tensile properties (Tensile strength, Young's modulus, and strain to failure) of both control and chemically treated jute fibers were studied by varying fiber span length (5mm, 15 mm, 25 mm and 35 mm). The effect of span length on those properties was also studied. Chemical concentration on the treated and control fiber have been studied by the thermal properties in terms of differential scanning calorimetric (DSC) and thermal gravimetric analysis (TGA). All the studies are made for the top, middle and bottom portion of the jute fiber. In order to observe the crystalline properties and surface morphology, x-ray diffractometry (XRD) and atomic force microscopy (AFM) have been carried out respectively.

Both the control and chemically treated fibers were incorporated as reinforcing agents in maleic anhydride grafted polypropylene (MAgPP) matrix composites through hot compression molding under specific pressure and temperature. The effect of fiber content on the mechanical properties of composites was studied by preparing composites with different percentage of fiber loading (20wt%, 25wt% and 30wt %) for each type of jute fiber. Tensile, three points bend and impact tests were conducted on all treated and control jute MAgPP composites. The Young's modulus, tensile strength, strain to failure, flexural strength, and flexural modulus increased in case of control, RR, FR and WR compared to matrix. Since scanning electron micrographs of the single fiber and fracture surface of composites were taken to examine the variation in failure mode and to

investigate the interfacial adhesion and bonding between fiber and matrix. Improve interfacial interactions were found for treated jute composites. Water absorption tests were carried out on rot, fire and water retardant fibers and their composites to investigate the chemical effect on the moisture absorption of hydrophilic jute and its composite. Reduced water absorption was found in case of rot and water retardant treated fiber and their composites.

Chapter 1

Introduction

1.1 Introduction

The performance and stability of fiber-reinforced composite materials depend on the development of coherent interfacial bonding between fiber and matrix. In natural fiber-reinforced composites there is a lack of good interfacial adhesion between the hydrophilic cellulose fibers and the hydrophobic resins due to their inherent incompatibility. Short, cellulose-based fibers will also tend to agglomerate making their use in reinforced composites less attractive. The presence of waxy substances on fiber surface contributes immensely to make ineffective fiber to resin bonding and causes poor surface wetting. Also the presence of free water and hydroxyl groups, especially in the amorphous regions, worsens the ability of plant fibers to develop adhesive characteristics with most binder materials. High water and moisture absorption of the cellulose fibers causes swelling and plasticizing effect resulting in dimensional instability and poor mechanical properties. Plant fibers are also prone to microbiological attack leading to weak fibers and reduction in their life span [1].

Fibers with high cellulose content have also been found to contain high crystallite content. These are the aggregates of cellulose blocks held together closely by the strong intra-molecular hydrogen bonds which large molecules, for example dyes, are not able to penetrate unless the cell wall is swollen. Fibers are, therefore, usually subjected to treatment such as mercerization and acetylation, with or without heat, to first bulk or swell the cell wall to enable large chemical molecules to penetrate the crystalline regions.

The mechanical properties of plant fibers are largely related to the amount of cellulose, which is closely associated with the crystallinity of the fiber and the micro-fibril angle with respect to the main fiber axis [2]. Fibers with high crystallinity and/or cellulose content have been found to possess superior mechanical properties. Sisal fibers with a cellulose content of 67% and micro-fibril angle of 10 -22° have tensile strength and modulus of elasticity of 530 MPa and 9-22 GPa respectively (Table 1.1). On the other hand, coir fiber with a cellulose content of 43 % and micro-fibril angle of 30 - 49° is reported to have tensile strength and modulus of elasticity of 106 MPa and 3 GPa

respectively [3]. Cellulose content of the jute fiber is 64% and micro-fibril angle is 8° which would affect the tensile strength and other mechanical properties. This variation in the cellulose content with increased micro fibril angle plays an important role in determining the mechanical properties of fiber reinforced composites. In addition it is necessary to optimize fiber alignment parallel with the direction of applied force to maximize tensile properties [4].

Table: 1.1 Properties of natural fiber [4].

Fibre	Density ($g\,cm^{-3}$)	Young's modulus (GPa)	Tensile strength (MPa)	Elongation (%)	Microfibrillar angle (°)
Cotton	1.5	5.5–27.6	300–1 500	3–8	–
Jute	1.3–1.5	13–26.5	393–800	1.2–1.8	8
Flax	1.5	27.6	345–1 500	2.7–3.2	5–10
Hemp	1.5	70	690	1.6	2–6.2
Ramie	1.55	61.4–128	400–938	1.2–3.8	7.5
Sisal	1.45	9.4–22	468–700	2–7	10–22
Coir	1.15–1.46	4–6	130–220	15–40	30–49
Viscose	–	11	593	11.4	–
Soft wood kraft	1.5	40	1 000	–	–
E-glass	2.5	70	2 000–3 500	2.5	–
S-glass	2.5	86	4 570	2.8	–
Aramide	1.4	63–67	3 000–3 150	3.3–3.7	–
Carbon	1.4	230–240	4 000	1.4–1.8	–

1.2 Objectives

To properly assess changes at the fiber surface and fine structure due to chemical treatment it is necessary to employ appropriate analytical characterization methods. A combination of two or more characterization techniques allows a much more thorough investigation of the effect of chemical treatment on cellulose based fibers. In present study, therefore, six characterization methods were employed. Wide angle X-ray analysis (WAXS), differential scanning calorimetry (DSC), thermo gravimetric analysis (TGA), Fourier transform infrared radiation (FT–IR) spectroscopy, atomic force microscopy (AFM) and scanning electron microscopy (SEM) were used to analyze the effect of rot retardant, fire retardant and water retardant treatment on the crystallinity and thermal characteristics of jute fiber.

1.3 Objectives of the Present Study

Present work is aimed at preparing rot retardant, fire retardant and water retardant fiber by chemical modification and characterizing those using different physical techniques.

The structural and mechanical properties of the control and treated jute fiber would also be investigated.

The aim of the present work is to improve the rot, water and fire retardant properties of jute fibers and its composite products. The main objectives are:

- To identify and locate the best segment (properties wise) from the total length of the jute fiber,
- To optimize the properties of chemically treated jute fibers,
- To incorporate modified jute fibers in polymer composites and to obtain better interfacial bond between fiber and polymer resin.

The blending of modified jute fiber (chemically treated) in thermoplastic matrix composite can be a viable approach for enhancing the mechanical properties and dimensional stability of jute composites and such modified composites may be used in household sectors as moderate load bearing structure.

The remainder of the thesis consists of six chapters. The second chapter of this thesis presents an analysis of the relevant literatures about natural fibers and natural fiber composites, especially jute fibers and their composites.

In the third chapter, experimental techniques are described that were used during the study. First, the technique used to perform single fiber tensile tests is explained. Next, a description of correction method by using some newly developed equations [5] is given. Several methods that were used to characterize the jute and chemically treated jute fiber such as tensile test, water absorption test, thermo gravimetric analysis (TGA), differential scanning calorimetry (DSC), Fourier transform infrared radiation (FTIR) spectroscopy, X-ray Diffractometer (XRD) and scanning electron microscope (SEM) are described. Then the production and characterization of fiber composites is highlighted.

In the fourth chapter, the experimental results are given, discussed and analyzed (comparisons with similar studies are also given).

Finally, in chapter five general conclusions and future works are drown based on the obtained results.

Chapter 2

Literature Review

2.1 Natural Fiber

Natural fiber filled polymer composites are materials that have natural fiber as the reinforcing agent in the composites. Natural fibers can be classified according to their origins as shown in Figure 2.1 . Vegetable fibers are generally comprised mainly of cellulose; for examples cotton, linen, jute, flax, ramie, sisal and hemp. Fibers are a class of hair-like materials that are continuous filaments or are in discrete elongated pieces, similar to pieces of thread. They can be spun into filaments, thread or rope. They can be used as a component of composite materials. They can also be matted into sheets to make products such as paper or felt. Natural fibers include those made from plant, animal and mineral sources.

Cellulose fibers serve in the manufacture of paper and cloth. Animal fibers generally comprise of proteins; examples include silk, wool, angora etc. Mineral fibers are naturally occurring fiber or slightly modified fiber procured from minerals. Among them asbestos is the only naturally occurring mineral fiber available.

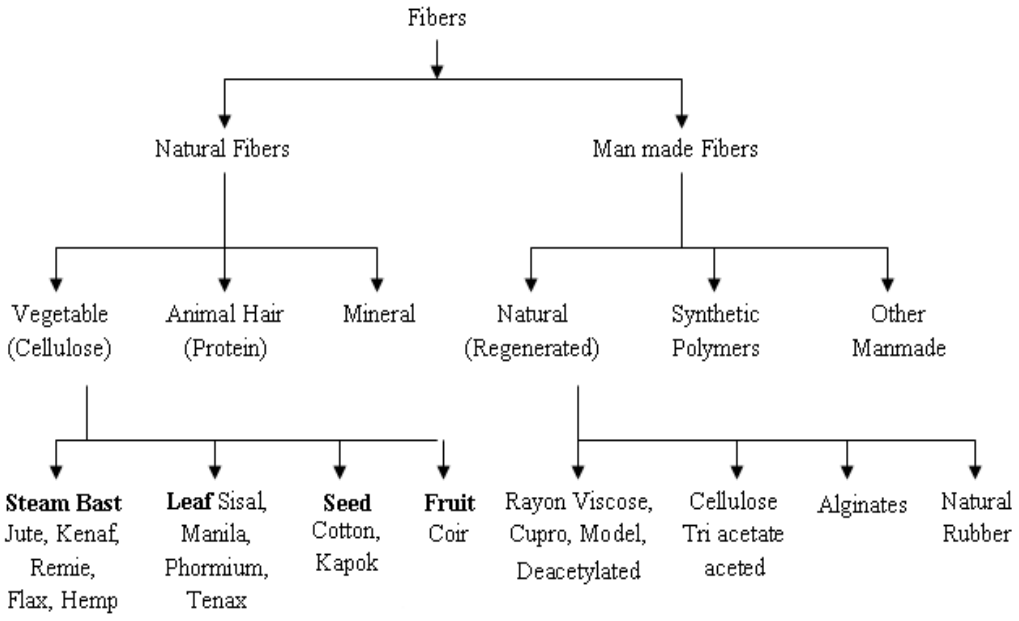

Figure 2.1: Classification of natural fiber [5]

2.2 Introduction of Jute

Jute is a biodegradable, cheap, non toxic, environment friendly, lignocellulosic bast fiber. It is versatile and fast growing renewable biomass and photo reactive crop with only 120-150 days duration from seed to fiber or maximum biomass. With the advent of cheap synthetic substitutes, bulk handling, containerization and storage in soils, jute and jute goods are losing market sharply in the important countries. Diversified use of jute is therefore essential to prevent further decline of the jute sectors [6].

Jute is an annually renewable resource of biomass. This, as a result, has stimulated growing interest among various developed and developing countries. Jute is abundantly available as an alternative source of composite. The stem of jute consists of two fibrous components, both of which are suitable for producing diversified products. The bark fiber is about 2.5 mm in length and constitutes 25-35% by weight of the stem. The shorter core fiber is about 0.6 mm in length and constitutes 60-65% by weight of the stem. Both are suitable for making diversified products. The bark is similar to soft fiber, while the core fiber has strength properties similar to that of hard wood fibers [6].

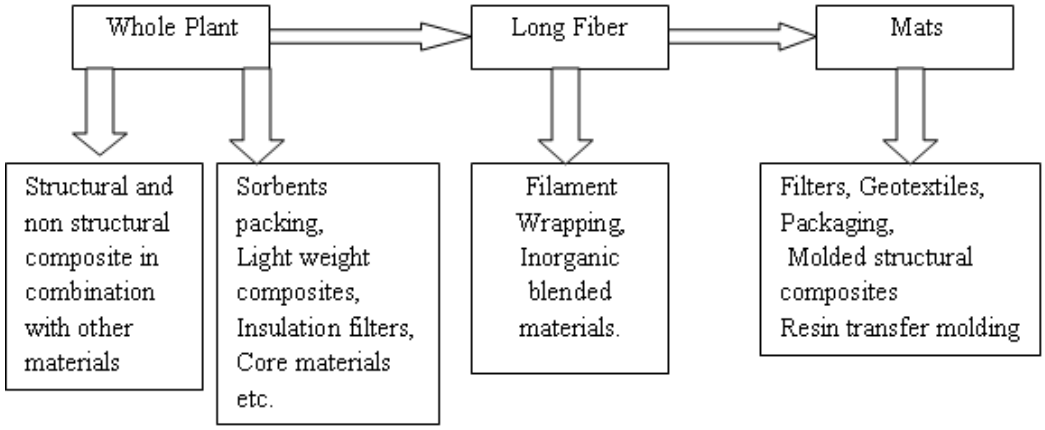

Figure 2.2: Diversified use of jute.

The traditional jute product market such as packaging materials for agriculture products (including sack, bags, backing cloth, packaging for fertilizer, cement and chemicals) are being eroded by the use of products based on synthetic substitutes. Diversified use [7] of jute (Figure 2.2) identifying major new market outlets is therefore essential to fend off further decline of the jute sector. One alternative to which great deal of attention had been given in the recent past is the possible utilization of jute composite production.

2.3 Chemical Composition of Jute Fibers

The two varieties of jute *Chorcorus olitrous* and *Chorchorus capsularis* are widely cultivated and most suitable for diversification use. The whole jute plant, jute fiber, jute stick and jute cutting can be used for various applications. The chemical composition of jute suitable for qualitative use is given in Table 2.1 [6].

Table 2.1: Chemical composition of jute and jute stick [6].

Element	Jute fiber (%)	Jute stick (%)	Element	Jute fiber (%)	Jute stick (%)
Cellulose	58-63	34.18-45.20	Water Soluble	0.6-1.2	-
Lignin	12-14	22.21-23.50	Polyuronide	4.8-5.2	-
Wax (Oil Materials)	0.4-0.8	7.18-7.25	Acetyl Value	2.8-3.5	-
Ash Content	-	0.37-0.4	Nitrogenous matter	1.56-1.87	-
Oxalic acid	-	13.3-22.3	Material Substances	0.5-0.79	-
Hemi-cellulose	20-23	-			

The genus of jute is chorchorus and the family is Tiliaceae. Jute fibers are finer and stronger than the mesta, and are therefore, better in quality. The natural fiber color of white jute is white creamy and that of tossa jute is golden. Depending on the demand, the annual production of jute and allied fiber in the world is increasing day by day.

2.4 Structure of Cellulosic Fiber

Structurally the jute fiber stem is composed of epidermis, cortex, large phloem, cambium, white xylem or wood and central pith tissue. The tissue, phloem, is most important as it is connected with fiber development. Bast is another name of the phloem tissue. Jute includes 40 species mostly distributed in the tropical regions. The vegetative period of jute is about 3-5 months. At the harvest stage varieties of *C. capsularis* attain a height of about 5-12 feet and those of *C. olitorus* attain a height of 5-15 feet or more. The stem of the both are cylindrical. The jute has shortest fiber length compared with mesta, ramie and flax. In the case of jute, the average length of fibers from outer parts of the wedge is 0.3-2 mm and that from the inner parts is about 1-5 mm only [8].

It is interesting to note that jute fiber has a hierarchical structure. Every fiber contains numerous elongated elementary fibers, or fiber-cells, which are about 20 to 30 μm in

diameter [8]. Each fiber cell wall is made up of a number of layers: the so called primary wall (the first layer deposited during cell development) and the secondary wall (S), which again is made up of three layers (S_1, S_2 and S_3 (Figure 2.3)) In all cellulosic fibers these layers contain cellulose, hemicelluloses and lignin in varying amounts. The individual fibers are bonded together by a lignin rich region known as middle lamella. Cellulose attains its highest concentration in the S_2 layer (about 50%) and lignin is most concentrated in the middle lamella (about 90 %) which, in principle is free from cellulose. The S_2 layer is usually by far the thickest layer and dominates the properties of the fiber [9].

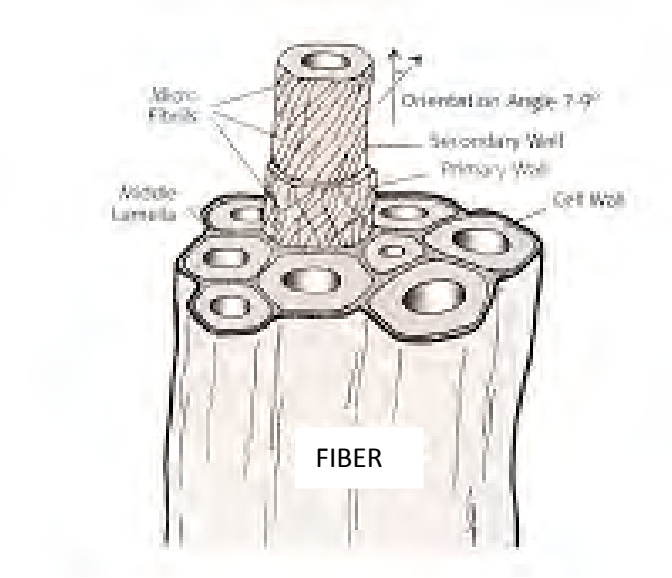

Figure 2.3: Micro structure of natural fiber.

Cellulose is the basic structural component of all plant fibers. It is the most important organic compound produced by plants and the most abundant in the biosphere. The cellulose molecule consists of glucose unit linked together in long chain, which in turn are linked together in bundles called micro-fibrils. The tensile strength of the cellulose micro-fibrils is very high. It is the strongest amongst the known material with a theoretically estimated tensile strength of 7.5 GPa or 1,087,500 pounds per square inch. In the S_2 layer, the micro-fibrils run almost parallel to the fiber axis. S_2 representing about 50% of the cell wall, gives the fibers a very high tensile strength [9].

Hemicelluloses are also found in all plant fibers. Hemicelluloses (Figure 2.4) are polysaccharides bonded together in relatively short, branching chain. They are intimately associated with the cellulose micro-fibril, embedding the cellulose in a matrix.

Hemicelluloses are very hydrophobic containing many sites to which water can readily bond [9].

Lignin compound gives rigidity to the plant. Without lignin, plant can not attain great height (as found in trees) or the rigidity (as found in some annual crops). Lignin is a three dimensional polymer with an amorphous structure and a high molecular weight. Of the three constituents of fibers, it is expected that lignin would be the one with least affinity for water. Another important feature of lignin is that it is thermoplastic (i.e. at temperature around 90°C it starts to soften and at temperature around 170°C it starts to flow) [9]. Lignin in jute makes the fiber resistance to microbial attack and provides better strength along with hardness and brittleness. The lignin and he micelluloses are responsible for most of the physical and chemical properties such as: biodegradability, flammability, sensitivity towards moisture of the thermo plasticity, degradability by UV-light, etc. Some structures of the monomeric units for the major polymeric constituents of cellulosic plant fibers are given in Figure 2.4.

Natural fibers are amenable to chemical modification due to the presence of hydroxyl groups. The hydroxyl groups may be involved in the hydrogen bonding within cellulose molecules, thereby activating these groups or introducing new moieties that form effective interlocks within the system. Surface characteristics, such as wetting, adhesion, surface tension or porosity of fibers can be improved upon chemical modification. The irregularities of the fiber surface play an important role in the mechanical interlocking at the interface. The interfacial properties can be improved by giving appropriate modifications to the components, which gives rise to changes in physical and chemical interactions at the interface. An enormous amount of work has been conducted in the field of fiber modification [7-13]. The present research has been conducted on rot, fire and water retardant modification of the jute fiber.

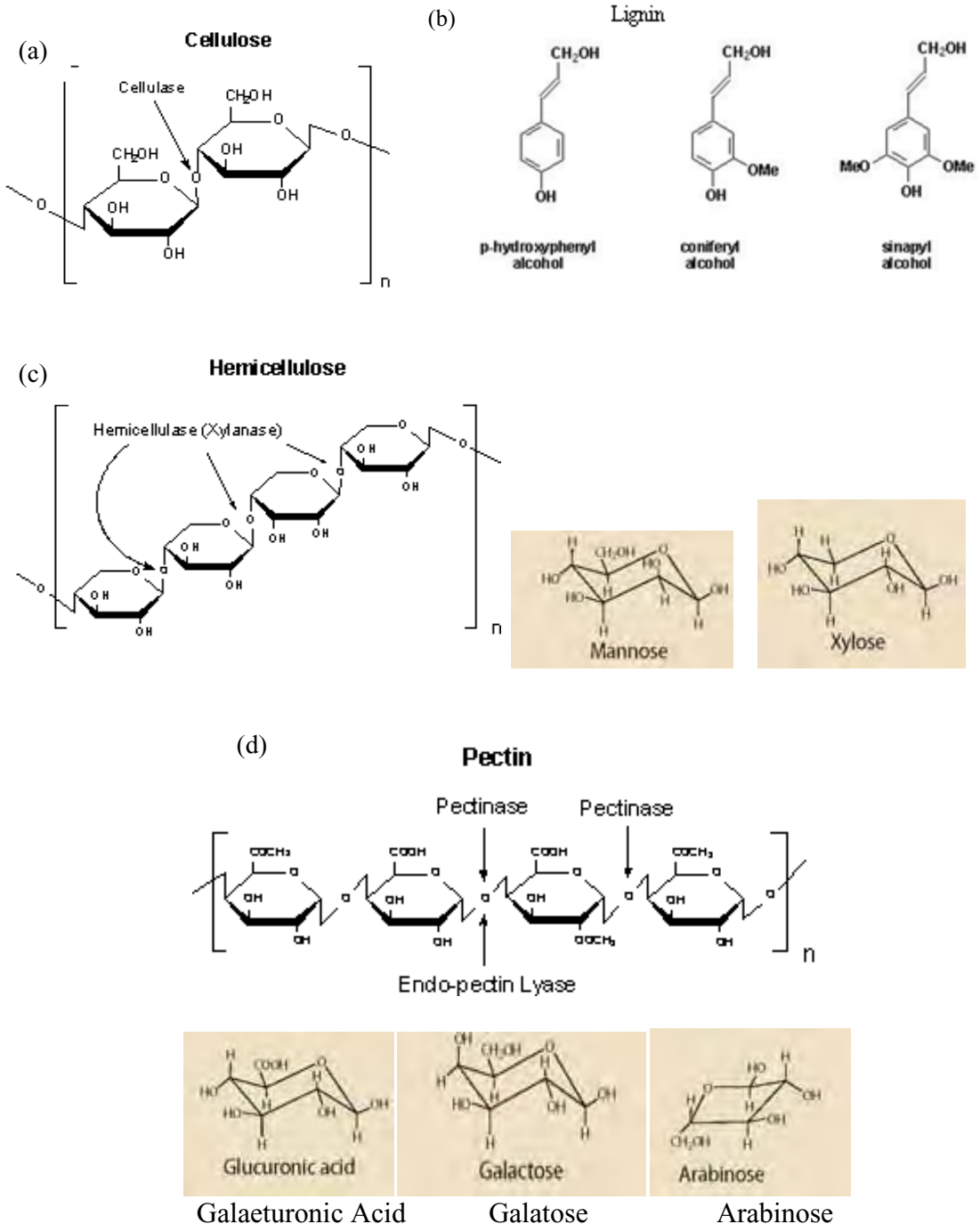

Figure 2.4: Polymeric constituent (a) cellulose, (b) lignin, (c) hemicelluloses and (d) pectin of jute plant.

2.5 Jute Scenario in Bangladesh

In 2007-2008, Bangladesh produced about 24.80% of world jute production. Jute and jute goods are the third most important source of foreign exchange earning after woven garments and knit garments. Jute is becoming more popular day by day because of its

environment friendliness compared to harmful synthetic substances. There are many kinds of jute products made in the world. Jute products can be classified into traditional products and diversified products. Traditional products comprise of hessian, carpet backing cloth and sacking, while diversified products include blanket, decorative fabrics, gift article, shopping bags etc [12].

Bangladesh is currently the second largest producer of jute fiber. The top spot is occupied by India. Highest quality jute fiber is grown in Bangladesh which supplies to the world. However, Bangladesh is falling behind other competitors due to recent technological advancements. In terms of world export of jute fiber and jute product, Bangladesh share more than 65%, which makes Bangladesh the largest exporter of jute fiber and jute product in the world. A study reveals that top five jute producing districts of the country are Faridpur, Rajbari, Madaripur, Kustia and Magura (Figures 2.5 and 2.6). These five districts contribute about 31.44% of the total jute production in Bangladesh. Mymensingh and Dhaka are well known for high quality jute production. But the jute production fluctuates due to weather condition and natural calamity. Hence the price also fluctuates. Table 2.2 shows the grade wise control jute price in BDT/bale in Bangladesh and Table 2.3 shows the diversified use of jute.

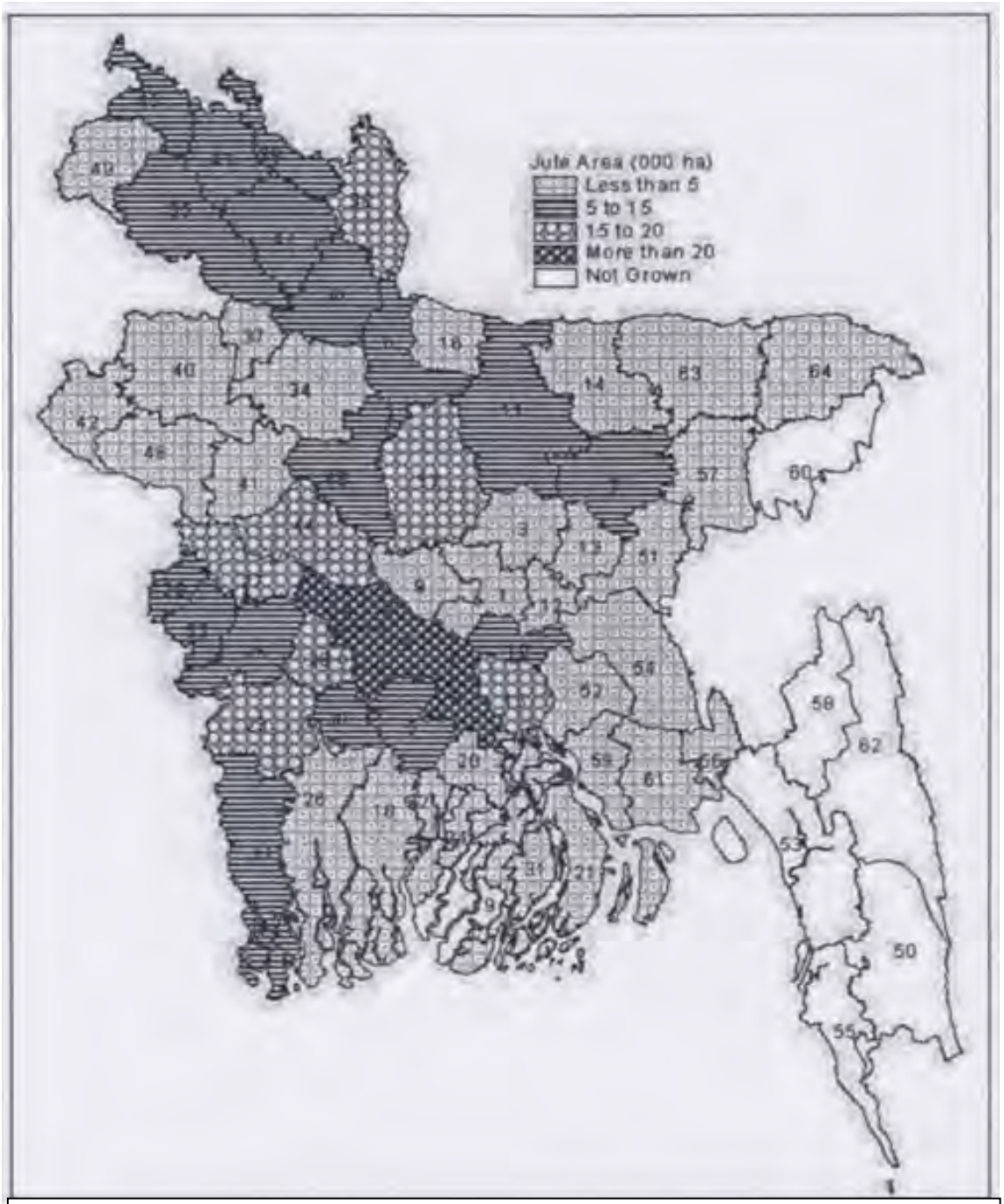

Note: 1 - Dhaka, 2 -Faridpur, 3 -Gazipur, 4 - Rajbari, 5 - Gopalgong, 6 -Jamalpur, 7 -Kishorgong, 8 -Madaripur, 9 - Manikgong, 10-Munshigong, 11-Mymensing, 12-Narayangong, 13-Norshingdi, 14-Netrokona, 15-Shariatpur, 16-Sherpur, 17-Tangail, 18-Bagerhat, 19-Bargona, 20-Barisal, 21-Bhola, 22-Chuadanga, 23-Jessore, 24-Jalakati, 25-Jhenaidah, 26-Khulna, 27-Kustia, 28-Magura, 29-Meherpur, 30-Narail, 31-Patuakhali, 32- Pirojpur, 33-Satkhira, 34-Bogra, 35-Dinajpur, 36-Gaibanda, 37-Joypurhat, 38-Kurigram, 39-Lalmonirhat, 40-Noagaon, 41-Natore, 42-Nawabgong, 43-Nilphamari, 44-Pabna, 45-Panchagor, 46-Rajshahi, 47- Rangpur, 78-Sirajgong, 49-Thakurgaon, 50—Bagerhut, 51 -Hramanbaria, 5 2-Chandpur, 5 3-Chittagong, 54 -Comilla, 5 5-Cox's bazaar, 5 6-Feni, 57 -Hobigong, 58-Khgrachari, 59-Lakshimpur, 60-Mawlaubibazar, 61-Noakhali, 62- Rangamati, 63- Srimongol, 64-Sylhet.

Source: Prepared by the author based on data collected from Bangladesh Bureau of Statistics.

Figure 2.5: Average jute production in Bangladesh (2005/06-2007/08) [11].

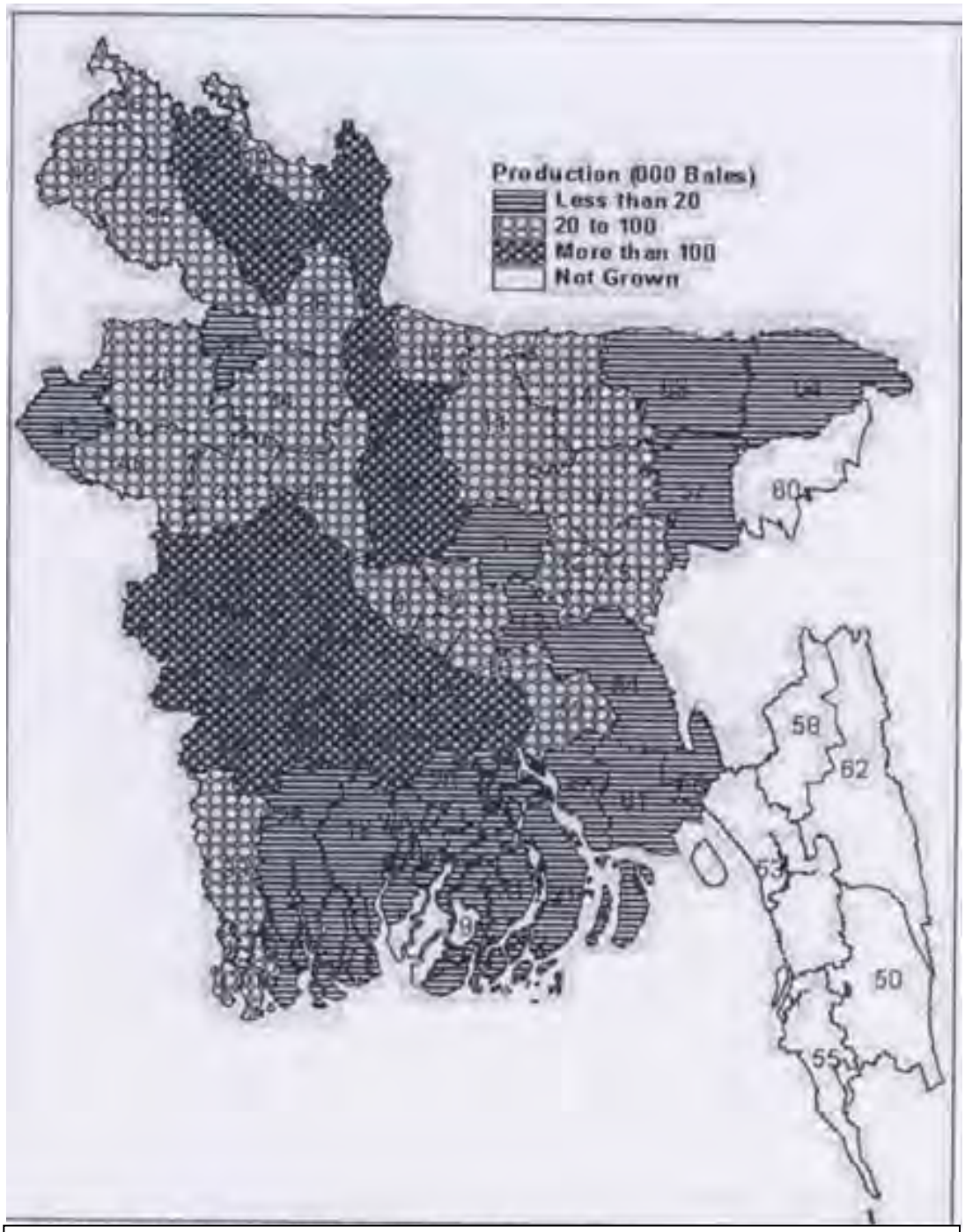

Note: 1- Dhaka, 2-Faridpur, 3-Gazipur, 4- Rajbari, 5- Gopalgong, 6-Jamalpur, 7-Kishorgong, 8-Madaripur, 9-Manikgong, 10 -Munshigong, 11 -Mymensing, 12-Narayangong, 13 -Norshingdi, 14 -Netrokona, 15 -Shariatpur, 16 -Sherpur, 17 -Tangail, 1 8-Bagerhat, 1 9-Bargona, 20 -Barisal, 2 1-Bhola, 22 -Chuadanga, 23 -Jessore, 2 4-Jalakati, 2 5-Jhenaidah, 2 6-Khulna, 27 -Kustia, 2 8-Magura, 2 9-Meherpur, 30 -Narail, 3 1-Patuakhali, 32- Pirojpur, 33-Satkhira, 34-Bogra, 35-Dinajpur, 36-Gaibanda, 37-Joypurhat, 38-Kurigram, 39-Lalmonirhat, 40 -Noagaon, 4 1-Natore, 4 2-Nawabgong, 43 -Nilphamari, 44 -Pabna, 45 -Panchagor, 46 -Rajshahi, 4 7- Rangpur, 78 -Sirajgong, 49 -Thakurgaon, 50—Bagerhut, 51 -Hramanbaria, 5 2-Chandpur, 53 -Chittagong, 54 -Comilla, 5 5-Cox's b azaar, 5 6-Feni, 57 - Hobigong, 5 8-Khgrachari, 5 9-Lakshimpur, 60 -Mawlaubibazar, 61-Noakhali, 62- Rangamati, 63- Srimongol, 64- Sylhet.

Source: Prepared by the author based on data collected from Bangladesh Bureau of Statistics.

Figure 2.6: Average jute growing areas in Bangladesh (2005/06-2007/08) [11].

Table 2.2 : Grade wise control jute price amount in BDT/bale in Bangladesh [11].

Grade	2008	2009
Excellent	6,825	8,175
Good	5,025	6,225
Medium	4,150	5,250
Poor	3,050	4,200

Table 2.3 : Different applications of jute fiber composites [12].

Application areas	Advantages
Automobile industries ➢ Door panels ➢ Seat backs ➢ Headliners ➢ Dash boards ➢ Trunk liners	▪ Lighter in weight ▪ Lesser control material ▪ Cost economic ▪ Serviceable mechanical properties ▪ Use of renewable resource
Building Component ➢ Door ➢ Window ➢ Wall partition ➢ Ceiling ➢ Floor	▪ Better physical properties ▪ Fire, termite and better moisture resistance properties ▪ Available at semi finished / finished state i.e. reduced labor and finishing cost
Transport Sector (railway coach & vehicle) ➢ Flooring ➢ Ceiling ➢ Seat and Backrest	▪ Better physical properties ▪ Fire, termite and better moisture resistance properties ▪ Available at semi finished / finished state i.e. reduced labor and finishing cost
Furniture ➢ Table ➢ Chair ➢ Kitchen cabinet etc.	▪ Better physical properties ▪ Fire, termite and better moisture resistance properties ▪ Available at semi finished / finished state i.e. reduced labor and finishing cost

2.6 Rot Retardant

2.6.1 Introduction

Biodegradation is a non specific process and it can be started in any space which is available to various organisms. Moreover, favorable conditions like heat, light, temperature, moisture and p^H value also have impact on the degradation. This biodegradation seems to occur through free radical mechanisms of jute and jute products. Quick biodegradation of jute product is advantageous in case of its disposal after use especially in land filling/land reclamation etc. It is more so since the degraded jute products have got definite fertilizing effect through increasing soil nutrient and biomass [13].

With increasing awareness of environment, the use of biodegradable natural fiber like jute is increasing. As the jute is a lingo-cellulosic bast fiber, the basic constituent of jute is cellulose- the element of which form the empirical formula $(C_6H_{10}O_5)_n$. Like all vegetable fibers, jute is prone to fungal and microbial attack in humid conditions leading to loss of strength and discoloration. It is also subjected to actinic and chemical degradation. Both bacteria and fungi can decompose cellulose when exposed in soil but are dependent on moisture content. The rate of degradation of control fabric is lower than that of alkali treated samples because some antifungal substances present in jute is removed by the alkali treatment.

2.6.2 Types of Deterioration

MacMillan [14] gave three chief causes of rotting in textile materials:

a) Photochemical, due to the action of light in combination with atmospheric effects.
b) Chemical, due to the action of agents such as acids, alkalis or salts.
c) Biological, which includes attack by agents such as rodents, insects and microorganism, chiefly fungi and bacteria.

Photochemical Deterioration

Sunlight especially combined with the effects of intermittent rain with cycles of wetting and drying, leads to considerable degradation in jute. Additionally, the action of direct sunlight, diffused light or artificial light causes yellowing. This effect being more pronounced with bleached jute [15, 16]. Jute is known to undergo more pronounced degradation in the presence of oxygen, although it has little or no effect on the yellowing.

Chemical Deterioration

Chemical agents such as acids, alkalis and salts can degrade textile materials. Industrial gases, such as sulfur di-oxide, are present in the atmosphere. These can be absorbed by jute with the development of strong acidity in the jute product. Chemical finishing operations can degrade jute materials as can chemicals packed in jute bags. Super phosphate fertilizers, for example, can lead to weakening of the jute materials [14].

Biological Deterioration

Rodent, insect and microorganisms are all responsible for deterioration of jute. Rats and mice often spoil textile, while a wide variety of insects attack and degrade jute materials. These insects include cockroaches, crickets, moths, beetles and silver fish. The microorganisms responsible for the rotting of the jute are mostly fungi and bacteria and occasionally actinomycetes and algae. In many cases these species of microorganisms, which attack one type of textile material will not attack another. For instance, *Chaetomium indicum* is very commonly found on jute but seldom found on cotton [12].

Of the three types of degradation, by far the most important would appear to be microbiological attack. Generally, the first indication that microbiological attack is in progress on cellulosic fibers is the development of a musty smell on the fabric followed by the formation of stain. This combine effect-mildew is due to the presence of mould on the surface. Moisture plays an important role in the formation of stains in jute. Staining is, nevertheless, aesthetically and hygienically disadvantageous and may render jute fabric difficulty to dye.

2.6.3 Effect of Degradation

Loss of strength is the most serious effect on jute caused by microbiological growth. Basu et al. [17] demonstrated that at a relative humidity between 80 and 100, a number of fungi grow on jute and decompose jute materials. Microbiological degradation of cellulose fibers occurs in stage, proceeding from breakdown of the long chain molecules to give cellulose molecule, followed by further breakdown of these to give glucose. Buston and Basu [18] reported that water extract of jute contains some vitamins, which accelerate the growth of some fungi. Lignin and hemicelluloses present in jute appears to have opposite effect in the fungal decomposition of jute as reported by Basu and Ghose [17]. The lignin

content in jute (12%-14%) does not provide suitable nutrition for most fungi and bacteria and so the higher the lignin content of a fiber the greater, generally, is the resistance to microbiological attack. Thus, white cotton, a dilignified fiber, loses strength more rapidly than jute under similar conditions. Coir, with lignin content of about 35%, is easily the most resistant to attack by microorganism. Bhattacharya and Basu [19] have established the fact that cotton canvases degrade totally within 5 days tested with compost, however the jute degrade much more slowly. When both jute and cotton were incubated with five especially selected fungi, there was particularly no decomposition of cotton canvas but jute canvas lost its tensile strength rapidly. The letter fact incorporated the earlier work of Macmillan et al. [20]. Resistance of natural fiber like jute to microbial damage may be dependent upon the physical properties such as crystalinity, chain length, orientation of ultimate cells etc. The higher the lignin content, the more resistance the fiber will be to rotting i.e. to fungal attack.

The method of protecting jute fabric against micro-biological attack depends on the introduction of a substance into or on the surface of jute fiber/product so that it acts as deterrent or provide toxicity to the micro organism and prevents its reproduction and growth. Past investigations have indicated that 0.5 -2% copper content gives maximum protection against rotting of jute products. The method that is long being used aims at forming a basic carbonate of copper on the jute fiber. The definite protective action of copper ions impregnated in the fabric has been proved by Doree et al [21]. To retard the process of decomposition or increase the durability of the jute products these need to be treated with copper compounds like copper sulphate, copper ammonium sulphate, copper ammonium carbonate, copper acetate, copper naphthenate, etc. Ali [22] showed the variation of copper number and carboxyl content of mesta, jute fiber and jute cellulose. The change of copper number of cotton fiber before and after boiling with sodium hydroxide was determined by Charles Doree [19]. Similarly different researchers [23, 24] studied the copper number and carboxyl content of jute cellulose. The copper number and carboxyl content of same quality of jute increased without any treatment even on storage. All the researchers were of the opinion that the copper number and carboxyl content are inversely proportional to the respective tensile strength of the fiber. Rahman et al. [25] studied the nature and degree of degradation of jute fabrics which were tested with different time period. They found out the copper number and carboxyl content in their research.

From the above discussion of the various causes of rotting of jute and other natural fibers, it is obvious that before considering the use of an anti rot agent, likely cause of any potential deterioration needs to be considered. This leads naturally to a consideration of the envisaged use of the material to be protected and hence the likely conditions to which it will be exposed. For example, there would be little need to protect a material from photochemical attack if it is predominantly to be used in shaded conditions.

2.6.4 Anti Rot Treatments and Their Application

Loss of strength and discoloration has long been a problem with jute exposed to strong sunlight. Peill [26] has stated that this is due to the presence of reactive phenolic groups in the lignin components of the fiber and it can be prevented by blocking these reactive groups by acetylation. MacMillan [27] pointed out that controlled acetylation of jute reduced degradation and yellowing, imparted a marked resistance to microbiological attack and reduced the moisture regain of the materials. However, acetylation treatments have proved so far too expensive for commercial adoption. The protection of jute against microorganism is usually based on three main principles:

a) Treatment with synthetic resins, which coat or react with the cellulose thus preventing it from being a readily available source of food for microorganisms.
b) Use of a finish that incorporated substances toxic to micro organism.
c) Modification of the fiber to make it non-nutritious to fungi and bacteria.

Treatment with Synthetic Resins

'Aminoplast', such as those based on melamine-formaldehyde and urea formaldehyde combinations have been used to introduce a physical barrier between the surface of the fiber and the fungi seeking to find nourishment there. This method, which would additionally allow the use of fungicides, appears to have been tried only on cotton. Nitrogenous phosphate resins, used to give flame retardant to cotton and other cellulosic fibers have also been found to give protection against microbiological attack. An advantage of this type of rot proofing is that it is resistance to leaching. A fairly recent method of rot proofing of jute using gamma-ray induced impregnation (grafting) of vinyl

plastic has been reported by Agarwal [28]. Styrene and methyl methacrylate system was applied, although the cost of grafting is likely to be high.

Use of Substances Toxic to Micro Organism

Treatment with such compounds usually called fungicides or bactericides is by far the most widely used manner of rot proofing jute materials. In general, an effective rot proofing agent should be toxic to both fungi and bacteria [13]. To be satisfactory, such a biocide would ideally have the following characteristics [13]:

a) Be toxic to a wide range of microorganisms under all conditions.
b) Exhibit low oral or dermal toxicity to man, presenting no health hazards in production or use of the treated textile.
c) Be relatively cheap.
d) Introduce no undesirable color or odour.
e) Have no effect on the 'handle' of any fabric made from the treated fiber.
f) Have no effect on its tensile strength, nor sensitize the materials
g) Have no adverse effect on other materials in close proximity to or enclosed in the treated materials.
h) Remain effective under all conditions of use through resistance to sunlight and leaching.

Not surprisingly, no single rot proofing treatment conforms to this entire stringent requirement and it is often necessary to apply two or more treatments, which is manually compatible. The most successful biocides for jute are those containing copper. Salt of zinc, chromium, iron and antimony also have rot proofing properties and the last three also inhibit photochemical degradation. Since jute appears to show a strong affinity for copper and copper compound resist leaching by water, treatments with compounds of this metal are fairly permanent. In particular, copper napthanate, copper-8-hydroquinolinolate and basic copper chromate appear to be especially resistant to leaching [27].

A process for prevention of mildew on cellulose fibers, using copper format followed by heat treatment has given encouraging result [13], however effectiveness on jute is not known. It is supposed that in fabric treated by this process, the copper is bound to the cellulose through cross linking.

Many organic chemicals provide rot-proofing to jute fabrics. Particularly effective in this group are chlorinated phenols and their sodium salts. These phenolic compounds are significantly volatile and so their effectiveness is reduced on exposure. Wilson has carried out long term tests on a number of rot proofing agents in which treated hessian samples were subjected to prolonged exposure to soil in column until a appreciable loss in strength had occurred in them. From the results, a number of rot proofing agents were listed in order of merit; using copper naphthenate (0.5% Cu) as a standard. The sequence of decreasing effectiveness is:

a) Copper pentachlorophenate (0.1% Cu)
b) Ammoniacal copper (0.5% Cu)
c) Copper naphthenate (0.5% Cu)
d) Rexcopine (39% in aqueous emulsion)
e) Rexcote (72% solutions applied as supplied)
f) Copper 8-hydroxyquinoline (0.1% Cu)
g) Lauryl pentachlorophenate (1.0% solution, solvent not specified)
h) Tributile tin oxide (0.1% in aqueous emulsion))
i) Di (5 chloro-2 hydroxyphenyl) methane [dichlorophen] (1.0 % solution. Solvent not specified.)

Chemical Modification of the Fiber

Chemical modification of the cellulose and associated components renders the fiber less easily metabolized as a source of food by fungi and bacteria. The acetylation of jute has been shown experimentally to impart a marked resistance to rotting by microorganisms, whilst also reducing absorption and discoloration by sunlight [13]. Other chemical modification has been done on the fiber application wise.

2.7 Fire Retardant

2.7.1 Introduction

The jute and jute products are vulnerable to fire. Hence it is desirable to make them fire resistant [29]. Fire may have been one of mankind's greatest innovations, however what it gives in warmth, light and cooking, it takes a way in power and destruction. Combustion or burning is the sequence of exothermic chemical reactions between a fuel and an oxidant accompanied by the production of heat and conversion of chemical species (Figure 2.7 (a)). The release of heat can result in the production of light in the form of either glowing or a flame. Fuels of interest often include organic compounds (especially hydrocarbons) in the gas, liquid or solid phase.

In a complete combustion reaction, a compound reacts with an oxidizing element, such as oxygen or fluorine and produces compounds of each element in the fuel with the oxidizing element. The simple word equation for the combustion of a hydrocarbon in air is:

$$\text{Fuel} + \text{Air} \rightarrow \text{Heat} + \text{Water} + \text{Carbon dioxide} + \text{Nitrogen} \quad (2.1)$$

The act of combustion consists of three relatively distinct but overlapping phases:

a) Preheating phase,

b) Distillation phase or gaseous phase and

c) Charcoal phase or solid phase,

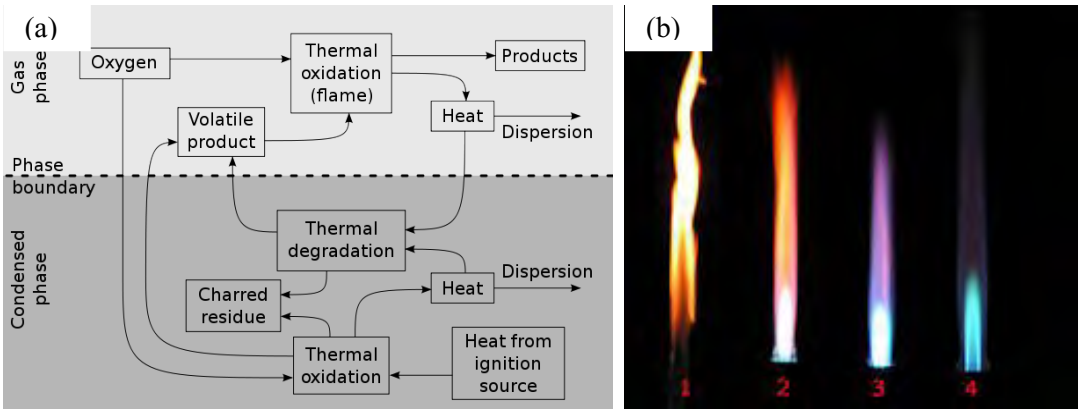

Figure 2.7: (a) Schematic diagram of combustion mechanism and (b) different flame types of a Bunsen burner [30].

2.7.2 Flame

A flame (from Latin flamma) is the visible (light-emitting) gaseous part of a fire. It is caused by a highly exothermic reaction (for example, combustion, a self-sustaining oxidation reaction) taking place in a thin zone. If a fire is hot enough to ionize the gaseous components, it can become a plasma [31].

Flame color is an important factor to identify the existing chemical in the fuel. Different flame types of a Bunsen depend on oxygen supply. On the left (Figure 2.7 (b)) a rich fuel with no premixed oxygen produces a yellow sooty diffusion flame. As seen from the right hand side of Figure 2.7 (b), a lean fully oxygen premixed flame produces no soot and the flame color is produced by molecular radicals, especially C-H and C_2 band emission. The purple color is an artifact of the photographic process [32].

Since flaming combustion and glowing combustion occur at different times and places and by distinctly different mechanisms, they may be expected to differ in the means by which they may be controlled. Effective flame-proofing agents may fail to retard glow and vice versa. They must therefore be considered separately. Flaming occurs earlier than glowing, progresses more rapidly and is more important in the spread of fire.

Theories of flame-proofing may be classified as coating theories, thermal theories, gas theories or chemical theories [33]. The theories, however, are by no means mutually exclusive because two or more of them may be and probably are operative in a given case.

The chemical theory of flame-proofing cellulosic materials [34-41] is based on changing the pyrolysis mechanism from that of fast pyrolysis to that of slow pyrolysis. If the pyrolysis of the cellulose could be directed to complete dehydration [39] according to the equation; Levoglucosan is a characteristic product of the primary pyrolysis of cellulose. It plays an important part in one of the modern theories of flame proofing cellulosic fiber or fabrics [41].

$$(C_6H_{10}O_5)_n = 6n\ C + 5n\ H_2O \qquad (2.1)$$

There would be no flammable gases from the major component until temperatures were high enough for the water-gas reaction to set in, by which time most of the water would escape. In fact, dehydration of the cellulose in the very first stage of the rmal decomposition may produce such ketones before hydrolysis or pyrolytic scission begins.

Substance added to a material or applied to a surface to suppress, reduce or delay the combustion of the material to a significant level called flame retardant or fire retardant (Figure 2.8). A fire retardant is a substance other than water that reduces flammability of fuels or delays their combustion. This typically refers to chemical retardants, but may also include substances that work by physical action, such as cooling the fuels. Examples of these include fire-fighting foams and fire-retardant gels. The name fire retardant may also be applied to substances used to coat an object, such as a spray retardant to prevent Christmas trees from burning. Fire retardants are commonly used in fire fighting [42].

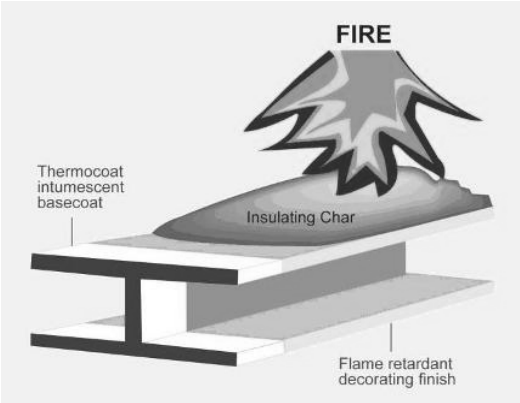

Figure 2.8: Fire retardant mechanism.

The effect of fire retardants on the charring temperature, the yield of products and the exothermic point suggests that jute is attacked chemically and partly decomposes before combustion can begin. The majority of retardants impair the strength of cotton/jute fiber or fabric to some extent even at ordinary or only slightly elevated temperatures [35]. Some materials that would otherwise be effective retardants cannot be used because they weaken wood, cotton or jute too seriously [43]. Desirable retardants should be harmless to jute at the temperatures of ordinary use, but should decompose or otherwise generate the effective reagent at a temperature above that of common use but well below that of combustion for control jute.

2.9.3 Working Principle of Fire Retardant

In general, fire retardants reduce the flammability of materials by either blocking the fire physically or by initiating a chemical reaction that stops the fire.

Physical Action

There are several ways in which the combustion process can be retarded by physical action such as by cooling, by forming a protective layer and by dilution. One commonly used fire retardant coating is aluminum hydroxide [42]. When heated, it dehydrates to form aluminum oxide (alumina, Al_2O_3), releasing water vapor in the process. This reaction absorbs a great deal of heat, thus cooling the material over which it is coated. Additionally, the residue of alumina forms a protective layer on the material surface.

Chemical Action

Chemical modificaation of cellulose with fire retardants gives products whose resistance to laundering and weathering is superior to that of finishes based on the physical deposition of the flame retardant within tha fabric, yarn or fiber. The reaction involved are either esterification or etherification. The latter is preferred because ether linkage are more stable to hydrolysis. The chemical action occurs at different phases such as [42]

a) Reactions in the gas phase,
b) Reaction in the solid phase,
c) Char Formation,
d) Intumescents

2.7.4 Flame Retardant

Flame retardants are materials that inhibit or resist the spread of fire. Many of the flame retardant chemicals are considered harmful, having been linked to liver, thyroid, reproductive/ developmental and neurological effects. Poly Chlorinated Biphenyl (PCBs) were banned in 1977 and the European Union (EU) has banned several types of brominated flame retardants as of 2008.

Aside from various conventional alternatives such as antimony or phosphorus-based retardants which have toxicological problems of their own, *Environmental Health*

Perspectives is also surveying the halogen-free alternatives. These include a technique to fuse flame retardants into products (so no chemicals leak). Nanoclays incorporating montmorillonite, an entirely new plastic, produces water when burned is called bishydroxydeoxybenzoin (BHDB). Inherently flame-resistant products are ideal and the aerospace industry uses such plastics, however they are too costly for widespread use. The annual consumption of flame retardants is currently over 1.5 million tones, which is the equivalent of a sales volume of approx. 1.9 billion Euro (2.4 billion US-$).

Mechanisms of Function

a) Endothermic degradation,
b) Dilution of fuel,
c) Thermal shielding,
d) Dilution of gas phase and
e) Gas phase radical quenching

Mechanism: cellulose, as such, has no appreciable vapor pressure and does not burn. However, on exposure to high temperature it decomposes exothermically into flammable compounds causing further degradation and decomposition until complete disintregration has taken place. Numerous studies have been made on burning of controland flame retardant-treated cellulose [42]. Decomposition normally takes place in two stages. Firstly thermal decomposition causes cellulose to decompose heterogeniously into gaseous, liquid, tarry and soil products. The flamable gases thus produced ignite, causing the liquids and tars to volatalize to some extent. This produces additional volatile fractions which ignite and produce a carbonized residue which does not burn easily. This process continues until only carbonaceous material remains. After the flame has subsided, the second stage begins. The residual carbonized residues lowly oxidizes and glowing continues until carbonaceous char is consumed.

Jute fiber consists hemi-cellulose, cellulose, lignin, pectin, fat and wax. Breakdown of the components, however, is not entirely simultaneous. The hemicelluloses, particularly its pentosans, are said to decompose first, largely between 200° and 260° C, followed by the cellulose at 240° to 350° C and finally by the lignin at 280° to 500° C [44-48]. Some investigators accordingly report three peaks in the exothermic region [45, 49-52].

Hemicellulose evolves more gases, less tar and about as much aqueous distillate as are formed from cellulose. However it differs from cellulose in that hemicelluloses yield no levoglucosan [53, 54]. Cellulose evolves water in the first stage of thermal decomposition before any other significant changes are observable.

Herodotus [55] wrote that the ancient Egyptians steeped wood in alum solution to impart resistance to fire. In the days of the Roman Empire, Romans soaked wood in vinegar and alum [38, 56] or coated it with clay, lime and loam, probably in an organic binder [56, 57]. In 1638 Nikolas Sabbattini recommended paint containing clay or gypsum for Italian theaters [57] and in 1820, Fuchs painted wood in the Munich Theater with sodium silicate [58, 59]. In 1735, Jonathan Wild received a patent in England for a treatment with alum, ferrous sulfate and borax [57]. Gay-Lussac [60] in 1821, at the request of Louis XVIII of France, tried many treatments for flameproofing cellulosic fabrics and recommended ammonium phosphate, a mixture of ammonium phosphate and ammonium chloride, or a mixture of ammonium chloride and borax.

Sengupta et al. [61] worked on ‘Bromination of jute fabrics’. They observed that bromination of jute imparts a fire resistance property which is handicapped by excessive after glowing and some strength loss. Menachem [62] reported that lignocellulosic material can be rendered flame resistant and resistant to biological deterioration through helagenation which is affected either by bromine or chlorine or by aqueous solution of these halogens in which p^H kept near the neutral point. Inorganic compound or these halogens are claimed to impart similar flame proofing effect to the lignocellulosic materials. Davis [63] observed that improved fire retardancy for lignocellulosic materials can be obtained by bromination or chlorination and phosphorilation. Robert [64] reported that ammonium salts of bromine, chlorine and iodine are effective in the prevention of after flaming and phosphoric acid and its sodium and ammonium salt are effective in the prevention of after glowing of the textile fabrics. Tyuganova et al. [65] reported that phosphoric acid is highly effective in flame proofing of the cellulosic materials. Robert et al. [66] also reported that chemical modification of cellulose for flame resistance can be achieved by introducing bromine or iodine and phosphorous in the esterification reaction in which halogen impart flame resistance and phosphorous imparts glow resistance. Hossain et al. [67] showed the effect of ammonium bromide and phosphoric acid on jute fabric for fire resistance properties. Camino et al. [68] showed the thermal degradation of

ammonium polyphosphate (APP), which is used as a commercial fire retardant. They blended it with polymethyl methacrylate (PMMA) and studied by thermal volatilization analysis (TVA) and identified the degradation products.

In case of gas phase radical quenching, chlorinated and brominated materials undergo thermal degradation and release hydrogen chloride and hydrogen bromide. These react with the highly reactive H and OH radicals in the flame, resulting in an inactive molecule and a Cl or Br radical. The halogen radical has much lower energy than H or OH and therefore has much lower potential to propagate the radical oxidation reactions of combustion. Antimony compounds tend to act in synergy with halogenated flame retardants. The HCl and HBr released during burning are highly corrosive, which has reliability implications for objects (especially fine electronics) subjected to the released smoke.

Thus best chemicals for impregnating jute for fire resistance are more than a century old. Meantime long lists of chemicals, as many as 400 in a single study [69], have been tested empirically [43, 71-76] without significant improvement as far as treatment of jute is concerned, except perhaps for the discovery that boric acid, when added to borax, imparts resistance to afterglow [77].

Coating Theory: In early as 1821, Gay-Lussac [60] suggested that fire resistance was due to formation of a layer of fusible materials which melted and formed a coating, thereby excluding the air necessary for the propagation of a flame. This was based on the efficiency of some easily fusible salts as flame retardants. Carbonates, borates and ammonium salts are good example of coating materials that produce foam on the fiber by liberation of gasses such as carbon dioxide, water vapor, ammonia etc. Monoammonium phosphate prevented both flaming and glowing and was highly effective against glowing at retention as low as 0.5 percent, although a considerably higher retention was necessary for good flame-proofing [78]. $NH_4H_2PO_4$ and other fire retardant materials are used as fire retardant, fire-proofing agent for wood, paper and fabric. These are used in manufacturing medicine and radio tube, phosphorus, nitrogen high efficient compound fertilizer. Food grade is mainly used as nutrient [79].

Fire resistance characteristics can change significantly when treated fabric is exposed to sunlight, followed by laundering, even though repeated washing and tumble drying of

samples of the same specimen did not indicate any significant changes, specially in the durability of the finish. Dry heat alone, followed by laundering or autoclaveing can also have a deleterious effect.

2.8 Water Retardant

Water is most abundant molecule in the earth surface. It can exist in three forms. Water-resistant fabrics (Figure 2.9) shed water because of their weave or because they have been treated. They will soak through in a heavy rain, however. Repeated exposure to chlorine, salt water or soaps accelerates this water retardant process.

Water-repellent materials (Figure 2.9) are more effective than water-resistant materials. They are either very tightly woven or coated with a finish that causes the water to make little beads when it hits the fabric rather than going through it. The finish may wear off over time or come off in dry cleaning. A silicone spray may rejuvenate the finish.

Water-proof fabrics can not be penetrated by water and should keep one dry, even in heavy rains. They may be extremely tightly woven, such as a fine polyester/nylon blend, rubber or plastic or other non-porous material or coated with a finish that makes them breathable but closed to water **[**80].

Jute fiber absorbs moisture from air, rain and other sources. In case of composite the fiber swell up or start to rot when they absorb moisture. Due to this the fiber delimitation occurs from the matrix. So the composite properties degrade. That is why water or moisture retardant is required to retain the composite properties for long time.

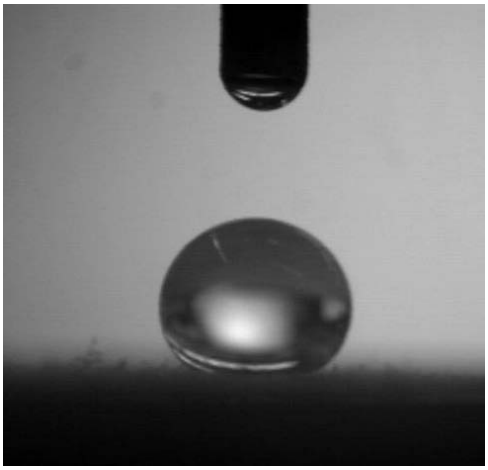

Figure 2.9: Water resistant surface.

2.8.1 Introduction

Jute and other lignocellulosic materials change dimensions with variable moisture content because the cell wall polymers contain hydroxyl and other oxygen-containing groups that attract moisture through hydrogen bonding. So the moisture absorption can be high [81]. The cell wall polymer affects the fiber properties as shown in Table 2.4. This hydrophilic behavior affects the properties of the fibers themselves as well as the properties of their composites. It leads to poor wetability of the polymers and weak interfacial bonding between fibers and hydrophobic polymers as the matrix. The hydrophilic character of fibers is usually incompatible with hydrophobic matrix materials unless a compatibilizer or coupling agent is used. This leads to poor interfacial adhesion between the fiber and matrix as well as poor fiber adhesion between the fiber and matrix, poor fiber dispersion [12].

Table 2.4: Cell wall polymers responsible for the properties of lingo-cellulosics in the order of importance [82].

Biological degradation	**Moisture aborption**	**Ultraviolet degradation**
Hemicellulose Accessible Cellulose Non-Crystalline Cellulose	Hemicellulose Accessible Cellulose Non-Crystalline Cellulose Lignin Crystalline Cellulose	Lignin Hemicellulose Accessible Cellulose Non-Crystalline Cellulose Crystalline Cellulose
Thermal degradation	**Strength**	
Hemicellulose Cellulose Lignin	Crystalline Cellulose Matrix (Non-Crystalline Cellulose + Hemicellulose + Lignin) Lignin	

The study of the water uptake behavior (e.g. the swelling) of the natural fibers, which have been used as reinforcements for polymers, is necessary for the construction of composite materials. The adhesive strength is influenced by absorption layers (in particular of water) at the common interface between the adhesive and the adherent component [83]. A major restriction in the successful use of natural fibers in durable composite applications is their high moisture absorption and poor dimensional stability (swelling), as well as their susceptibility to rotting [84]. Swelling of fibers can lead to micro-cracking of the composite and deteriorated mechanical properties. A deeper understanding of the complex nature of natural fibers and their surface properties is still needed in order to optimize natural fiber surface modification processes. This might help to increase the usefulness of those fibers as reinforcing material for polymers and to gain insights about the interaction between these materials [8].

2.8.2 Moisture Effect

Water is one of jute's worst enemies. Whether in the form of vapor or liquid, water can cause shrinking and swelling, which can lead to dimensional changes of the jute and degradation of the finish. Water causes decay or rot of the jute and it accelerates the weathering of jute exposed materials.

2.8.3 Shrinking and Swelling

In general, jute shrinks as it loses moisture and swells as it gains moisture. More precisely, jute changes dimension between an absolutely dry state (completely free of moisture) and its fiber saturation point (the point at which the wood fibers are completely saturated with moisture). This fiber saturation point typically occurs at about 30% moisture content for most species. At this point, all the water in the jute is bound within the cell wall. As moisture content changes above fiber saturation, the cell cavities take on or lose unbound water but the jute cell walls do not change dimensionally. Below the fiber saturation point, however, the jute changes dimension with changing moisture content.

2.8.4 Water Vapor and Water Effects

Shrinking and swelling of jute occur whether the water is in the form of vapor or liquid. For example, jute swells during periods of high humidity and shrinks during periods of low humidity; it also swells and shrinks as it gets wet from liquid water and then dries. As

discussed, jute can swell until it reaches fiber saturation. If jute is exposed to water vapor, such as occurs indoors, the moisture content can only reach the fiber saturation point. This requires exposure to 100% relative humidity for an extended period. Since jute is seldom exposed to this level of relative humidity for short periods, it easily reaches fiber saturation because of high humidity. However, if the jute gets wet from liquid water, it can quickly reach or even go beyond, fiber saturation. Problems with poor performance of jute occur when the moisture content of jute reaches or goes beyond fiber saturation — this is almost always caused by liquid water. Throughout the remainder of this report, the term water refers only to liquid water, the term water vapor to humidity and the term moisture to both water and water vapor.

2.8.5 Mildew

Mildew is caused by a type of stain fungi, which differ from decay fungi. Mildew is not capable of degrading the structural components of jute. Therefore, it does not cause a decrease in jute strength. Unlike decay fungi, mildew fungi do not tunnel through the jute but live only on the surface. Like decay fungi, mildew fungi often flourish when excessive water is present. Moisture also encourages the growth of lichens and other microorganisms that discolor the jute surface [85].

Microbial growth as associated with fibers of biologic origin such as cotton, wool, linen and silk, in the field of marine use, the high relative humidity renders even synthetic polymer textiles such as polyesters and polyamides subjected to microbial growth, which is also true of many other outdoor uses. To overcome problems associated with water absorption and stain resistance, report has been made to synthetic leathers and polyvinylchloride (vinyl) coated fabrics [86].

Applications of fluorochemicals such as the well known SCOTCHGUARD™ and similar compounds also may confer a limited degree of both water repellency and stain resistance. However, for optimal water repellency, it is necessary to coat fabrics with thick polymeric coatings which completely destroy the hand and feel of the fabric. Examples include vinyl boat covers, where the fabric backing is rendered water resistant by application of considerable quantities of polyvinylchloride latex or the thermoforming of a polyvinyl film onto the fabric. The fabric no longer has the hand and feel of fabric, but is plastic-like. Application of polyurethane films in the melt has also been practiced

with similar results. However, unless aliphatic isocyanate-based polyurethanes are utilized, the coated fabric will rapidly weather [87].

To overcome the above problem water resistance or repellant or proof properties is important. Report has been made to synthetic leathers and polyvinylchloride (vinyl) coated fabrics to overcome problems associated with water absorption and stain resistance [87]. Cross linking agents suitable for use in the present invention include both chemical agents which promote cross linking of crosslinkable groups along the latex copolymer chains as well as crosslinkable resins which may crosslink with the copolymer or which are themselves crosslinkable. A preferred cross linking agent which facilitates copolymer cross linking is zinc ammonium carbonate. Preferred self-cross linking resins are the various melamine/formaldehyde and phenol/formaldehyde resins and their variants, particularly CYREZ.RTM. 933 . Other phenol, melamine, urea and dicyandiamide based formaldehyde resins are available commercially, for example, from the Borden Chemical Company. Preferably, melamine/formaldehyde resin in the amount of 0.1 to about 1.0 weight percent, preferably about 0.25 weight percent based on the weight of the aqueous treating composition is used. Other crosslinkable resins such as oligomeric unsaturated polyesters, mixtures of polyacrylic acid and polyols, e .g. polyvinyl alcohol and epoxy resins may also be used, together with any necessary catalysts to ensure cross linking during the oven drying cycle [88].

Acetylation has been shown to be beneficial in reducing moisture absorption of natural fibers. Reduction of about 50% of moisture uptake for acetylated jute fibers and of up to 65% for acetylated pine fibers has been reported in the literature [20]. Acetylation has also been found to enhance the interface in flax/polypropylene composites [21]. In case of silane treatment chemicals are hydrophilic compounds with different groups appended to silicon such that one end will interact with matrix and the other end can react with hydrophilic fiber, which act as a bridge between them. The uptake of silane is very much dependent on a number of factors including hydrolysis time, organofunctionality of silane, temperature, and pH. Alkoxy silanes are able to form bonds with hydroxyl groups. Silanes undergo hydrolysis, condensation, and the bond formation stage. Silanols can form polysiloxane structures by reaction with hydroxyl group of the fibers [22].

But no such work has been conducted on the jute fiber or fabrics.

2.9 Composite Materials

2.9.1 Introduction

The word 'Composite' means "a substance, which is made up by mixing two or more distinct different substance". In most cases mixing is done by physical process. In a few cases it is also done partly by chemical reaction. Polymer composites consist of one or more discontinuous phases embedded in a continuous phase polymer matrix. The discontinuous phase is usually harder and stronger than the continuous phase and is called reinforcement. The matrix can be classified as thermoplastic or thermoset [7].

Table 2.5: Main advantages and disadvantages of lingo-cellulosic fibers [8].

Advantages	**Disadvantages**
Low cost	High moisture absorption
Renewable	Poor microbial resistance
Low density	Low thermal resistance
Nonabrasive	Local and seasonal quality variations
Low energy consuming	Demand and supply cycles limited.
High specific properties	
High strength and elasticity modulus	
No skin irritations	
No residue when incineration	
Fast water absorption/ desorption	
Good thermal conductivity	
Biodegradability	

Natural fiber reinforced composites are inferior to synthetic fiber reinforced composites in tensile strength and modulus, but they exhibit significantly higher elongation [10]. This provides better tolerance to composite damage. However, a major problem of natural fiber reinforced composites is the ir susceptibility to fungal and insect attack and degradation by moisture. The high moisture absorption of the natural fiber and their low microbial resistance are disadvantageous (Table 2.5) that need to be considered, particularly during shipment and long term storage as well as during processing of the composites. In addition their hydrophilic behavior affects the properties of the fibers themselves as well as the properties of their composite [7].

2.9.2 Lignocellulosic Fiber Reinforced Thermoplastic Composite

In general, cellulosic fillers or fibers have higher Young's modulus as compared to commodity thermoplastics, thereby contributing to the higher stiffness of the composites. The increase in the Young's modulus with the addition of cellulosic materials depends on many factors such as amount of fibers used, orientation of the fibers, interaction and adhesion between the fiber and matrix. In general dispersing agents and or coupling agents are necessary for the property enhancement, when fibers are incorporated into thermoplastic [9]. Dispersing agent facilitates the fiber dispersion and improves the interfacial adhesion between the fibers and the polymer matrix. Although grafting can improve the properties of the composite to a significant extent, this process increases materials cost of the system. The use of dispersing agents and or coupling agents is a cheaper route to improve properties and makes more practical sense for high volume, low cost composite system [10].

In a natural fiber-thermoplastic composite the lingo-cellulosic phase is present in a wide range of diameter and length. Some of them are in the form of short filaments and others are present in the form that seems closer to the individual fiber. The high shearing energy of blending the filaments and the polymer in a matrix results in fiber attrition but can also axially separate the filaments into discrete individual fibers. Cellulosic fiber/ fillers can be classified under three categories depending on their performance when incorporated to plastic matrix. Wood dust and other low cost agriculture based dust can be considered as particulate filler that enhance the tensile and flexural moduli of the composite with little effect on the composite strength. Wood fiber and recycled newspaper fiber have higher aspect ratios and contribute to an increase in the moduli of composite. They can also improve the strength of the composite when suitable additives are used to improve stress transfer between the matrix and the fibers. The improvement in moduli is not significantly different than the cellulosic particulate fillers. The most efficient cellulosic additives are natural fibers such as jute, kenaf, flax etc. The specific Young's modulus, the specific flexural modulus, the ratio of the composite modulus to the composite specific gravity of composites with natural fibers such as kenaf are significantly higher than those with wood fibers. The specific moduli of high fiber volume fraction of bast fibers polypropylene (PP) composites are high and in the range of glass fiber-pp composites. The most efficient

natural fibers having high cellulose content coupled with a low micro fibril angle attain high filament mechanical properties.

2.9.3 Reinforcement in Composite Material

The role of the reinforcement in a composite material is fundamentally one of increasing the mechanical properties of the neat resin system. All of the different fibers used in composites have different properties and so affect the properties of the composite in different ways. However, individual fibers or fiber bundles can only be used on their own in a few processes such as filament winding. For most other applications, the fibers need to be arranged into some form of sheet, known as a fabric, to make handling possible. Different ways for assembling fibers into sheets and the variety of fiber orientations are possible leading to various types of fabrics, each of which has its own characteristics.

2.9.4 Interphase

When composites are manufactured, a small region (1μm) known as the fiber-matrix interphase is formed between the fiber and the matrix. This region exhibits properties distinguishably different from the properties of the bulk matrix. The fiber-matrix interphase transfers stress between fiber and matrix, the efficiency of this stress transfer process and a composite's durability are controlled by the properties of this region.

The interphase of composites is the region where loads are transmitted between the reinforcement and the matrix. The extent of interaction between the reinforcement and the matrix is a design variable and may vary from strong chemical bonding to weak frictional forces. This can be controlled by using an appropriate coating on the reinforcing fibers. Generally, a strong interfacial bond makes the composite more rigid but brittle. A weak bond decreases stiffness but may enhance toughness.

2.9.5 Thermoplastics

Thermoplastics require heat to make them formable and after cooling, retain the shape they were formed into. These materials can be reheated and reformed into new shapes a number of times without significant change in the ir properties. Most thermoplastics consist of very long main chains of carbon atoms covalently bonded together. Sometimes nitrogen, oxygen or sulfur atoms are also covalently bonded in the main molecular chain. Pendant atoms or groups of atoms are covalently bonded to the main chain atoms. In

thermoplastic the long molecular chains are bonded to each other by secondary bonds [89].

Polypropylene

Polypropylene (PP) is a thermoplastic polymer. It is one of the most extensively used plastics both in developed and developing countries. Polypropylene is available with many different reinforcing agents or fillers, such as talc, mica or calcium carbonate; chopped or continuous strand fiber. Many additives have been developed to enhance the thermal stability of polypropylene to minimize degradation during processing. One of the most important requirements of the polypropylene used in the manufacture of composites is that it should be relatively pure and free of residual catalyst [90, 91]. PP provides most of the advantages with regards to economic (price), ecological (recycling behavior) and technical requirements (higher thermal stability).

Molecular Structure of Polypropylene

In isotactic PP, each monomer unit in the chain is arranged in a regular head-to-tail assembly without any branching. Furthermore, the configuration of each methyl group is the same**.** Occasionally, some imperfect monomer insertion gives the type of fault shown in Figure 2.10.

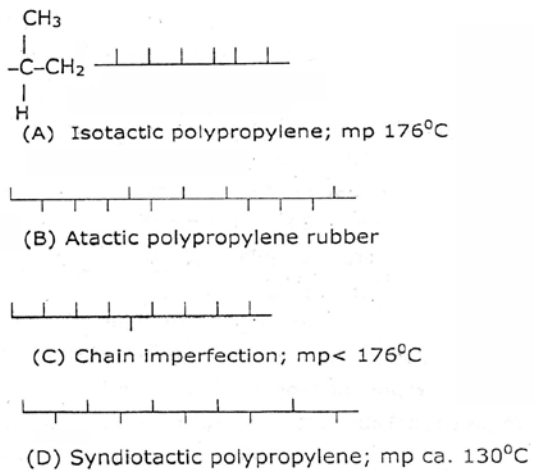

Figure 2.10: Poly propylene chain structure [92].

An extreme example of clamfests is a tactic PP (Figure 2.10), with complete loss of steric control. In syndiotactic configuration, methyl groups are alternatively on either side of the carbon chain [92].

Properties of PP

Polypropylene is a linear hydrocarbon polymer containing little or no instauration. Some typical properties of PP are given in Table 2.6. The final melting point of commercial PP lies in the range 160-170ºC, with purified polymer reaching 176ºC. Within the range of commercial polymers, the greater the amount of isotactic material, the greater the crystalline hence, greater the softening point, stiffness, tensile strength, modulus and hardness. The crystalline and non-polar nature of PP confers good resistance to a wide range of aqueous and polar media, including emulsifier solutions with their strong stress cracking abilities [92].

Table 2.6: Properties of PP [92].

Parameters	**Standard used**	**Values**
Crystallinity, (%)	-	82
Melting temperature, (ºC)	-	165-171
Specific gravity	ASTM D792	0.90-0.91
Tensile modulus, (GPa)	ASTM D638	1.10-1.55
Elongation-to-break, (%)	ASTM D638	100-600
Tensile strength, (MPa)	ASTM D638	31-41
Rockwell hardness (R-scale)	ASTM D785	90-95
Impact strength, notched Izod,(j $m^{-1)}$	ASTM D256	21-53
Heat Deflection temperature, (ºC), at 455 KPa	ASTM D648	225-250

Maleic Anhydride Grafted Polypropylene (MAgPP)

Effective application of polymer composites is determined by the interfacial interaction between polymer and fiber. In polymer composites, the role of interaction is more critical because of non-polar hydrophobic nature of the polymer phase and the hydrophilic character of fibers. The polarity of the polymer matrix can be increased (Figure 2.11) by several methods. One of the most common processes is to use a functional monomer with a pendant reactive polar group. The most widely used functionalities are unsaturated acids and their derivatives. The Maleic Anhydride Grafted Polypropylene (MAgPP) is at present a classical example of the reactive functionality [93].

MA grafting to the backbone of a polypropylene gives improved properties (Table 2.7) of polymers by providing polarity to promote hydrophilicity and adhesion. It gives functionality for cross linking and other chemical modifications and to promote

compatibility with other materials. Currently, *MA-graft* PP is the most effective coupling agent between PP and natural fibers [9].

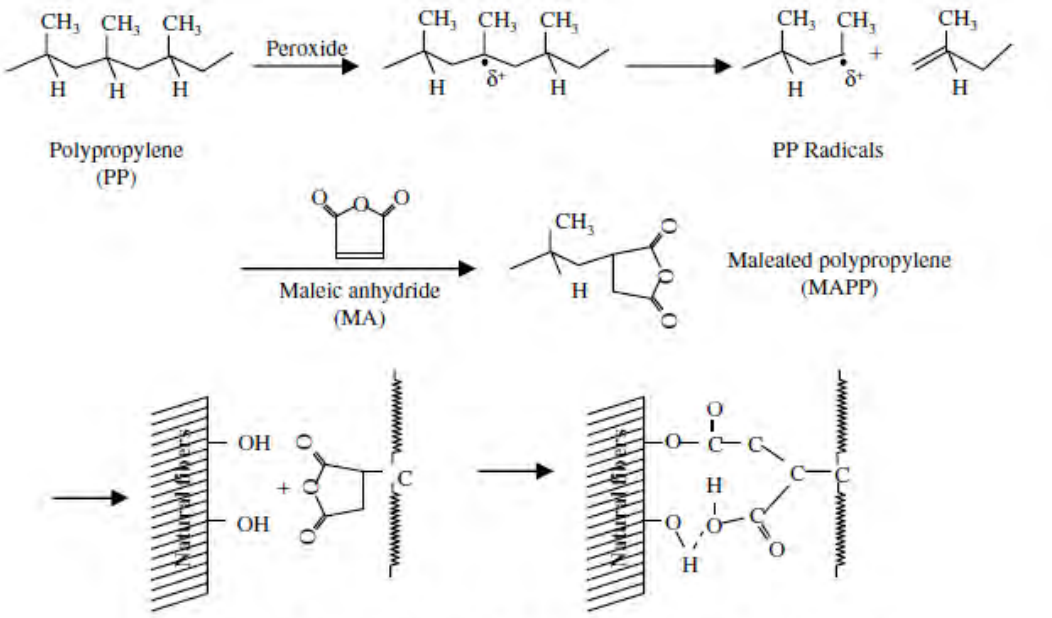

Figure 2.11 Chemical reaction mechanism of the natural fiber and MAgPP matrix.

A commonly used method for inducing compatibility between polyamide and polyolefin (i.e. polypropylene) is by chemical modification of the polyolefin to contain pendent carboxyl groups, often by grafting with maleic anhydride or similar compounds. This forms chemical linkages to the polyamide via the terminal amine groups Bonner and Hope, 1993 . For many years, following the early pioneering advances by Ide and Hasagawa 1974 , maleic anhydride grafted polypropylene (PP- g-MA) has been used extensively for compatibilization of PP and PA6. In the melt, the maleic anhydride groups can easily react with the amine end groups of PA6 to form block or graft copolymers. These resulting copolymers efficiently reduce the interfacial tension between PP and PA6. Thus, reducing the size of dispersed PA6 phase and enhancing the mechanical properties of the blends. Sathe et al. 1996 reported that PA6/PP blends containing PP-g-MA showed more regular and finer dispersion, different dynamic properties and improved mechanical properties due to the better adhesion between the two phases. In addition, the addition of PP-g-MA into the PA6/PP blends also lower MFI and water absorption properties due to the formation of PP-g-PA6 copolymer during melt mixing. According to Marco et al . 1997, the presence of PP-g-MA in the PA6/PP leads to a

reduction in the crystallinity of the polyamide 6 and in its rate of crystallization, due to the diluents effect of the polypropylene. A similar compatibilization effect of PP-g-MA in the PP/PA6 blends was also reported by Tseng et al. 2001, Roeder et al. 2002 and Zeng et al. 2002. Roeder et al. 2002 found that the compatibilized PP/PA6 blends absorbed less water than corresponding uncompatibilized systems, probably related to fewer N-H groups due to amide linkage formation. The compatibilized blends can form a hydrogen bond that reduces the interfacial tension and the possibility of forming capillaries between domains and matrix. Then, the interfacial layer formed with the addition of PP-g-MA increases the adhesion between the phases and reduces voids and water uptake [96].

Table 2.7: Properties of MAgPP.

Properties	Value	Test method
Melting temperature, (ºC)	167	DSC
Tensile strength, at Break, (MPa)	22	ASTM D 638
Flexural modulus, (MPa)	880	ASTM D 638
Elongation at break,(%)	12	ASTM D 638
Melt Flow Index, g/10 mm	10	ASTM D 1238

Jute is a lignocellulosic bast fiber which is prone to bacterial effect, easy to ignite, biodegradable and highly hydrophobic. Recent research and development in jute fiber reinforced composite as potential structural materials has attracted attention of material scientist all over the world because of their low cost, easy availability, light weight, renewable and biodegradable nature. In addition, low density and high specific strength jute reinforced polymer composites make them the most suitable candidates for low load bearing applications [97-99]. However, natural fiber reinforced materials have substantially inferior mechanical and water resistance properties compared to conventional glass fiber reinforced composite. In order to overcome these disadvantages, several treatments have been proposed in the literature [100-102]. In the case of jute fibers, in addition to the matrix/fiber interface modification, different changes on the interface between the elementary fibers, as well as on the roughness and density of the technical fiber could be also induced by the chemical treatment [103,104]. These treatments remove pectin from the middle lamella, thereby separating fiber bundle into their individual components. This fibrillation of fiber bundles increases the surface area which would affect the surface bonding properties.

Chapter 3

Experimental Procedure

3.1 Introduction

Chapter three include experimental procedures of the present research that can be divided into following steps:

Chemical modification and conformation of their presence/ existence were completed by chemical treatment and Fourier transform infra red (FTIR) spectroscopy. Fiber characterization was accomplished by mechanical testing of different portion for chemically treated and control fiber. To enlighten the mechanical properties, X-ray diffraction (XRD) analysis was completed. To monitor the thermal properties, differential scanning calorimetry **(**DSC) and thermo gravimetric analysis (TGA) were conducted. To observe the surface morphology, scanning electron microscopy (SEM) and atomic force microscopy (AFM) were accomplished. Composite characterization was done by evaluating mechanical and other related properties. The total experimental detail is specified bellow.

3.2 Materials

3.2.1 Control Fiber

The jute fibers were collected from the Bangladesh Jute Research Institute (BJRI), Faridpur regional station, Bangladesh. The supplied jute fiber was CVL-1 (*Corchorus capsularis L.*). The whole jute fiber was cut into three portions as top, middle and bottom/cutting (Figure 3.1). Three different types of chemical modification were conducted on each portion of the jute fibers (Figure 3.2).

Figure 3.1: Cutting process of whole jute.

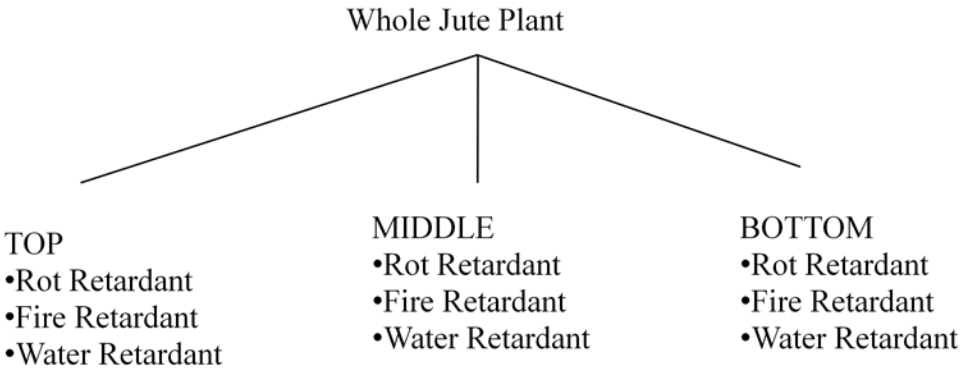

Figure 3.2: Chemical treatment on three portions of the jute.

3.2.2 Chemicals

The copper sulfate ($CuSO_4$) and sodium carbonate (Na_2CO_3) were used for rot retardant (RR) treatment, di ammonium hydrogen phosphate ($NH_4H_2PO_4$) and Lissapol-N were used for fire retardant (FR) treatment and poly vinyl chloride (PVC), magnesium chloride ($MgCl_2$), acetic acid (CH_3COOH) and perapret were used for water retardant (WR) treatment.

3.3 Rot Retardant

The control fibers were first cut into three (top, middle and bottom) different portions. For rot retardant the three portions of fiber were immersed in 4%, 8% and 20% $CuSO_4$ (Figure 3.3) solution at room temperature. After 30 minutes 1%, 2% and 5% Na_2CO_3 were added as a catalyst. After 1 hour the jute fibers were pulled out from the solution and air dried at room temperature for 2 days. The chemical composition is presented in Table 3.1.

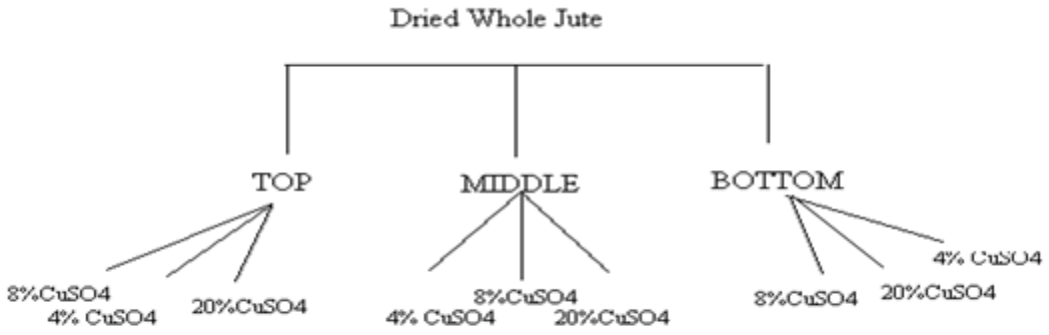

Figure 3.3: Rot retardant jute fiber.

Table 3.1: Chemical composition of rot retardant jute fiber.

Jute	**4%RR**		**8%RR**		**20%RR**	
50gm	$CuSO_4$	Na_2CO_3	$CuSO_4$	Na_2CO_3	$CuSO_4$	Na_2CO_3
	2g	0.2g	4g	1g	10g	2.5g

3.3.1 Compositional Analysis

Cu content of the rot retardant jute fiber (4%, 8% and 20%) was measured by Iodometric method [106,107]. Stock solution was prepared by using the chopped fiber, 20% H_2SO_4, CH_3COOH, KIO_3 and Na_2CO_3 were mixed with the stock solution and placed in dark room for 5 minutes. The cu content was measured by using the thio ($NaHS_2O_3$) for titration. The color of different rot retardant treated fiber was different as shown in Figure 3.4 (a). The moisture content of the above treated jute fiber was measured by conventional method [108]. The chopped fiber were weighted at room temperature and oven dried at 105°C± 3°C for 6 hours and placed in a dedicator with anhydrous silica gel in order to cool for at least 15 minutes. The moisture content was measured by the weight difference compared to the initial weight and the percentage was made.

Figure 3.4: Rot retardant (a) chopped jute fiber (b) moisture content measurement and (c) oven.

3.4 Fire Retardant

The control fibers were first cut into three (top, middle and bottom) different portions. For the fire retardant, the fibers were immersed in 20%, 25% and 30% $NH_4H_2PO_4$ solution (Figure 3.5) at room temperature. After 10 minutes, lissapol-N was added as a catalyst. After 1 hour reaction, the jute fibers were pulled out from the solution and air dried at

room temperature for 2 days. For fire retardant treatment, the chemical composition is presented in Table 3.2.

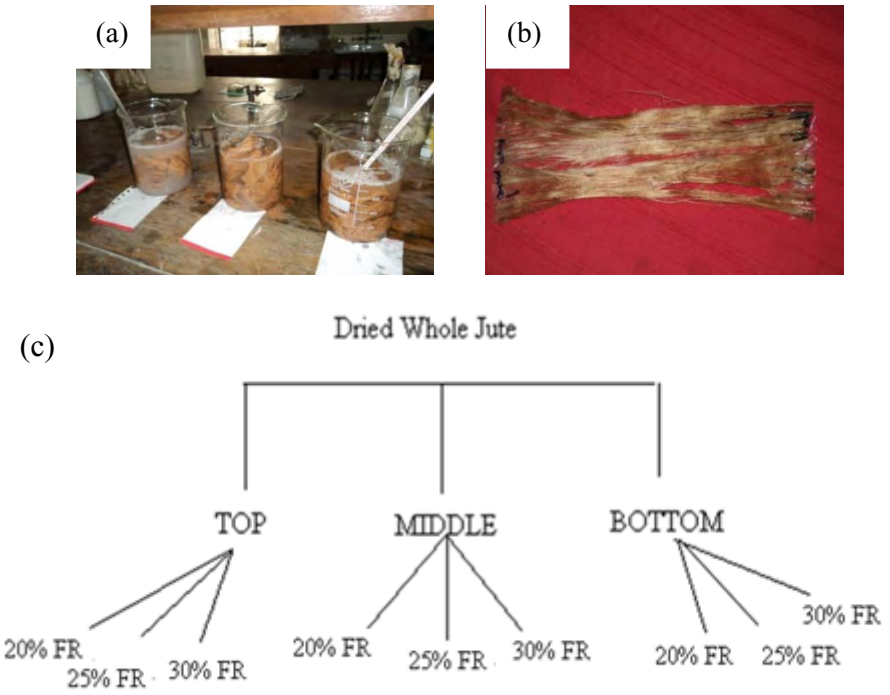

Figure 3.5: (a) Soaking of jute fiber for fire retardant, (b) fire retardant sample for flaming test and (c) fire retardant of jute fiber.

Table 3.2: Chemical composition of fire retardant treatment.

Jute	**20% FR**		**25% FR**		**30% FR**	
200g	$NH_4H_2PO_4$	Lissapol	$NH_4H_2PO_4$	Lissapol	$NH_4H_2PO_4$	Lissapol
	200g	1 tbs	250g	1tbs	300g	1tbs

3.4.1 Flammability Test

Preliminary test was conducted to determine the fastest burning direction of the fibers. Samples were preheat in a woven at 105 °C ± 3 °C for 30 ± 2 minutes and placed in a dedicator with anhydrous silica gel in order to cool for a tleast 15 minutes. Five specimens were prepared having dimension of 50 by 150 mm. The flammability was tested by a Flammability Tester. The test procedure required that a 16 mm (Figure 3.6 (a)) flame impinged on a specimen mounted at a 45° angle for 1 second (Figure 3.6 (b)). The specimen was allowed to burn to its full length or until the stop thread was broken at a

distance of 127 mm. The results of several specimens were averaged and a *Class* designation was made based on the flammability performance and surface characteristics of the sample [109].

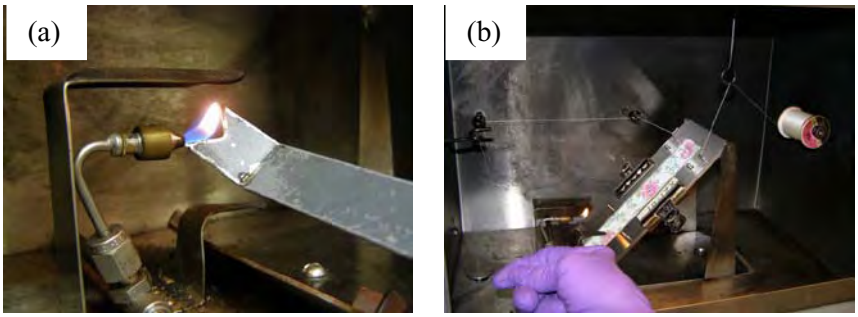

Figure 3.6: (a) Determination of flame length and (b) flammability test.

3.5 Water Retardant

For the water retardant treatment, the fibers were immersed in 10%, 15% and 20% PVC, perapert, acetic acid and $MgCl_2$ solution (Figure 3.7 (a) and (b)) at room temperature. After 1 hour the jute fibers were pulled out from the solution and air dried at room temperature for 2 days. For water retardant, the chemical composition is presented in Table 3.3.

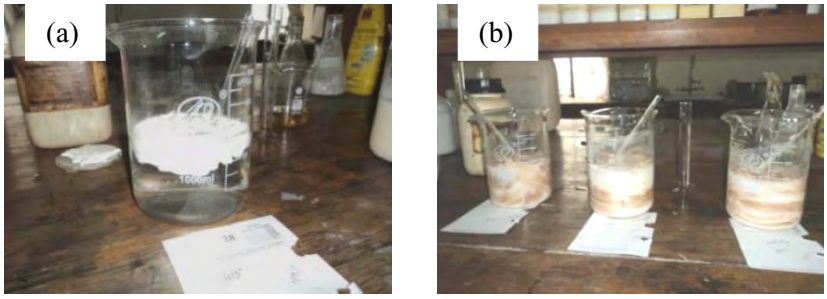

Figure 3.7: (a) Water retardant solution preparation and (b) soaking method of jute fiber for water retardant.

Table 3.3: Chemical composition of water retardant treatment.

Jute	**Liquor ratio**	**Acetic acid**	**$MgCl_2$**	**10% WR**		**15%WR**		**20%RR**	
50g	0.048611	2-1 drop	10g/l	PVC	Perapert	PVC	Perapert	PVC	Perapert
				50g	10g	150g	10g	100g	10g

3.6 Characterization of Single Fiber

3.6.1 Tensile Properties

Tensile testing was carried out using an Instron universal testing machine (Model no 3369) by varying span length (5 mm, 15 mm, 25 mm and 35 mm (Figure 3.8). The cross-head speed and load cell used were 5 mm/min and 5N respectively.

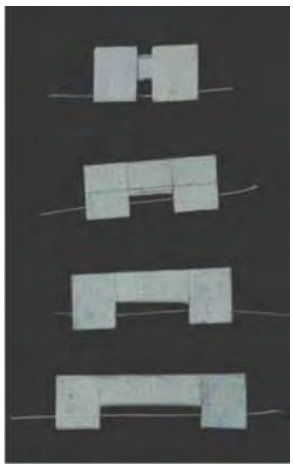

Figure 3.8: Sample preparation of tensile test.

Specimen Preparations and Measurement

a) At first, single treated and control jute fibers from top, middle and bottom portions were chosen randomly, which were cut down to a particular length.
b) The diameter of single fiber was measured using a scanning electron microscope (SEM).
c) The fibers were stacked between two paper frame (Figure 3.8) to conform good gripping to the clamps of test machine and to provide straight direction during test. This paper frame was clamped in the machine jaws and cut the paper frame carefully before the start of the test at room temperature and humid conditions.
d) The crosshead speed was maintained at 5mm/min. and 5 N load cell was used.

The tensile strength was calculated using these following formulas

Tensile Strength, $\sigma = \frac{F_{max}}{A}$ (3.1)

Where,

F_{max} = Maximum force.

A = Cross sectional area.

Cross sectional area $A = \pi \left(\frac{d}{2}\right)^2$ (3.2)

Where

d = diameter.

Young's modulus was measured from the stress/strain curve.

3.6.2 Fourier Transform Infra-Red (FT-IR) Spectroscopy

The wave response properties of the control (top, middle and bottom) and treated jute (rot, fire and water retardant) jute fiber were characterized by FT-IR using a Digital Fourier Transform Infrared spectrophotometer, Model Nicolet-380, USA using a technique of Attenuated Total Reflectance (ATR). The analyses were run using the KBr pellet technique. The mixture was pressed and molded into a flat sheet by hydraulic press. The spectrum was obtained after placing it into the FTIR machine. The transmittance range of scan was 370 to 4000 cm^{-1}. FTIR spectroscopy works by shining infrared radiation on a sample and observing which wavelengths of radiation in the infrared region of the spectrum are absorbed by the sample. Each compound has a characteristic set of absorption bands in its infrared spectrum. Characteristic bands found in the infrared spectra of jute and chemically treated jute fiber was detected.

3.6.3. Morphological Study

Scanning Electron Microscopy (SEM)

The morphological properties were observed by using a scanning electron microscope (XL 30 Philips, Netherland). Very Small portion from each one of the sample was cut and placed on the sample holder. Since treated and control jute samples are not conductive, the samples were needed to be made conductive. It was done by applying a gold coating sputtering technique. The thin gold coating caused the electron to interact with the inner atomic shells of the sample.

Atomic Force Microscopy (AFM)

Topographic images were recorded on an atomic force microscope (AFM) at Cincinnati University; model NanoScope IV[110], from Digital Instrument. Measurements were performed in air on dry film using tapping mode with a silicon tip having a 280 kHz tuning frequency. To measure the thickness of the film using the AFM, a scratch was initially made on the silicon wafer with a sharp pair of tweezers. The AFM image of the step edge allowed the later measurement of the thickness.

3.6.4 Thermal Properties

Thermo Gravimetric Analysis (TGA)

Thermo-gravimetric analysis was carried out on 8-10 mg treated and control jute fibers at a heating rate of 5° C/min in a nitrogen atmosphere using a Thermo-gravimetric Analyzer (TA Instrument SDT Q50). Chemically treated and control fiber were subjected to TGA in high purity nitrogen under a constant flow rate of 5 ml/min, sample purge flow of 60ml/min and balance purge flow of 40 ml/min Thermal decomposition of each sample occurred in a programmed temperature range of 30-450°C. The continuous records of weight loss and temperature were measured and analyzed to determine the following: thermal degradation rate (% weight loss/min), derivative weight loss (Figure 3.9 (a)) initial degradation temperature, 10% and 50% weight loss temperature and residual weight at 450°C.

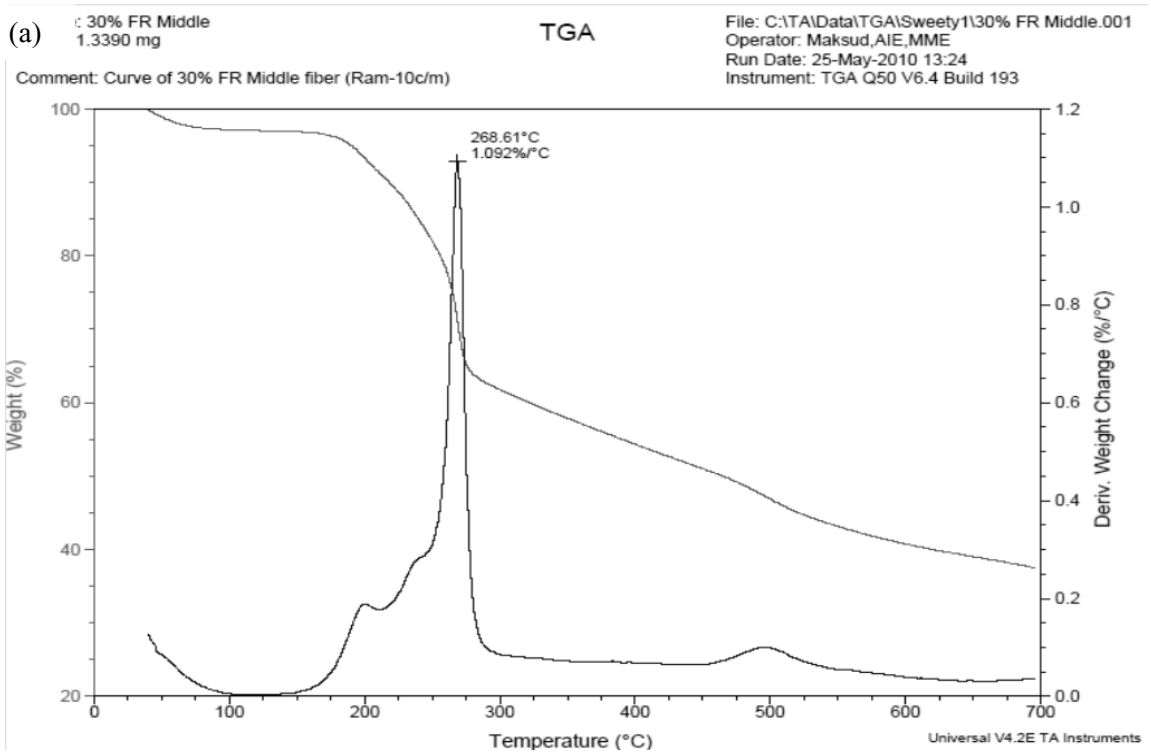

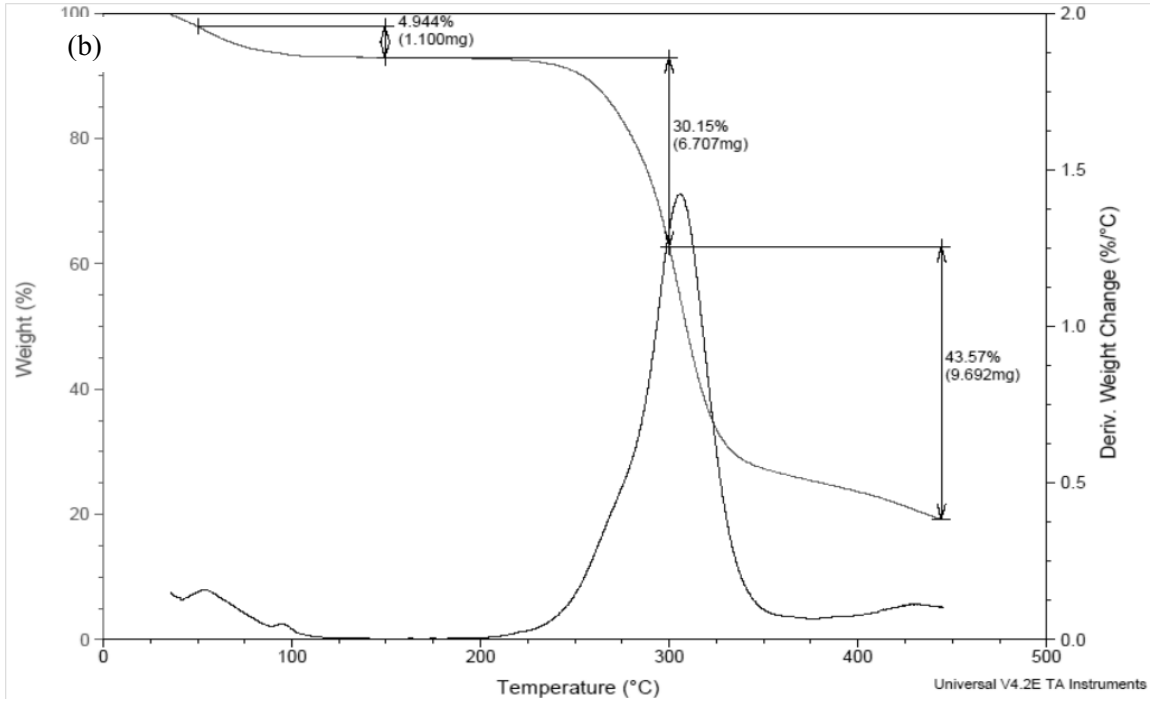

Figure 3.9: (a) Derivative weight percentage determination and (b) weight change of sample at different temperature.

Differential Scanning Calorimetry (DSC)

Differential scanning calorimetric analysis provides a rapid method for determining fiber/polymer crystalinity based on the heat required to melt the polymer. All differential scanning calorimetric (DSC) measurements were made on a DSC Q10 (TA instrument) thermal system using a sealed aluminum capsule. Each test specimen was weighed to about 7-8.5 mg. Each sample was held at a single heating rate of 5°C/min and scanning temperature from 30-600°C. Each of the data reported represents an average of three runs. Glass transition temperature T_g, melting temperature T_m, melting onset temperature (Figure 3.10 (a)), melting peak temperature and enthalpy (Figure 3.10 (b)) was measured and presented in the result and discussion section [111, 112].

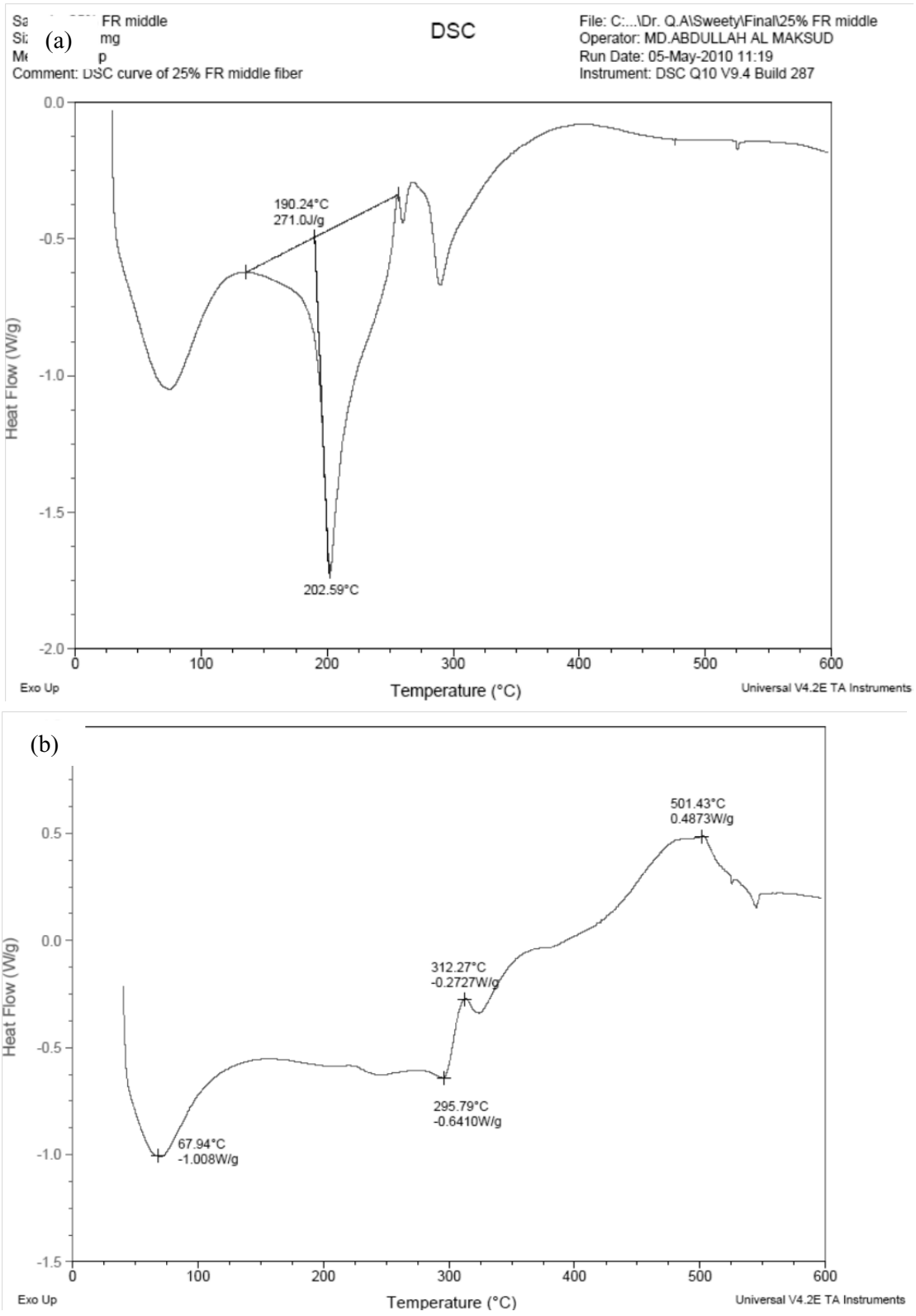

Figure 3.10: (a) measurement of enthalpy and (b) Peak temperature from DSC Curve.

3.6.5 Moisture Absorption

Moisture absorption study of control and treated jute fiber were determined by a change in mass method in accordance with BS EN ISO 62: 1999 [97]. The specimens were dried in an oven at 50°C and were allowed to cool to room temperature in desiccators before weighing them to the nearest 0.1 mg. This process was repeated until the mass of the specimen reached a constant value. Water absorption tests were conducted by immersing the fiber specimens in distilled water, 10% HCl and 10% NaCl (Figure 3.11) solutions in a beaker for different time at room temperature. Samples were periodically taken out of the solutions, wiped with tissue papers, reweighed and reemerged in the solution. The specimens were reweighed to the nearest 0.1 mg within 1 min of removing them from the water. The moisture absorption was calculated by the weight difference. The percentage weight gain of the sample was measured at different time interval. The process was carried out till equilibrium was established. The percentage of water absorption was calculated by weight difference between the samples immersed in water and the dry samples using the following equation [113].

$$\Delta M(t) = \frac{m_t - m_0}{m_0} \times 100 \qquad (3.3)$$

Where,

m_t = the weight of the specimen after immersion in the solution

m_0 = initial weight of the specimen

• $M_{(t)}$ = water absorption

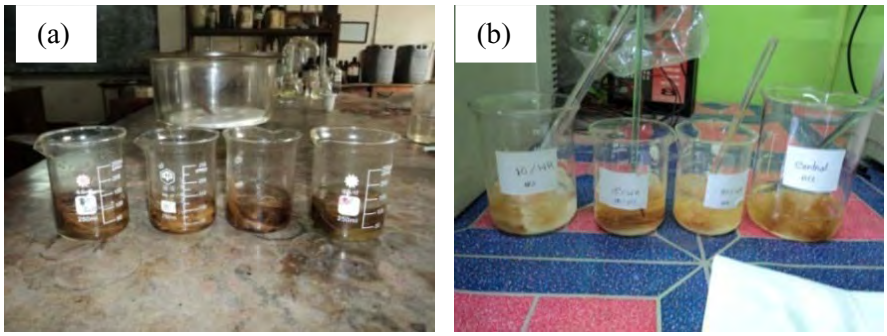

Figure 3.11: Water Absorption test at (a) distilled water and (b)10% HCl of different sample.

3.6.6 Contact Angle Measurement

To realize the concentration of the chemical on the fiber surface, droplet shape and size were measured. This was done by photographing droplets of liquid on treated and control jute fibers using a 12.1 Mega pixel, 4X Optical zoom, 28mm wide angle lance, SONY CORP, digital still camera, Model no .- DSC-W310. One drop was applied to the substrate using syringe. Three liquids were used to characterize the liquid droplets [114]

a) distilled water,
b) acetone,
c) glycerol

3.6.7 X-Ray Diffraction Test

To determine crystallinity, a Norelco type 120-101-85 Philips electronic diffractometer with nickel filtered copper K• was used. It had radiated at an operating voltage of 40 kV and a filament current of 30 mA. The measurements were conducted at 30°C and 65% relative humidity by taking finely chopped and pressed in tablet form (Figure 3.12) samples. The degree of crystallinity was determined by comparing the crystalline areas of the samples with that of ramie [7-9]. Jute polymers are not highly absorbing to x-rays. The dominant experiment is a transmission experiment where the x-ray beam passes through the jute and treated jute sample (Figure 3.12).

Figure 3.12: Sample for XRD.

X-ray diffraction data were collected from the Equatorial diffraction profiles using 5 step15 steps scanning (2•), Method- "Top of smoothed peak", fiber diagram. A wide angle diffractometer equipped with a scintillation counter. Linear intensities were

recorded between 10º and 65° (2• -angle range) at 25°C. The crystalinity index (I_c) was determined by Segal empirical method as equation 3.4[4].

$$I_c = \frac{I_{002} - I_{am}}{I_{002}} \times 100 \quad (3.4)$$

Where $I_{(002)}$ = counter reading at peak intensity at a 2• angle close to 22º and

$I_{(am)}$ = amorphous counter reading at a 2• angle of about 18º

3.7 *Characterization of Composite*

3.7.1 MAgPP Resin Collection

MAgPP resin was collected from Belgium. Measured Young's modulus, tensile strength and density of the resin are 1.17GPa, 20.38MPa and 0.86 g/cc respectively.

3.7.2 Determination of Fiber Volume Fraction

Maleic Anhydride Grafted Polypropylene (MAgPP) was collected from Belgium. The fiber volume fraction was measured after prepared composites by using the following equation

$$V_f = \frac{\rho_m \times W_f}{\rho_f \times W_m + \rho_m \times W_f} \quad (3.5)$$

Where,

ρ_m = density of matrix

W_f= weight of fiber

ρ_f= density of fiber

W_m = weight of matrix

3.7.3 Fabrication of Composites

Three types of 4mm directional short jute fiber composites were manufactured using maleic anhydride grafted PP at varying fiber weight percentage (20%, 25%, 30%), using hot press machine (Figure 3.13). Manufacturing steps are given below:

a) At first middle portion of control and treated jute fiber was weighted according to the required weight percentage needed. The fibers were chopped into approximately 3mm length and oven dried at 105°C±3°C for 6 hours.

b) Sufficient amount of maleic anhydride was taken on a beaker and weighted. To prevent voids, water bubbles, poor fiber matrix adhesion the polypropylene was dried in an oven at about 100±3°C for 3 hours.

c) Jute and MAgPP were heated at 120 °C (Figure 3.14 (a) and (b)) to mix the jute with MAgPP.

d) Mould surface was cleaned very carefully and Frekote FRP90-NC polymer mould release agent was sprayed over the mould surface for the easy removal of the product. Teflon sheet and waxy cloth were also used for easy removal of the product.

e) The female mould with a mixture of short fiber and MAgPP was covered by a male mould and teflon sheet.

f) Plates were placed in hot pressing machine (Figure 3.15) under 160°C temperature and 40KN pressure for about 15 minutes. Finally at 185 °C, 30KN pressure was applied for 10 minutes. Then the system was cooled slowly using water cooling system.

g) At last the specimen (Figure 3.16) was carefully discharged from the mould. The composition of the jute and MAgPP is given in the Table 3.4.

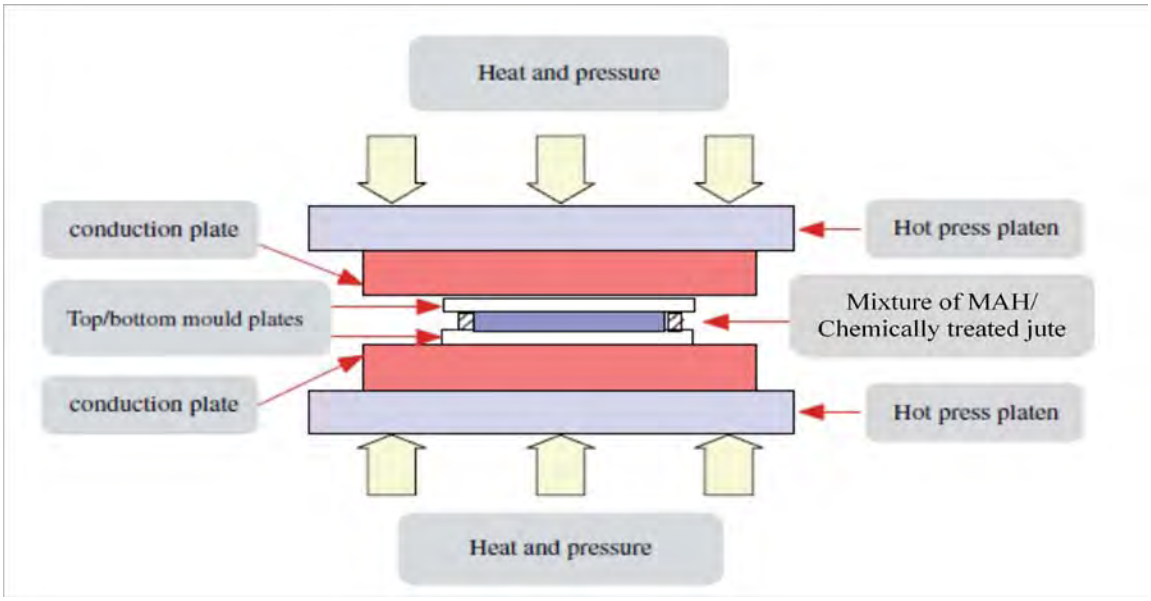

Figure 3.13: Schematic of the composite consolidation.

Figure 3.14: Jute composite production process (a) treated and control jute and MAgPP heated (b) heated sample and (c) mixture placed on the mould.

Figure 3.15: Hot pressing machine.

Table 3.4: Sample designation and composition of ingredients used in the study.

Sl. No.	Sample (Designation)	Composition by wt.%	
		MAgPP	Fiber
1	MAgPP	100	-
2	20%RRM/MAgPP	70	30
3	20%FRM/MAgPP	70	30
4	15%WRM/MAgPP	70	30
5	Jute M/MAgPP	70	30
6	20%RRM/MAgPP	75	25
7	20%FRM/MAgPP	75	25
8	15%WRM/MAgPP	75	25
9	Jute M/MAgPP	75	25
10	20%RRM/MAgPP	80	20
11	20%FRM/MAgPP	80	20
12	15%WRM/MAgPP	80	20
13	Jute M/MAgPP	80	20

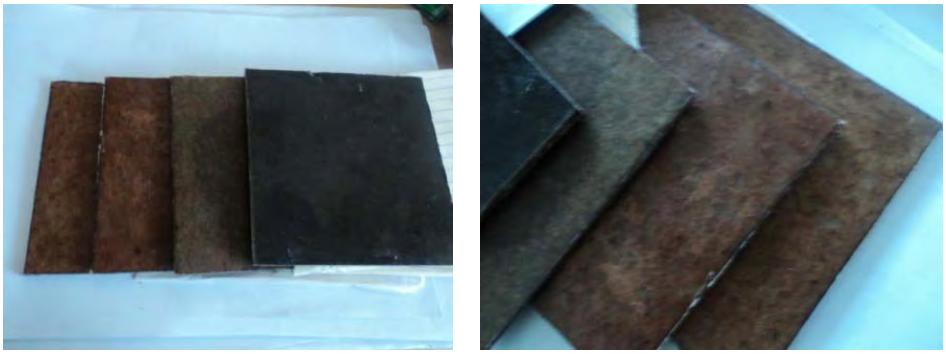

Figure 3.16: Different types of perpared composites.

3.7.4 Mechanical Characterization of Composites

Tensile Test

Test specimens of required shape were cut from the composite part. Tensile properties as determined by the test method helps to know the stress of the composite specimen (Figure 3.17), their fracture characteristics under tensile load, load strain behavior bearing properties of fiber and the matrix materials. At least three samples were tested for each specimen and a load cell of 30kN was used during the test.

The following steps were performed during tensile test (ASTM D 638-01) [115].

a) The test machine was calibrated
b) Dimensions of the specimen were taken
c) Cross head speed was set 3 mm/min
d) The tensile strength were measured by

$$\sigma = \frac{Load}{width \times thickness} \qquad (3.6)$$

e) The ultimate tensile strength (UTS), modulus were calculated from the following formula-

$$UTS = \frac{Maximum\ Load}{Initial\ Area} \qquad (3.7)$$

$$\sigma = \frac{P_{max}}{A} \qquad (3.8)$$

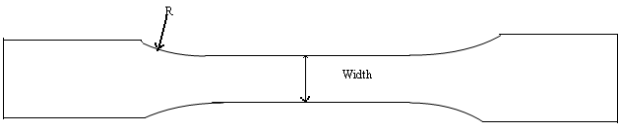

Figure 3.17: Tensile test specimen.

Impact Test

The impact test is a standardized high strain-rate test which determines the amount of energy absorbed by a material during fracture. This absorbed energy is a measure of toughness of a given material. The standard sample dimension is shown in Figure 3.18. The impact energy was calculated using the following equations [116].

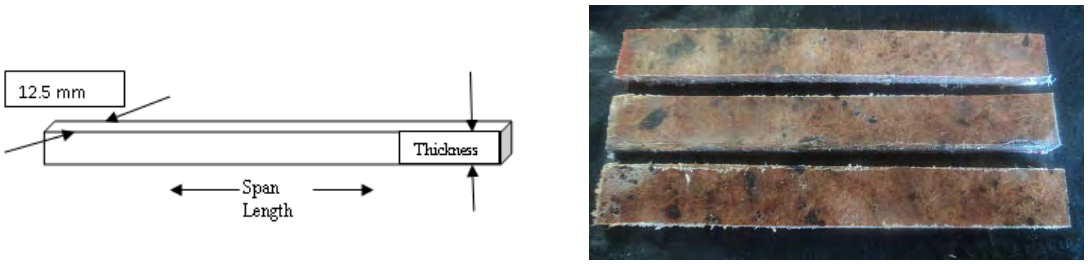

Figure 3.18: Impact test specimen.

$$\text{Average impact energy } \left(\frac{\text{kJ}}{\text{mm}^2}\right) = \frac{\text{Impact (J)}\times 1000}{\text{width (mm)}\times\text{thickness (mm)}} \qquad (3.9)$$

Flexural Test (3PBT)

The three-point bend test was carried out by universal testing machine. The flexural test specimen (Figure 3.19) was prepared according to ASTM D 790-98 [117]. It says that, "the depth of support span shall be 16 times the depth of beam. Specimen width shall not exceed one fourth of the support span for specimens greater than 3.2 mm in depth".

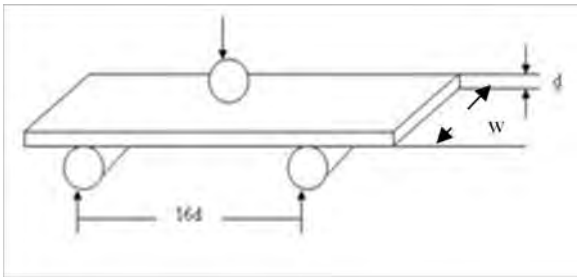

Figure 3.19: Flexural test dimension.

Five specimens of each composite were tested and the average values were reported. The load displacement curves were obtained from the electronic chart recorded and the maximum (peak) load values were also recorded by the instrument, which were recalled after the completion of the test.

The following procedure was performed to carry out the test:

a) The test machine was prepared
b) Dimension of the specimens were taken
c) The rate of cross head motion was calculated using the following formula

$$R = \frac{ZL^2}{6d} \quad (3.10)$$

Where,

R = rate of cross head motion mm/min

d = depth of beam, mm

Z= rate of straining of the outer fiber which was set at 0.01

d) The loading nose and supports were aligned in such a way that the axis of the cylindrical surfaces was parallel and the loading nose was midway between the supports.
e) The load was applied to the specimen at the specified cross head motion and simultaneously load deflection data was taken.
f) The test was terminated when rupture occurred at the outer surface of the test specimen.
g) The flexural stress was calculated by using of the following equation:

$$\sigma_f = \frac{3PL}{2bd^2} \quad (3.11)$$

Where,

- $_f$ = stress in the outer fibers at mid point, MPa

P = load, N

L = support span, mm

b = width of beam, mm

d = depth/ thickness of beam, mm

h) Flexural strain $\varepsilon_{3pB} = \frac{6Dd}{L^2 * 100}$ (3.12)

Where,

D = elongation, mm

i) Flexural modulus, $E_B = \frac{L^3 m}{4bd^3}$ (3.13)

Where,

m = slope of linear portion of load-deflection curve.

The crosshead speed and depletion were calculated using the following equations

$$Deplection = \frac{0.05L^2}{6d} \quad (3.14)$$

$$Speed = \frac{0.01L^2}{6d} \quad (3.15)$$

3.7.5 Water Absorption Test

The effect of water absorption on jute fiber reinforced composites was investigated in accordance with ASTM -570 -02:1999 [118]. The specimens were cut into 76.2 mm X 25.4 mm dimension, dried in an oven at 50 °C and were allowed to cool to room temperature in desiccators before weighing them to the nearest 0.1 mg. This process was repeated until the mass of the specimen reached a constant value. Water absorption tests were conducted by immersing the specimens in distilled water in a beaker for different time at room temperature. Samples were periodically taken out of the solutions, wiped with tissue papers, reweighed and reemerged in the solution. The specimens were reweighed to the nearest 0.1 mg within 1 min of removing them from the water. The process was carried out till equilibrium was established. The percentage of water absorption was calculated by using equation 3.3.

Chapter 4

Results and Discussion

Fiber Characterization

4.1 Introduction

Control and chemically treated fibers were characterized using tensile, thermal and structural testing. Tensile properties of control, rot, fire and water retardant treated single jute fibers of span length of 5 mm, 15 mm, 25 mm and 35 mm from top, middle and bottom portions were measured by Universal tensile testing machine. Thermal properties were measured by Thermo gravimetric analysis (TGA) and differential scanning Calorimetric (DSC), structural properties were determined by scanning electron microscope (SEM), X-ray diffractometry (XRD), Fourier transform infrared (FTIR) spectroscopy and atomic force microscopy (AFM).

4.2 Tensile Properties of Control Jute Fiber

The tensile properties of control jute fiber are shown in Figure 4.1. From the figure, it seems that the middle portion had higher Young's modulus, tensile strength and strain to failure compared to the top and bottom portions. The fiber of bottom portion is over mature and their surface is rough, however the middle portion contain smooth surface compared to the bottom portion due to sufficient amount of cellulose and lignin. On the other hand the top portion fibers are immature to bear the load and contain low amount of cellulose. Another important thing is that the bottom portion contains more defects and non homogeneities compared to the middle and top portion. As mentioned by Bledski and Gassan [118], the longer the stressed distance of the natural fiber is, the more non homogeneities and defect points will be in the stressed fiber segment, weakening the structure. Thus strength and strain to failure decreased with increasing span length. However the situation is reverse for Young's modulus. The Young's modulus increased (Tables A.1 and A.2) with increase in span length**.** The strength decreased with span length due to the presence of more flows and defect in longer span length fiber that make the probability of failure larger. Fibers with longer span length have larger surface area, which indicates more surface defects as compared to short span length.

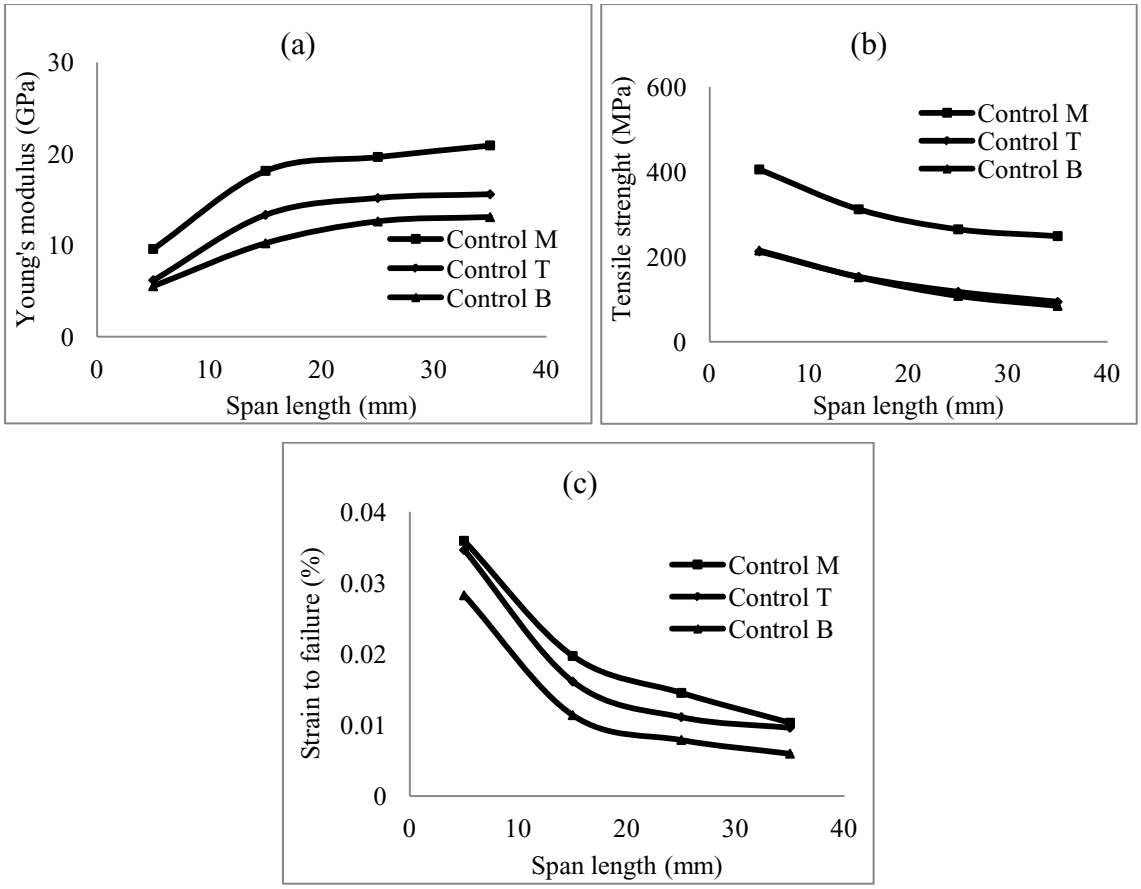

Figure 4.1: (a) Young's modulus (b) tensile strength and (c) strain to failure of three portions of control single jute fiber.

The Young's modulus decreased by 25% and 37.48% in case of top and bottom portion compared to the control middle portion. The tensile strength decreased 66% in case of top and bottom portion compared to the middle portion. This is due to more pores present in case of bottom portion and immaturity of top portion fiber.

4.2.1 Correction of Tensile Properties

During test s ome s lippage por tions always o ccur. Large s pan length mini mizes the slippage portion more compared to smaller ones. Thus Young's modulus found higher for larger span length which was not desired. So correction is required for Young's modulus. Young's modulus can be corrected by using the following steps [16]:

1. $\bullet_i = \bullet L_{total} / F - L_0 / E_0 . A_i$ (4.1)

2. $\bullet L_{\mathbf{total}} / F = \bullet . L_0 / \bullet . A_i = 1 / E . L_0 / A_i$ (4.2)

3. Strain correction

a) $\bullet L_{grip} / L_o = \bullet_1 (A_i . \bullet) / L_o$ (4.3)

b) $\bullet L_{fiber} / L_o$ (Corrected) = $(\bullet L_{Total} / L_o - \bullet L_{grip} / L_o)$ (4.4)

Where, α_i is machine displacement for each fiber, L_0 is original span length, E is the Young's modulus for each fiber, E_0 is extrapolated Young's modulus, A_i is cross-sectional area for each fiber, F is force, ε is strain and α is stress.

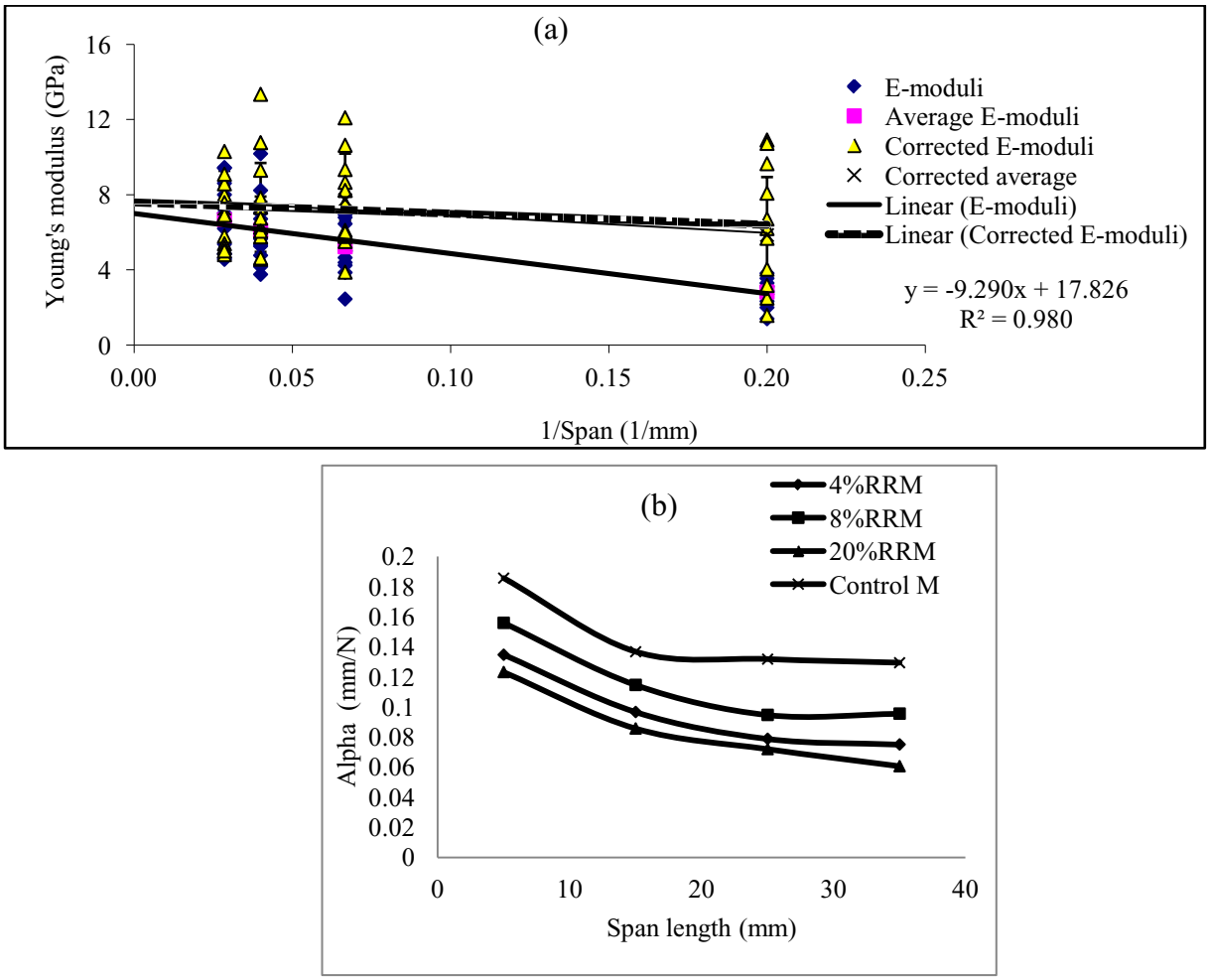

Fig 4.2: (a) Correction of single fiber Young's modulus and (b) span length effect on machine constant.

Due to slippery portion of the tensile machine gripper, the Young's modulus changed with the change of span length. Figures 4.2 (a) and 4.3 show the corrected Young's modulus. The slippery portion is higher for smaller span length compared to higher span

(Figure 4.2 (b**)**. This is why strain to failure became higher and Young's modulus became lower at smaller span length.

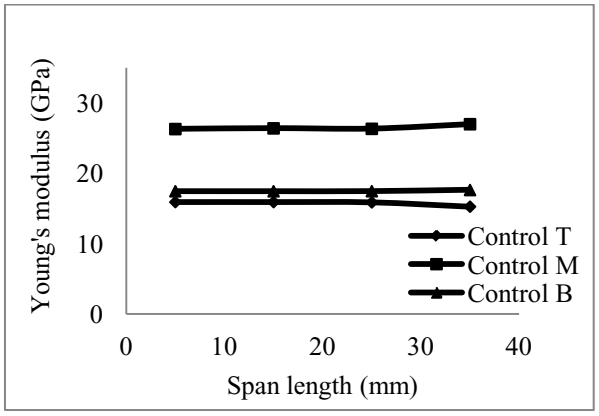

Fig 4.3: Corrected Young's modulus control single fiber.

After correction, (Figure 4.3) the Young's modulus became independent of span length. The tensile strength and strain to failure are fiber span length dependent property, so they need not to be correct by using these types of formula.

4.3 Results of Rot Retardant (RR) Jute Fiber

4.3.1 Tensile Properties

The uncorrected tensile test results of rot retardant (RR) and control fibers are mentioned in Appendix 1 (Tables A.3 and A.20) and shown in Figure 4.4. The tensile strength follows the decreasing trend because the lower testing span length was much affected by fiber properties and machine parameters. It is observed that tensile strength of control jute fiber (middle portion) was higher than those of the rot retardant jute fiber. The strength of the rot retardant jute fiber decreased due to the decrease in crystalinity compared to the control jute fiber. The decreasing trend of the crystalinity is also concentration dependent.

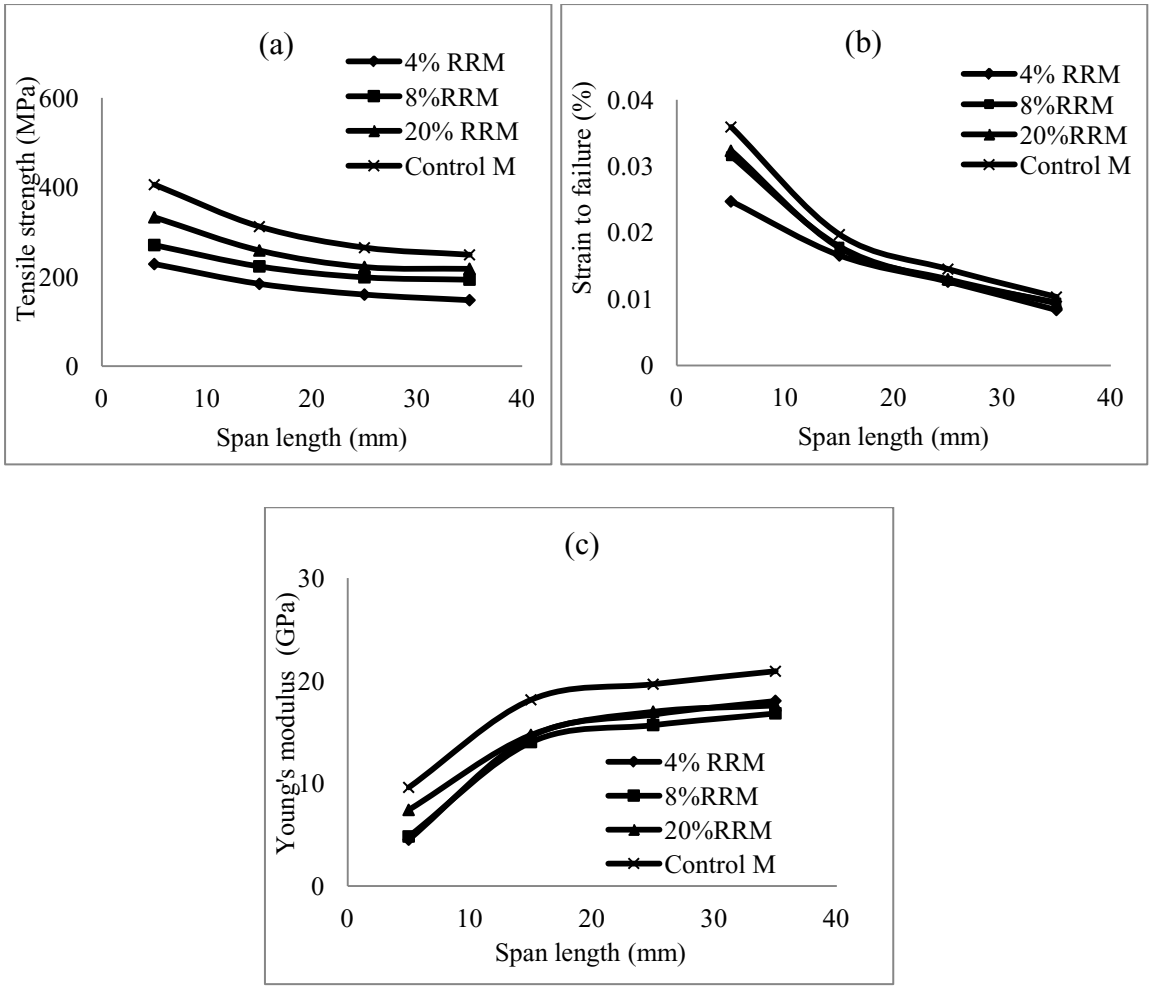

Figure 4.4: Uncorrected (a) tensile strength (b) strain to failure and (c) Young's modulus of RR single jute fiber.

Individually 4 %RR t op, m iddle a nd bot tom por tion e xhibited approximately s imilar results i n c ase of t ensile s trength p roperty (Figure 4.5 (a)). Similar r esults a re also observed i n c ase o f 8 %RR a nd 20% RR t op, middle a nd bot tom por tions jute f iber (Figures 4.5 (b) and (c)). The co ating property of t he r ot r etardant i s concentrations dependent. In case of 4%RR, the coating of the chemical is similar in case of top, middle and bottom portions. So their tensile properties became similar. Due to this, similar result were obt ained in c ase of 8% RR a nd 20% RR t op, m iddle a nd b ottom por tions individually.

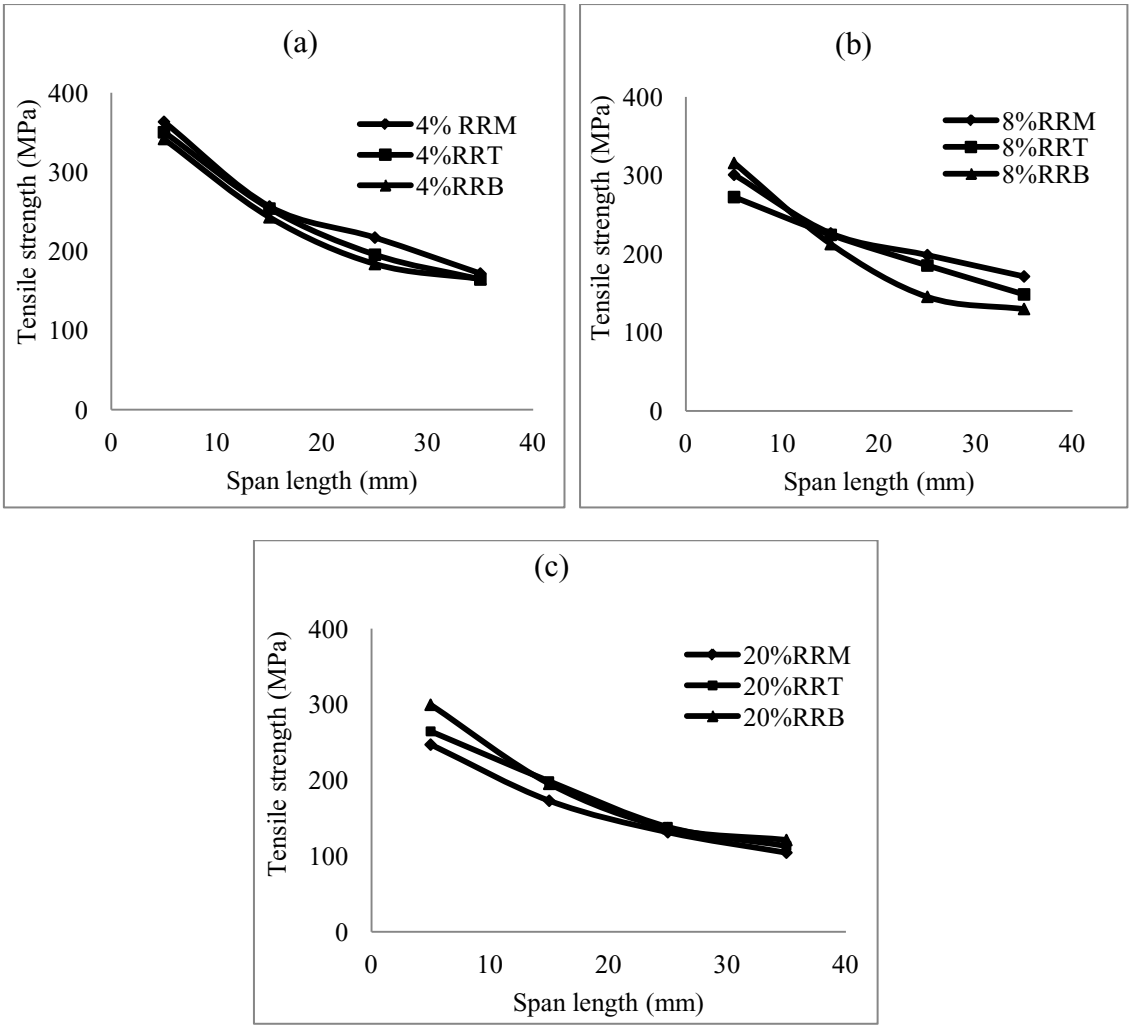

Figure 4.5: Uncorrected tensile strength of top, middle and bottom portions with (a) 4%RR, (b) 8%RR and (c) 20%RR concentrations.

An improvement has been observed in tensile properties of different portion rot retardant treated single jute fiber with respect to chemical concentrations. With the increase of chemical concentration, the tensile strength of middle portion jute fiber decreased more compared to the control fiber. The tensile strength increased in case of top and bottom portions compared to the control fiber (Figure 4.6). The tensile strength of RR middle portion decreased with the chemical concentration compared to the control middle portion due to the decrease of surface roughness and crystalinity with rot retardant chemical concentration.

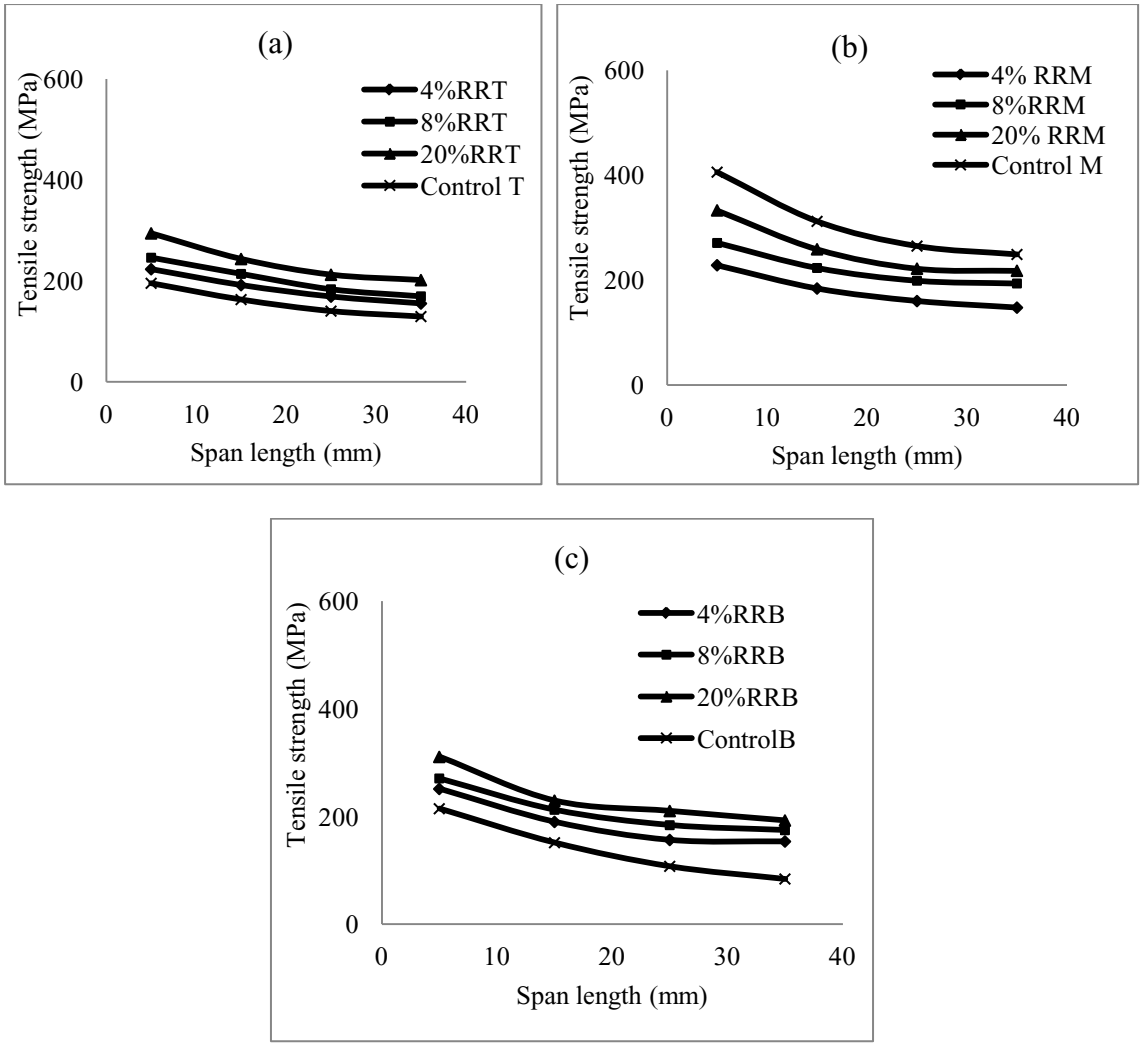

Figure 4.6: Tensile strength of (a) top, (b) middle and (c) bottom portion single rot retardant jute fiber.

The comparison of the Young's modulus of treated and control fibers are shown in the Figure 4.7. It is observed that top and bottom portion rot retardant treated jute fibers obtained higher Young's modulus compared to the control jute fiber. But it was reverse in case of middle portion (Figure 4.8 (b)). Due to the correction, it is also observed that the Young's modulus became span length independent.

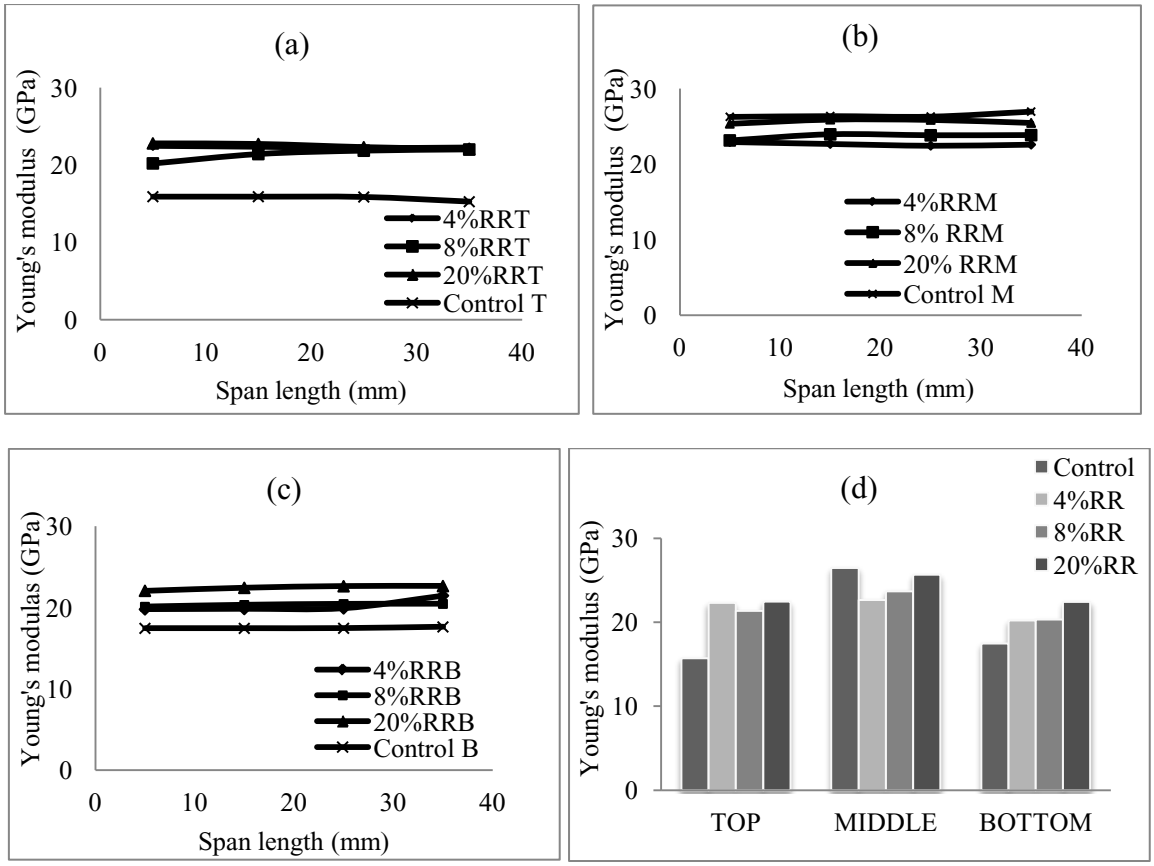

Figure 4.7: Corrected Young's modulus of (a) top, (b) middle, (c) bottom portion single rot retardant jute fiber and (d) comparison of Young's modulus of RR fibers.

The top, middle and bottom portion 4% RR, 8% RR and 20% RR treated jute fiber had Young's modulus in the range 20 -25 GPa. The middle portion had higher Young's modulus compared to the top and bottom portions. This may be due to the higher cellulose content in the middle portion. After rot retardant treatment with different chemical concentration, the Young's modulus of top, middle and bottom became approximately similar (Figure 4.7 (d)). Where as the middle portion of control jute fiber had higher Young's modulus compared to the top and bottom portions.

After rot retardant treatment, the strain to failure became quite similar for different concentrations. With increase in concentration of chemical, the strain to failure increased (Figure 4.8 (c)) compared to the control fiber in case of bottom portion. The increase of strain to failure with the chemical concentration may be due to the increase in amorphous

component of jute fiber [104]. However in the case of top and middle portions (Figures 4.8 (a) and (b)), the strain to failure decreased compared to the control fiber.

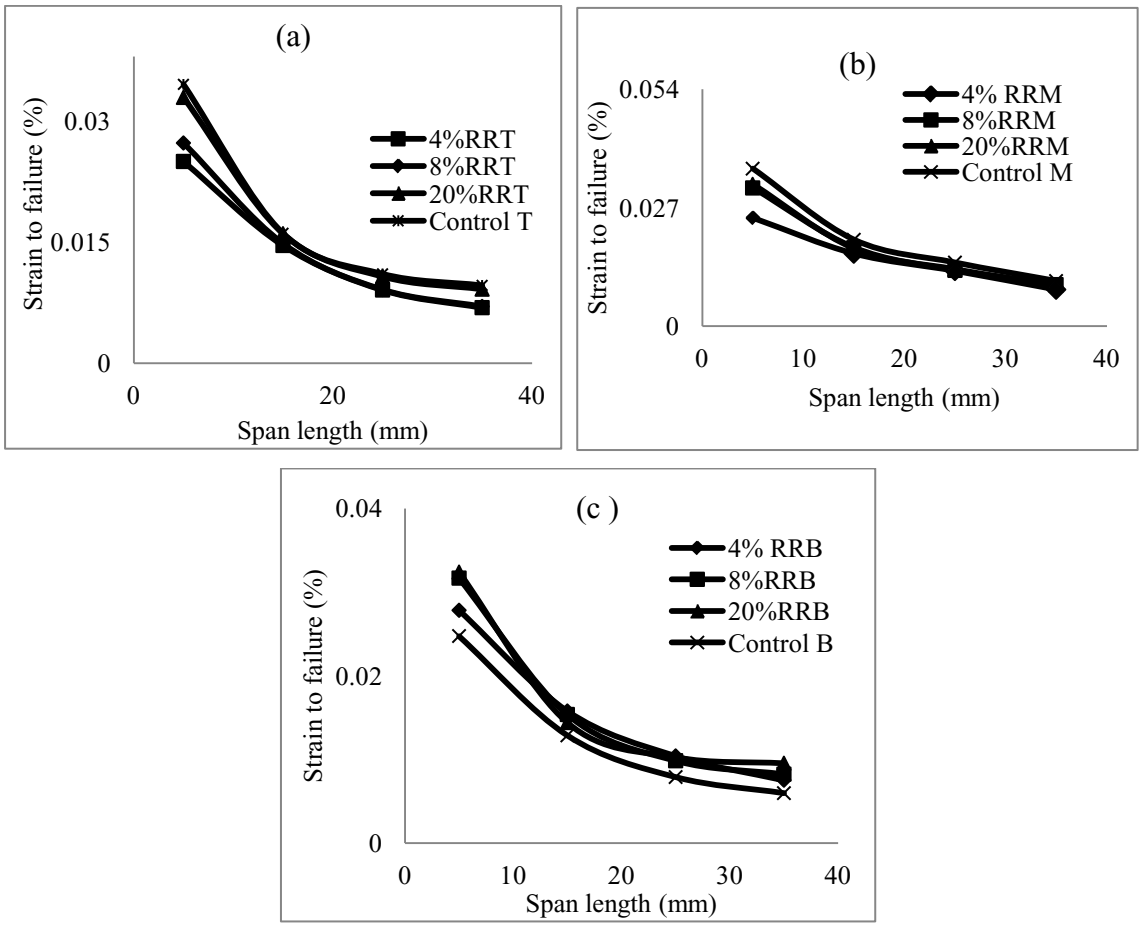

Figure 4.8: Strain to failure of (a) top, (b) middle and (c) bottom portions rot retardant jute fiber.

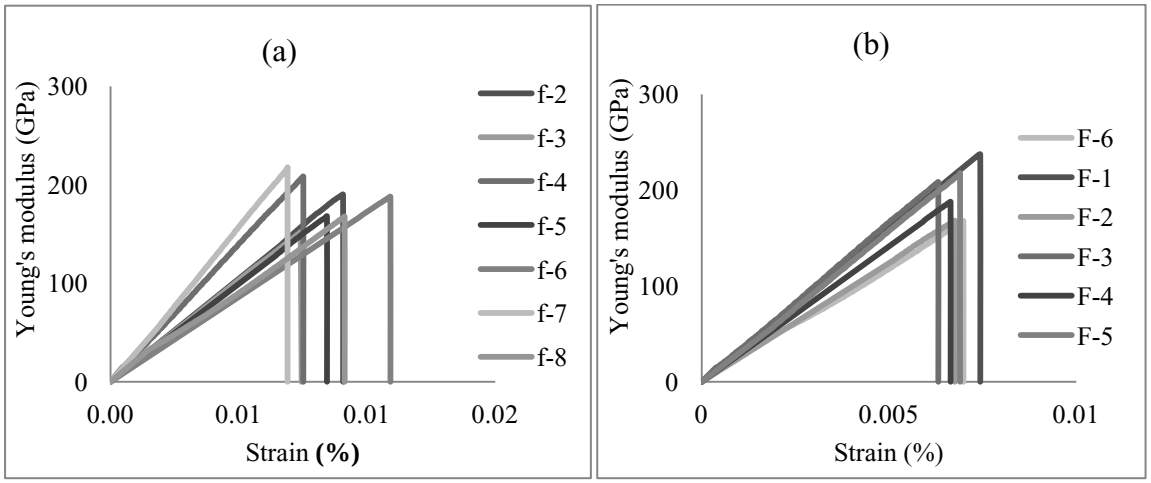

Figure 4.9: Corrected Young's modulus for (a) 5mm and (b) 35mm span length.

Corrected Young's modulus for 5mm and 35mm has been shown in Figures 4.9 (a) and (b) respectively. The slopes (Figure 4.9) were not similar due to non homogeneity of natural fiber.

Copper (Cu) content was measured due to variation of mechanical properties for control and rot retardant jute fiber. The Cu content of the rot retardant middle portion jute fiber was higher compared to the top and bottom portion as shown in Figure 4.10 (a). With increasing chemical concentration, the Cu content increased linearly (Figure 4.10 (b)) because the adsorption of Cu was pH dependent. The adsorption increased as the pH increased from 2 to 5. However, Cu adsorption was still excellent at pH 2.0. Due to coating of Cu on the treated fiber, the mechanical properties changed. At 30%RR, the Cu content did not increase compared to 20%RR. That is why the 20%RR was used due to cost effectiveness.

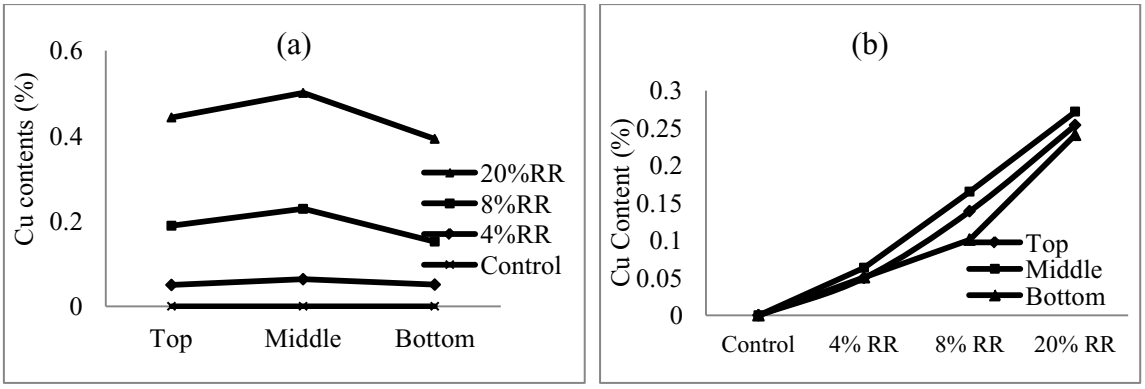

Figure 4.10: Copper (Cu) content of jute fiber at (a) different portions and (b) various chemical concentrations.

4.3.2 FTIR Spectroscopic Analysis

Both control and rot retardant jute fiber were characterized by FTIR using attenuated total reflectance (ATR) scanning to confirm the chemical reaction between $CuSO_4$ and cellulose backbone of jute fiber. The results of the spectra as depicted by the transmittance versus the wave number are presented in Figure 4.11 for the range of 4000-700 cm^{-1}. Broad peak appeared in the range of 3600-3200 cm^{-1} wavelength due to strong bond formation between cellulose, hemicelluloses and lignin of the jute and chemical [122]. A distinguished transmission peak is also observed at around 3600-4000 cm^{-1} in

case of 8% RR and 20% RR jute fiber due to noise. New absorption bands are found at 2100-2300 cm^{-1}[123]. The absorption shifts are concentration dependent [124]. The O-H bond shifted right wards and became wider due to other retardant chemical concentration. This fact confirms that SO_4/CO_3 group of $CuSO_4$/ $NaCO_3$ reacted with cellulose. The intensity of the O-H peak increased with the RR chemical concentration. Higher absorption is observed in the region around 3400 cm^{-1} for the unmodified jute moss over the 20% rot retardant (RR) jute fiber since more hydroxyl groups were present. The observed transmittance peak with the wavelength is given in Table 4.1 and the shifting of the same peak is shown in Table 4.2.

Table 4.1: Related FTIR peak of the control jute fiber [7, 122].

Band position (cm^{-1})	**Functional group**
~3600-3200	•(OH) broad, strong band from the cellulose, hemicelluloses and lignin of jute
~3450–3400	O–H alcohol
~3000-2900	•(C-H) in aromatic ring and alkenes
~2930–2910	C–H methyl and methylene groups
~1740–1730	C=O carbonyls
~1750-1710	•(C=O) most probably from the lignin and hemicelluloses
~1650-1630	Possibly aromatic ring
~1640–1618	C=C alkenes
~1630-1642.6	Probably absorb water
~1515–1504	•(C=C) aromatic in plane
~1501-1510	•(C=C) aromatic skeletal ring vibration due to lignin
~1462–1425	CH_2 cellulose, lignin
~1460-1468	•(C-H:C-OH) 1^o and 2^o alcohol
~1422-1428	•(C-H)
~1384–1346	C–H cellulose, hemicelluloses
~1365-1377	•(C-H)
~1315	•(C-H)
~1280	•(C-H_2) twisting
~1260–1234	O–H phenolic
~1170–1153	O–H alcohols (primary and secondary) and aliphatic ethers
~1155	•(C-C) ring breathing , asymmetric
~1112	•(C-O-C) glycosidic
~1055	•(C-O-C) 2^o alcohol
~1033	•(C-O-C) 1^o alcohol
~910	C=C alkenes
~895	•(C-O-C) in plane, symmetric

Table 4.2: Shifting of FTIR transmittance peak (cm^{-1}) of control and RR treated middle portion jute fiber.

Bond type	Control	4% RR	8%RR	20%RR
Intermolecular hydrogen bonding, O-H stretching	3415.9	3426.4	3411.7	3433.5
C-H stretching	2915.8	2915.8	2915.4	2917.8
Carboxylic anhydride	1736.2	1737.7	1738.0	1753.6
C-H bending	1376.3	1377.2	1371.6	1371.6
C-H bending	1247.2	1246.2	1249.3	1247.3
C-C Stretching	1034.3	1059.6	1060.4	1060.2

To distinguish all peaks in the rot retardant jute fiber is very difficult because of the weak transmission. The 1600 cm^{-1} band was found due to lignin [125].

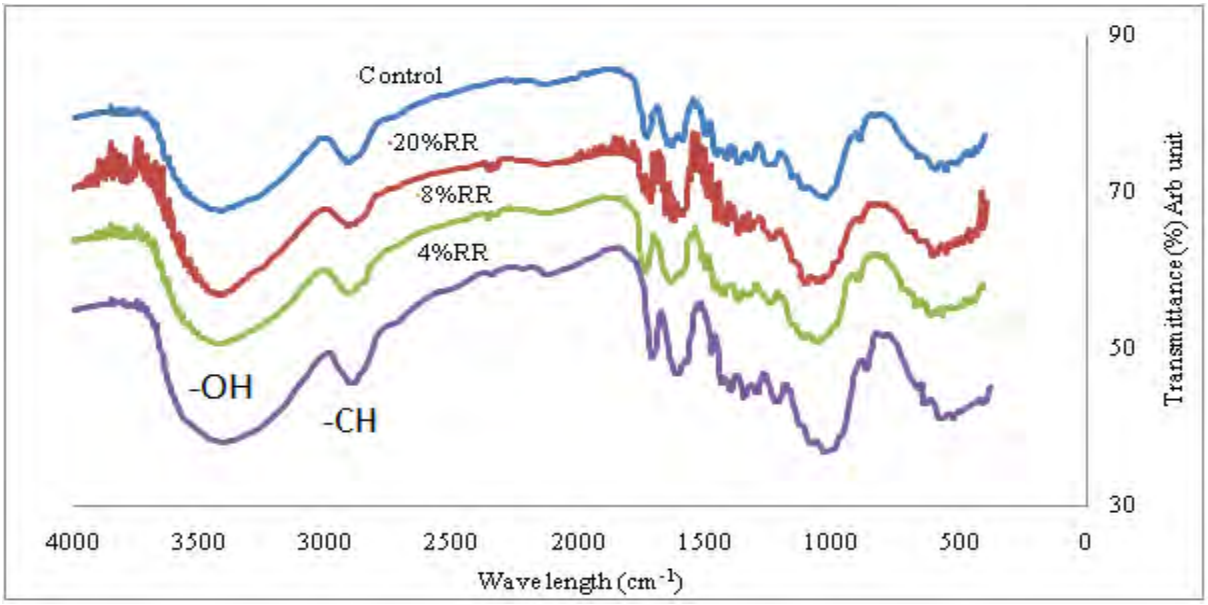

Figure 4.11: ATR- FTIR of control, 4%RR, 8%RR and 20%RR jute fibers.

4.3.3 X-ray Diffraction Analysis

The diffraction pattern of control fiber in Figure 4.13 (a) shows peaks only at 2theta =22.58, which is derived from cellulose I [126]. On diffractogram after rot retardant treatment, additional peak from cellulose were registered in case of 20%RR and merge in case of 4%RR. In Figure 4.12 (b), the X-ray diffraction pattern of top, middle and bottom portions 20% RR fibers are shown. As the concentration of $CuSO_4$ increased, x-ray diffraction of rot retardant fiber showed an overall decrease in crystalinity due to bond formation of O-H and rot retardant chemicals . This was attributed to the better packing

and stress relaxation of cellulose chains as a result of the removal of pectin and other amorphous constituents from the fiber [127]. The existing phase according to plane is not possible to explain due to insufficient peak.

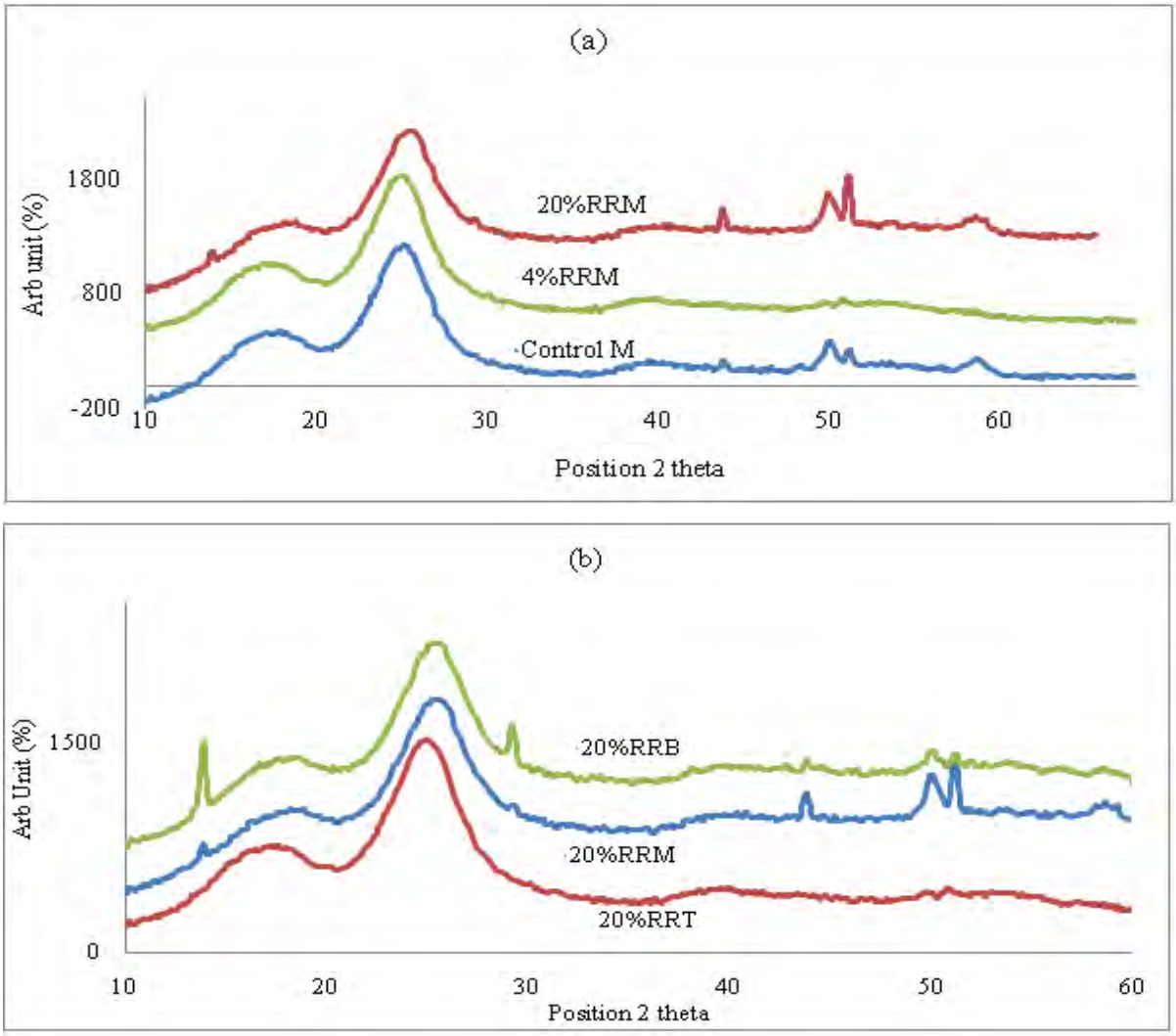

Figure 4.12: XRD of (a) different (%) rot retardant jute fiber and (b) 20%RR top, middle and bottom portion jute fiber.

The decrease in crystalinity obtained due to rot retardant jute fibers is thought to be the main contributing factor for the decrease in fiber strength. The degree of crystalinity of control fiber was 92.02%.

It can be observed that the major crystalline peak on each pattern occurred at around 2y ¼ 22.58°, which represents the cellulose crystallographic plane (002) [128]. The X-ray diffractograms hows that the intensity of the crystallographic plane (002) was as

significantly increased due to $CuSO_4$ treatment of the jute fiber. The crystalinity and proposed heat of fusion of the RR treated jute fibers is expressed in Table 4.3.

Table 4.3: Crystalinity and heat of fusion of the RR treated jute fibers.

Sample	18^0 Intensity	22^0 Intensity	Crystalinity (I_c) (%)	100% Crystalline jute	
				Heat of fusion (H_f)	Enthalpy (From DSC)
20%RRM	07.52	34.29	78.06	108.7622	84.91
4%RRM	100.00	47.00	-112.76	-70.4911	79.49
Control M	7.98	100.00	92.02	179.2002	164.9

The heat of fusion of 100% crystalline RR and control treated jute fiber jute is calculated as follows:

$$\Delta H_C = \frac{\Delta H_f}{X_c} \qquad (4.5)$$

Where,

- H_C= enthalpy of fusion
- H_f =100% crystalline materials enthalpy of fusion

X_C = crystalinity

4.3.4 Morphological Studies

Scanning Electron Microscopy (SEM)

Surface morphology of control fiber and rot, fire and water retardant treated jute fibers were observed by using scanning electronic microscope (SEM). Figures 4.13 and 4.14 represent surface morphology of top, middle and bottom portion control and rot retardant treated jute fibers. With the increase in chemical concentration, the surface become smoother as observed from the SEM images of Figure 4.13. Due to increase of coating properties with the concentration of $CuCO_3$, the treated top, middle and bottom portion of fibers gradually became smoother.

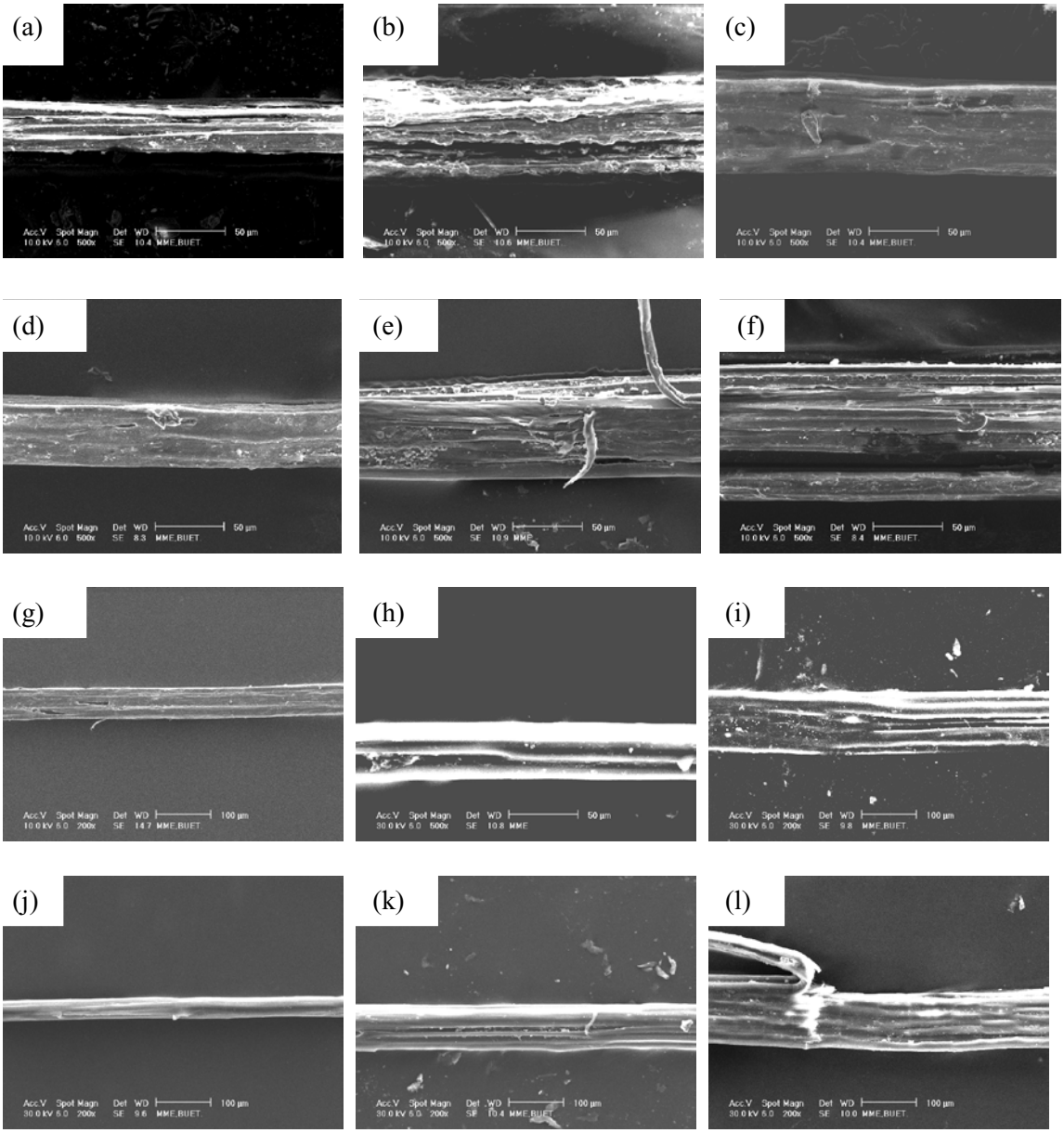

Figure 4.13: Surface morphology of (a, b, c) control; (d, e, f) 4%RR; (g, h, i) 8%RR and (j, k, l) 20%RR jute fiber. First, second and third columns are showing morphology of top, middle and bottom portion jute fiber respectively.

Control jute fiber surface was rough **(**Figure 4.14 (a)), which reduced the fiber strength. Jute fiber treated with $CuSO_4$ (Figure 4.14 (b)) had rather smoother surface and increased diameter as compared to the control jute fiber.

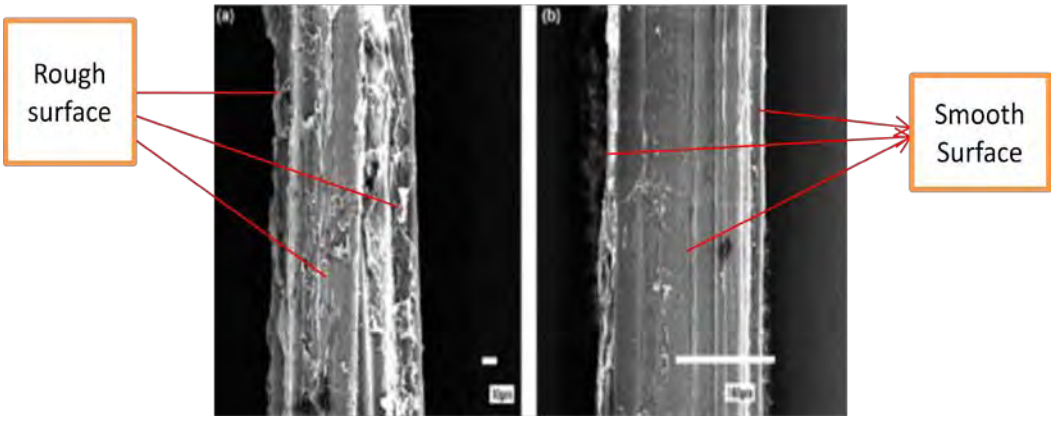

Figure 4.14: SEM micrographs of (a) control and (b) 20% RR treated jute fiber.

Atomic Force Microscopy (AFM)

The atomic force microscopic analysis shows that the surface roughness of fiber decreased with the employment of rot retardant treatment (Figure 4.15). Control jute fibers exhibited a rougher surface, whereas the rot retardant jute fibers exhibited smoother surface. This is considered as a proof for the surface coverage of the fibers with a coating layer resulting in decreased surface roughness.

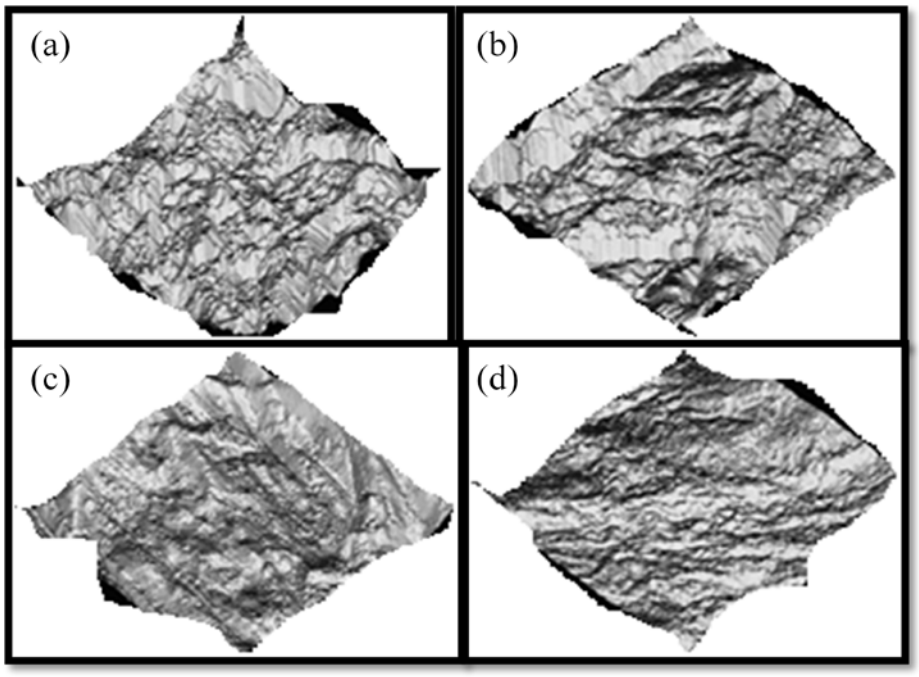

Figure 4.15: Atomic force microscope (AFM) topographic pictures of (a) control, (b) 4% RR, (c) 8% RR and (d) 20% RR jute fiber.

4.3.5 Thermal Properties

Thermo gravimetric Analysis (TGA)

From thermo-gravimetric analysis (TGA) curves of control and rot retardant jute fiber (Figure 4.16 (a)), it is seen that control fiber was stable up to 281°C, while rot retardant treated jute fiber was stable up to 265°C. TGA was used to monitor the fiber decomposition as a function of temperature. DTGA thermographs (Figure 4.16 (b)), clearly show main decomposition peaks for each sample. Control fiber had high derivative loss compared to the rot retardant fiber. After 350°C, mass loss followed the trend of 20%RR<8%RR<4%RR<Control. A small loss in mass occurred in the first stage when the fibers reached about 50-100°C. This is due to the loss of absorbed water. The TGA curve remained relatively flat until the main decomposition reaction occurred at about 225 to 275 ^{o}C in nitrogen. The main pyrolytic transformation occurred over a narrow temperature range (275-350°C) involving a substantial break-down of the main polymer network structure by a random scission process [119]. 10% and 50% weight loss [120] data are presented in Table 4.4. After rot retardant treatment, the weight change due to temperature, decreased compared to the control fiber. After rot retardant the residue is increased compared to control jute fiber due to volatile components coated by non volatile material.

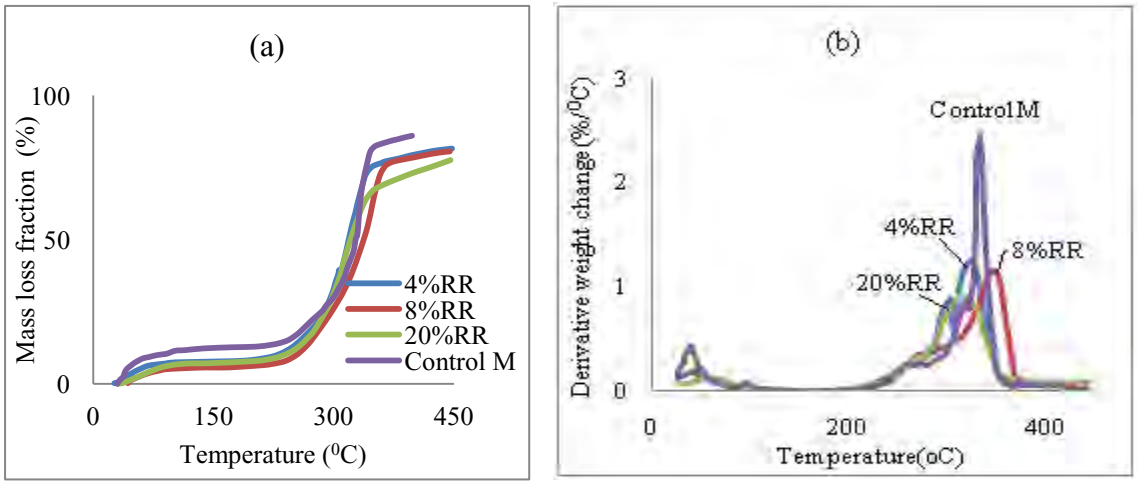

Figure 4.16: (a) TGA and (b) DTGA thermograph of control and rot retardant jute fiber.

Table 4.4: Residual, weight and derivative weight change at different temperature of control and RR jute fiber.

Sample Name	Weight change between 50-200°C (%)	Weight change between 200-350°C (%)	Weight change between 350-450°C (%)	Derivative weight change in temp (°C)	10% weight loss temp (°C)	50% weight loss temp (°C)	Residual weight (%)
4% RRM	4.443	67.26	5.952	323.33	228.84	319.48	18.35
8% RRM	4.713	57.88	16.46	347.65	235.44	337.67	19.50
20%RRM	6.097	59.23	10.15	313.43	236.05	321.42	20.09
Control M	5.926	17.20	55.81	332.85	76.31	327.10	13.96
4% RRC	5.720	28.09	43.37	346.58	245.73	340.35	21.14
8% RRC	5.443	55.74	18.03	350.40	253.44	339.58	19.50
20%RRC	5.357	59.04	14.16	345.06	255.04	334.56	20.75
Control C	6.815	55.23	17.31	347.35	246.82	341.09	18.80
20%RRT	4.039	45.43	33.07	355.88	269.65	349.01	12.79
Control T	1.205	62.02	15.79	346.26	269.85	335.01	17.08

Differential Scanning Calorimetric (DSC) Analysis

Differential Scanning Calorimetric **(**DSC) thermographs obtained from the control and rot retardant jute fibers exhibit both endothermic and exothermic transitions as shown in Figure 4.17 (a). The peak-temperatures appeared differently with respect to the sample conditions. The exothermic transition (upward peak) (Table 4.5) or melting temperature (Table 4.6) for control sample was 396.82 °C, while that for rot retardant jute fibers shifted to lower temperatures. On the other hand, the 1st exothermic peaks for the rot retardant jute fiber samples decreased and this change may be due to the presence of reactive groups in the rot retardant jute fiber. The appearance of both endo and exothermic peaks could be related to the possible morphological changes that occurred by the decomposition of hemi-cellulose and cellulose respectively [119].

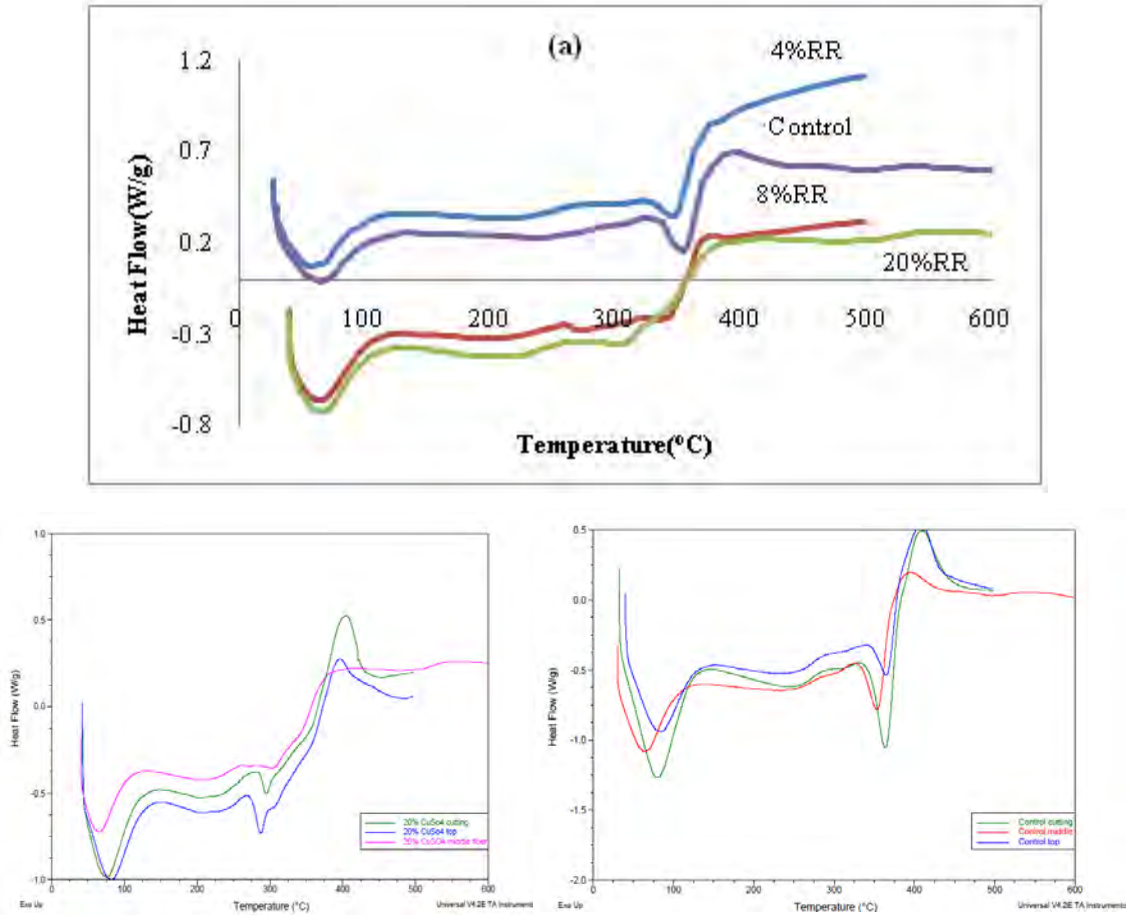

(b) (c)

Figure 4.17: DSC curve of (a) control and RR, (b) control fiber and (c) 20%RR jute fiber.

At temperature range of 60 to 100°C, the control and treated jute fiber had endothermic peak due to water or moisture release [120]. Around 300 °C, sufficient energy was available for a rapid cleavage of the glycisidic bond that resulted in products evaporation, levoglucosan and formation of other tarry products [119]. Hemicelluloses, on the other hand, showed an exothermic peak between 250 -350°C [119]. The peak at 297 °C corresponds to pyrolysis of hemicelluloses; the peak at 360 °C was due to depolymerization of cellulose and the peak around 432°C resulted from decomposition of lignin [119]. One important thing is that the heat flow gradually decreased after rot retardant treatment i.e. the oxidation resistance increased due to RR treatment except 4%RR.

The values of enthalpy from DSC curves give the idea of crystalinity (Table 4.6). Using the value of 100% crystalinity, the heat of fusion value of crystalinity can be obtained. But 100% crystalline value of the jute and rot retardant jute fiber is not known.

Table 4.5: Peak temperature and nature of peak from DSC data of rot retardant treated jute fiber.

Sample	1st Peak temp (°C)	2nd Peak temp (°C)	3rd peak temp (°C)	Nature of 1st peak	Nature of 2nd peak	Nature of 3rd peak
Control T	85.27	365.91	409.50	endo	endo	exo
4% RRM	58.40	345.45	398.90	endo	endo	exo
8%RRM	64.997	337.85	376.66	endo	endo	exo
20% RRT	82.89	205.89	396.37	endo	endo	exo
Control M	65.07	353.83	396.82	endo	endo	exo
20%RRM	65.79	304.39	319.03	endo	endo	exo
Control B	79.90	364.12	410.10	endo	endo	exo
20%RRB	75.72	295.45	404.72	endo	endo	exo

Table 4.6: "As received" DSC characterization of control and rot retardant treated jute fiber.

Sample	Melt onset temp (°C)	Melt peak temp (°C)	Enthalpy (J/g)	Crystalinity (%)	Melting temp T_m (°C)	Glass transition temp T_g (°C)
Control M	331.48	354.78	164.9	Very high	353.35	81.92
4%RRM	324.29	347.66	76.49	Very low	245.85	75.72
8%RRM	327.78	344.54	78.09	Low	338.71	83.30
20%RRM	287.29	339.66	84.91	High	305.38	82.72

The first exothermic peak reflects the stability of the fibers as a function of Cu concentration on the fiber surface.

4.3.6 Moisture Absorption Characteristics

The variation in moisture absorption of control and chemically treated jute fiber as a function of time for different RR treatment is shown in Figure 4.18 (a). It is evident that the initial rate of moisture absorption increased with increase in time. The increasing moisture absorption was caused, among other factors by the hydrophilic nature of jute fiber. When the RR treated fiber is exposed to moisture, the hydrophilic jute fiber swelled. The high cellulose content in the jute fiber, further contributes to more water penetration into the fiber. Moisture absorption behavior of rot retardant jute fiber in

water, 10% HCl (Figure 4.18 (b)) and 10% NaCl (Figure 4.18 (c)) at room temperature is quite different.

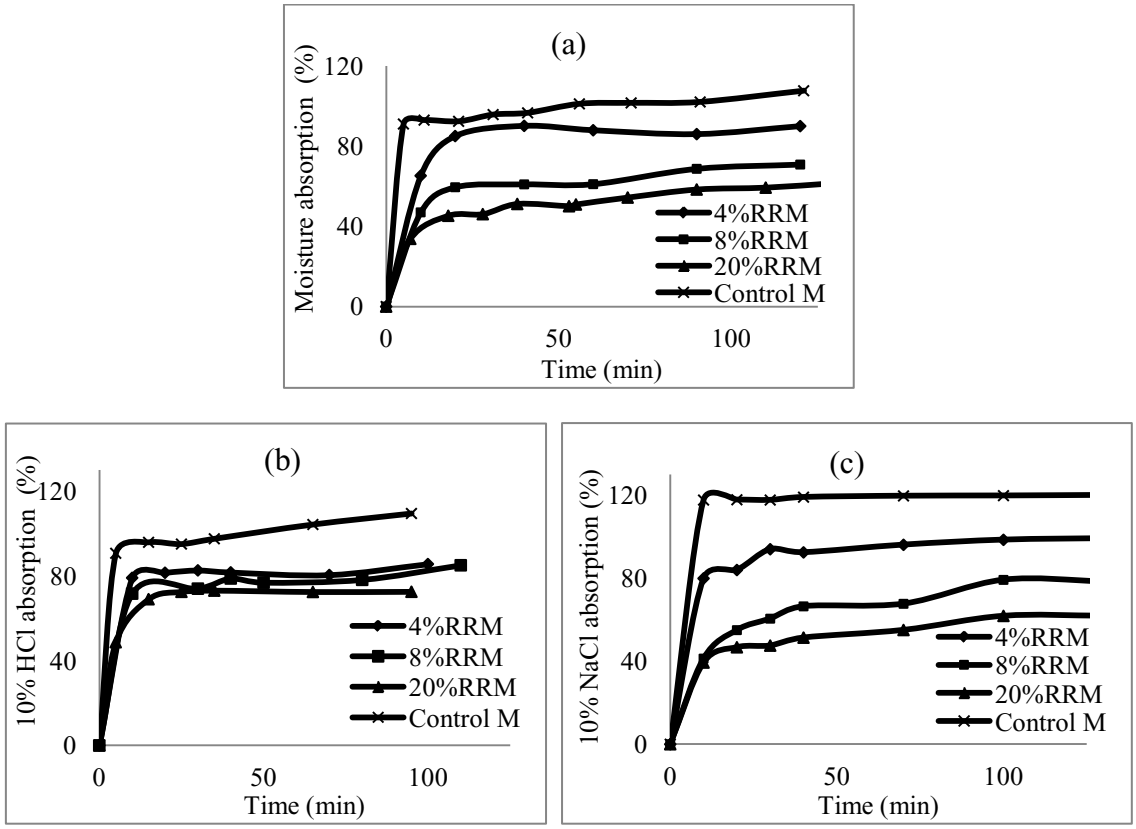

Figure 4.18: Moisture absorption behavior in (a) water, (b) 10%HCl and (c) 10%NaCl of control and rot retardant treated jute fiber.

Due to coating properties of the rot retardant chemicals, the molecule of moisture could not penetrate the barrier to reach the porous fiber. Thus the moisture absorption value decreased compared to the control jute fiber with the rot retardant chemical concentration. The decreased value is also concentration dependent because higher chemical concentration gives higher barrier. Among three different moisture conditions, the absorption in water and NaCl are similar except 10%HCl. Because the HCl solution can easily remove the coating partially from the rot retardant treated jute fiber surface.

4.3.7 Contact Angle Analysis

To observe the wettability of the rot retardant jute fiber, contact angle was measured at different conditions. Contact angle analysis was conducted using distilled water and

glycerol. In case of distilled water, the chemically treated fiber became more hydrophobic with chemical concentration. Control fibers showed higher adhesion force (Figure 4.19 (a)) and were most hydrophobic. With increase in chemical concentration, adhesion force decreased (Figures 4.19 (b), (c) and (d)) due to copper coating of the surface.

i

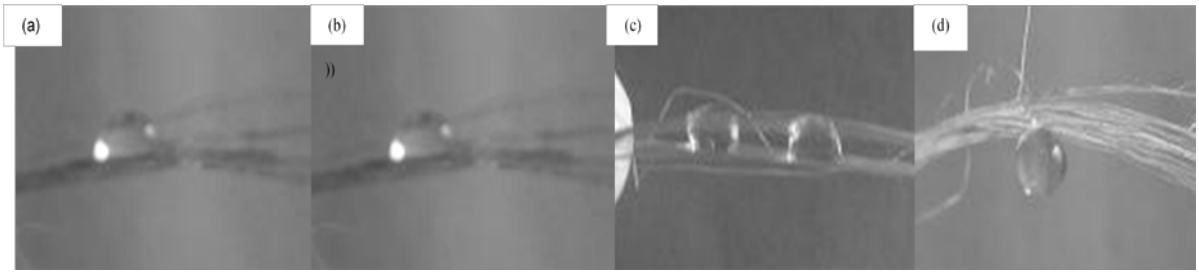

ii

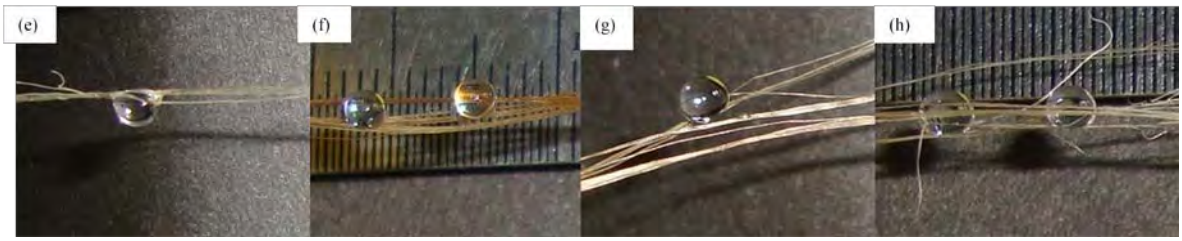

Figure 4.19: Interaction of i) distilled water with (a) control fiber (b) 4%RR (c) 8%RR (d) 20%RR and ii) glycerol with (e) control (f) 4%RR (g) 8%RR, and (h) 20%RR.

The interaction between the jute fiber and the copper salt treated fiber with water was investigated to provide a qualitative observation of wetting characteristics. The water formed high contact angle with the surface of the control fiber. In contrast, copper salt treatment permitted lower wetting of the fiber surface and lower tendency for rapid absorption of water into the fiber. Due to the decrease of wettability, the drop size also decreased with the chemical concentrations (Figure 4.19 (ii)). In case of acetone it was not possible to measure the drop sixe because the chemical was fully absorbed by the control and treated jute fiber.

4.3.8 Weight Percentage Gain (%)

The weight percentage gain (WPG) increased with the rot retardant chemical concentration as shown in Figure 4.20. This is due to the participation of large amount of

rot r etardant che mical in the r eaction with increase i n chemical con centration. Due t o higher chemical concentration, coating property was also improved that were observed by AFM i mages. The i ncreases of w eight i nfluenced t he m echanical, t hermal and morphological properties [129, 130].

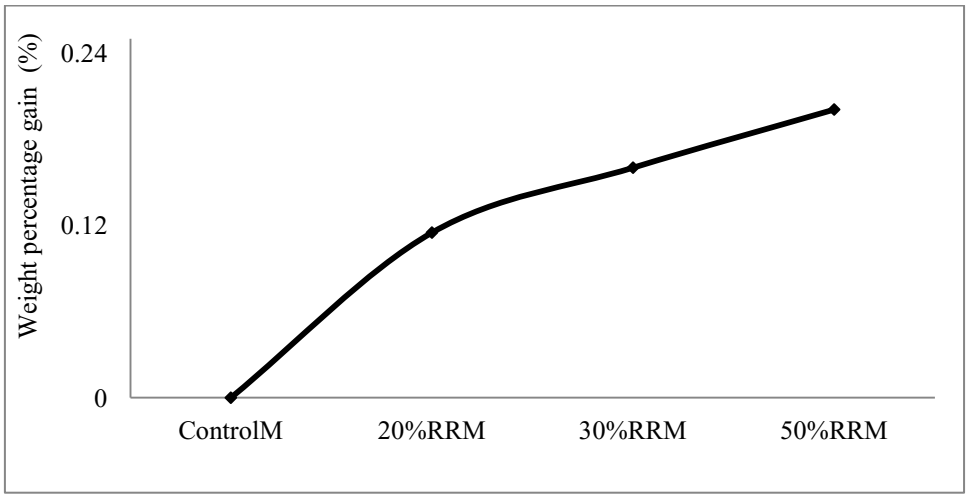

Figure 4.20: Weight percentage gain (%) of RR jute fiber.

4.3.9 Moisture Content

Moisture c ontent is a n important tool to investigate the quality of f iber a nd t heir application. Cellulose molecules of jute fiber contain hydroxyl groups which are pol ar in nature and attract moisture f rom t he a tmosphere w hich a re not de sirable f or good application. The m oisture c ontent gradually d ecreased with the r ot retardant che mical concentration c ompared t o t he control fiber (Figure 4.21) . In m oisture c ondition, the moisture content is higher compared to the room and dry condition. The coating property of the rot retardant may be less pol ar compared to hydroxyl group of control j ute fiber. So, t he m oisture a bsorption pr operty of r ot r etardant j ute f iber decreased which will improve the dimensional stability. Thus after rot retardant treatment the treated fiber rot later compared to the control fiber.

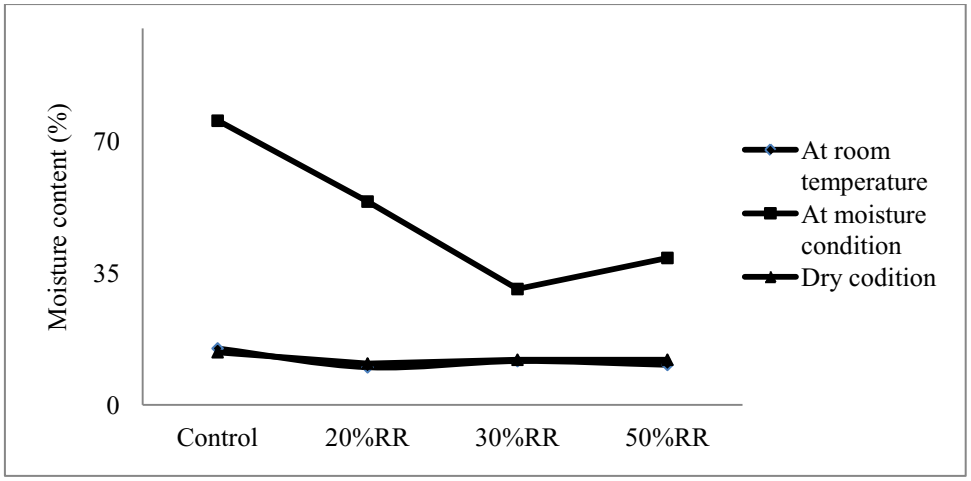

Figure 4.21: Moisture content of the RR jute fiber.

4.4 Result of Fire Retardant (FR) Jute Fiber

4.4.1 Weight Percentage Gain (%)

The weight percentage gain (WPG) increased with the fire retardant chemical concentration as shown in Figure 4.22. This is due to the participation of large amount of fire retardant chemical in the reaction with increase in chemical concentration. Due to higher chemical concentration, coating property was also improved that were observed by AFM images. The increase in weight influenced the mechanical, thermal and morphological properties [129, 130].

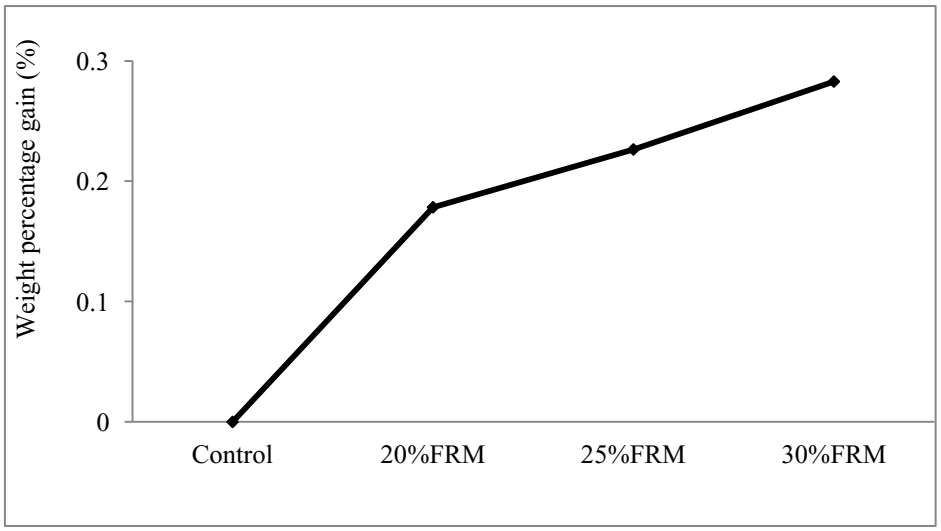

Figure 4.22: Weight percentage gain of the FR jute fiber.

4.4.2 Flammability Test of FR Jute Fiber

The flammability of the fire retardant was higher for 20%FR compared to the 25%FR and 30%FR as shown in Figure 4.23. Due to fire retardant chemical property that is concentration dependent, the burnt portion linearly decreased. After 30%FR, the burned portion did not decrease significantly. Thus the use of 20%FR was cost effective.

Figure 4.23: Flammability test of (a) 20%FR (b) 25%FR (c) 30%FR treated single jute fiber.

4.4.3 Tensile Properties

The Tensile test results of fire retardant treated and control fibers are mentioned in Appendix 1 [Tables A.21 to A.26]. The tensile strength of different portion of control and fire retardant (20%FR and 30 %FR) jute fibers are shown in Figure 4.24. After fire retardant treatment, the tensile strength of top and middle (Figures 4.24(a) and (b)) portions jute fiber decreased compared to control jute fiber. The top portion of FR jute fiber decreased approximately by 31.28% compared to control jute fiber. Tensile strength of middle portion 20% FR and 30% FR jute fiber decreased by 41.74% and 55.69% respectively compared to middle portion control jute fiber. However with increase in concentration of fire retardant chemical, the tensile strength increased in case of bottom portion by 62.07% compared to the control bottom portion jute fiber (Figure 4.24 (c)). The Young's modulus of top and bottom portion jute fiber (Figures 4.25 (a) and (c) increased after fire retardant treatment compared to the control top and bottom portion jute fiber. However the reverse results were obtained in case of middle (Figure 4.25 (b)) portion jute fiber.

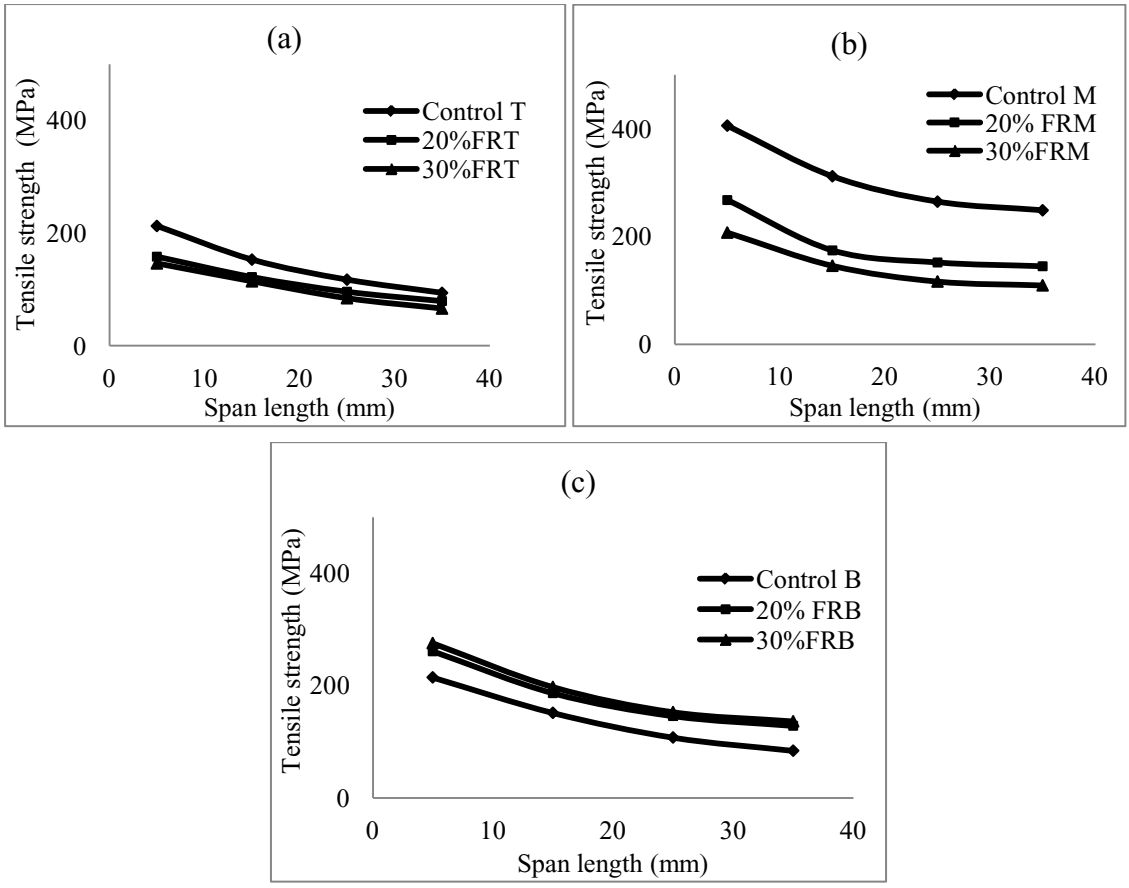

Figure 4.24: Tensile strength of (a) top (b) middle and (c) bottom portion FR single jute fiber.

After correction the Young's modulus became span length independent. The Young's modulus of fire retardant top, middle and bottom portion 20%FR and 30%FR jute fiber is shown in Figure 4.25. The middle portion control and fire retardant treated fibers had higher modulus compared to the top and bottom portions jute fiber. The Young's modulus of 20% FR and 30 % FR middle portions of FR jute fiber decreased by 15.85% and 27.50% respectively compared to the control's middle portion jute fiber. However, the Young's modulus of bottom portion FR jute fiber increased by 13.04% over the control bottom portion jute fiber.

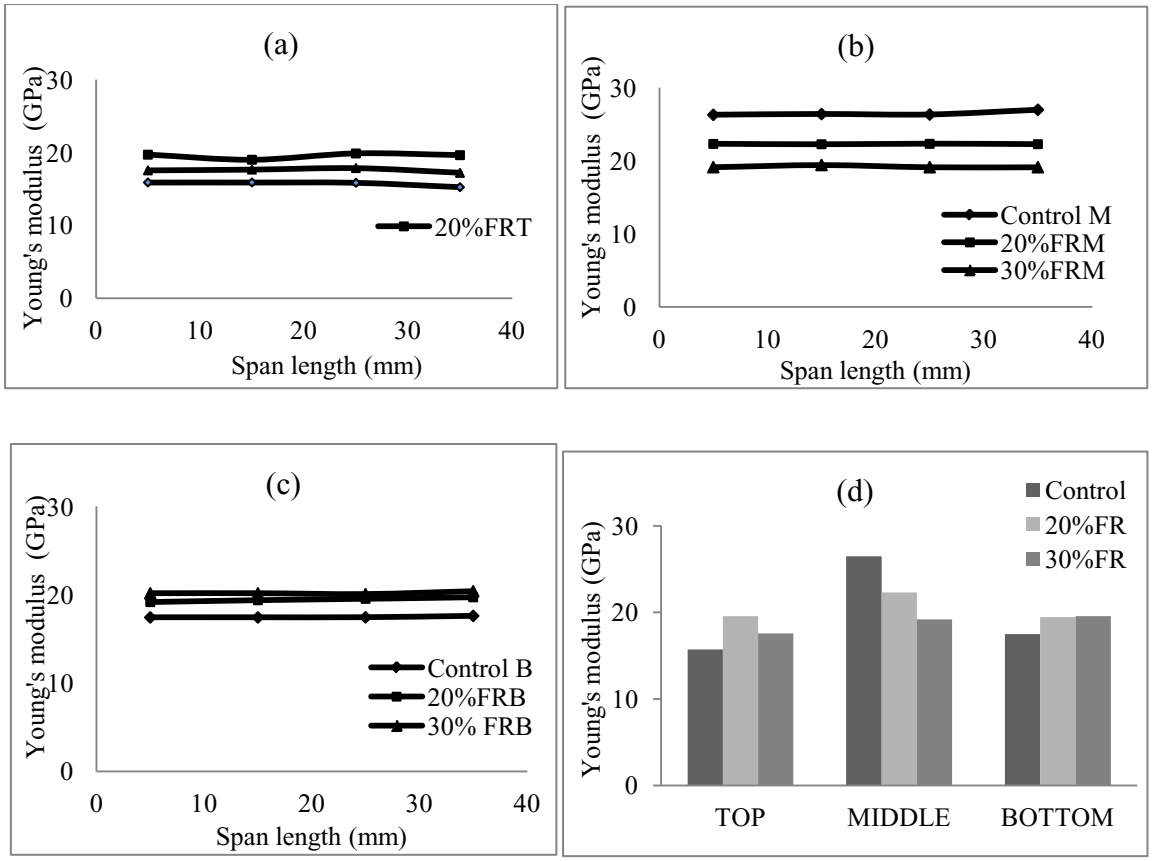

Figure 4.25: Corrected Young's modulus of (a) top (b) middle (c) bottom and (d) comparative Young's modulus of FR treated single jute fiber.

After fire retardant treatment, the strain to failure became span length dependent and followed decreasing trend. With increase in concentration of chemical, the strain to failure followed decreasing in case of top and middle portions (Figures 4.26 (a) and (b)) jute fiber compared to control fiber. However, after FR treatment the strain to failure became similar for bottom portion (Figure 4.16 (c)).

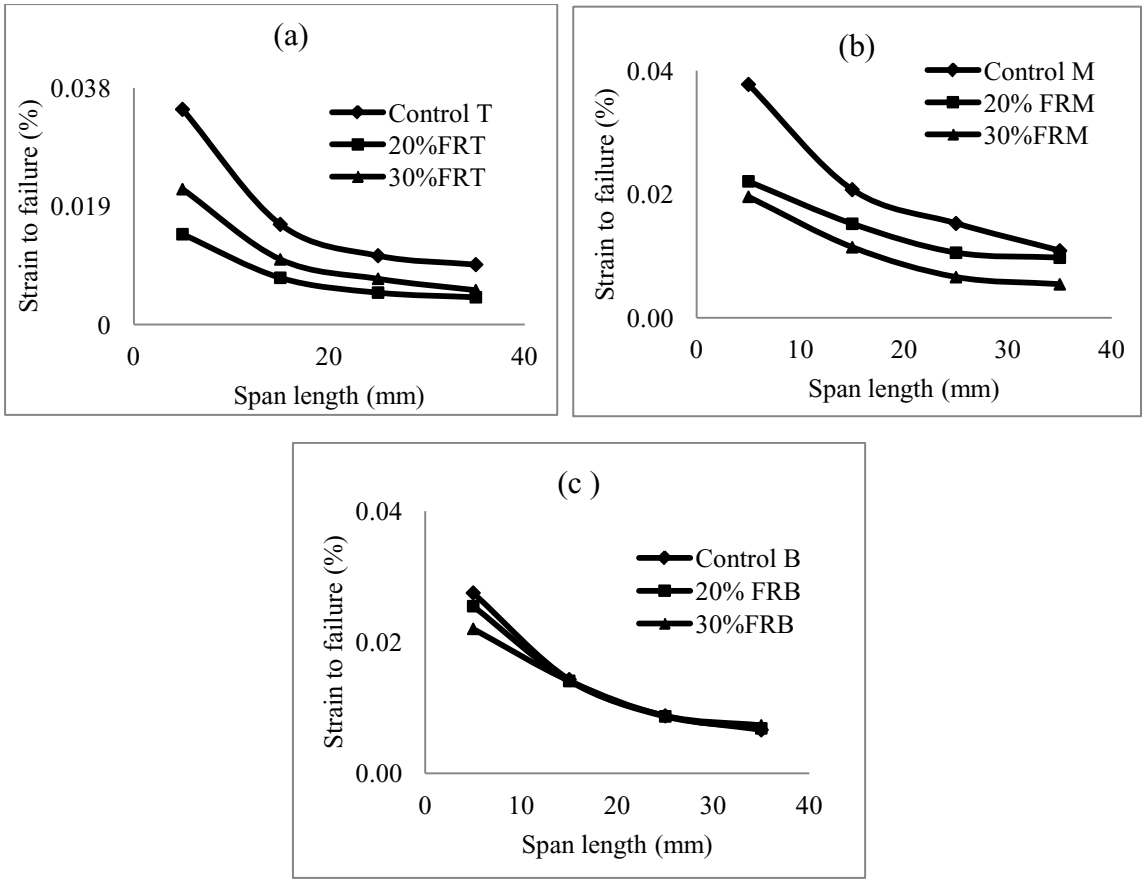

Figure 4.26: Strain to failure of (a) top (b) middle (c) bottom and (d) different portion FR treated single jute fiber.

4.4.4 FTIR Spectroscopy Analysis

Figure 4.27 shows a decrease in the intensity of the O–H absorption band at 3450–3400 cm^{-1} indicating that the hydroxyl group contents in jute were reduced after fire retardant reaction of top, middle and bottom portions jute fiber. However after the FR treatment, this absorption bands occurred at higher wavelengths. That means strong bond was produced with the chemical concentration, but top and bottom portion formed weak bond with the FR chemical. There is one thing that the peak of the treated fiber became sharper. Absorption in the first region is obtained from O-H stretching vibrations in hydroxyl, phenol and carboxyl groups. The intensity of the O-H peak also increased due to more hydroxyl group present in fire retardant treated jute fiber. After fire retardant treatment, the C-H peak is clearly abolished. The intensity of C-H stretching decreased with the fire retardant chemical concentration. Approximately around 1430 cm^{-1}, N-H bending observed due to fire retardant chemical i.e. NH_4. There are two new peaks observed after

fire r etardant t reatment at 400 a nd 500 cm^{-1} [144]. The a bsorption a t t he l ower b and (1300-800 cm^{-1}) is also present may be due to esterification [122].

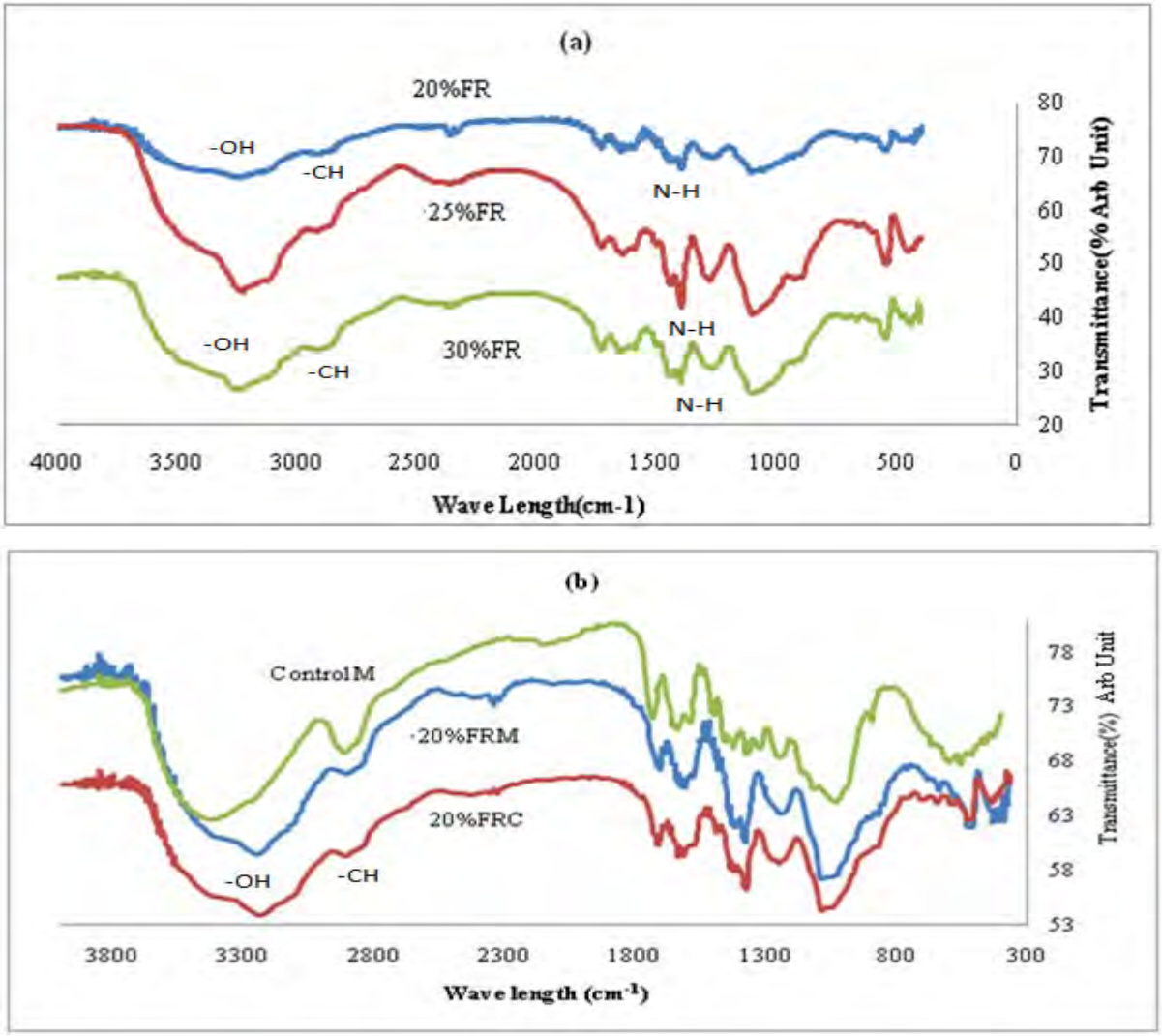

Figure 4.27: ATR-FTIR of (a) different concentration and (b) different portions fire retardant jute fiber.

4.4.5 XRD Analysis

The XRD results with various chemical concentrations are shown in Figure 4.28. Figure 4.28 (b) shows the top, middle and bottom portions XRD results. XRD pattern of the top, middle a nd bot tom por tion were found s imilar. However with t he concentration of the chemicals o f f ire r etardant, some extra pe ak occured. W ith t he FR che mical concentration, all t he pe aks shifted t o t he r ight ha nd s ide. S o i t c an be concluded t hat there w as some degree of che mical r eaction between the j ute and the f ire r etardant chemicals. The XRD pattern shows ther are double phase and formation of structure. By

analyzing the XRD patterns it is observed that the position of the peaks comply with $NH_4H_2PO_4$ and SiO_2. Peaks are shown in the XRD pattern are identified with their miller indices.

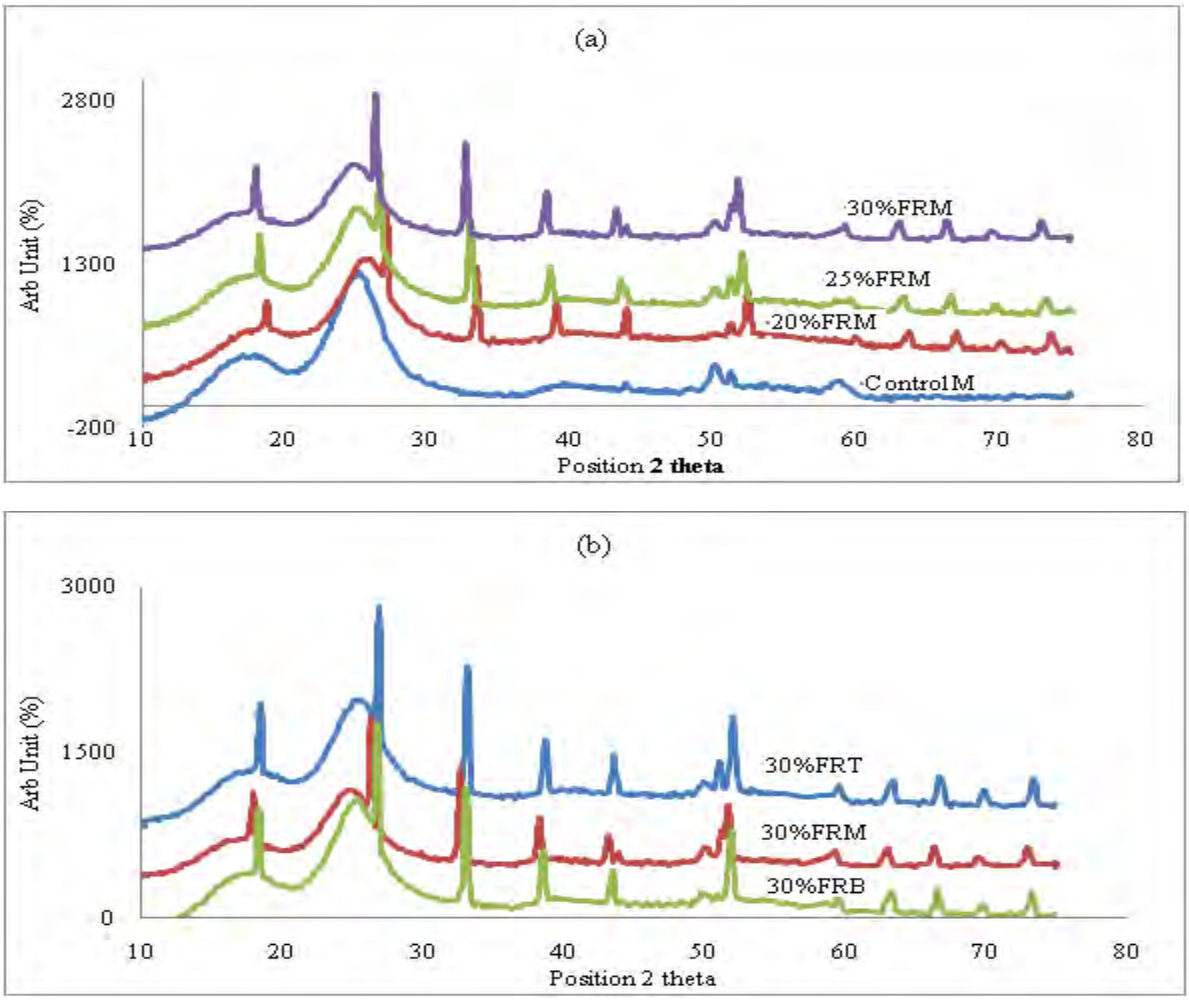

Figure 4.28: XRD of FR with (a) chemical concentrations and (b) different portions of jute. fiber.

Table: 4.7: Crystalinity and heat of fusion of the FR treated jute fibers.

Sample	18° Intensity	22° Intensity	Crystalinity (I_c)	100% Crystalline jute	
				Heat of fusion (H_f)	Enthalpy
20%FR M	17.83	38.93	54.19	366.97	198.9
25%FRM	35.00	50.33	30.45	889.72	271.0
30%FRT	34.53	23.53	-46.74	-579.48	270.9
Control M	07.98	100	92.02	179.20	164.9

Table 4.7 shows the cristalinity of the fire retardant jute fiber. It is observed that the crystalinity decreased with the percentage of chemical concentrations compared to the control jute fiber. Due to this, the tensile properties of the fiber decreased after fire retardant treatment in case of middle portion. The proposed enthalpy of fusion (for 100% crystalline FR treated jute fiber) of the FR treated jute fibers is expressed in the above Table 4.7.

4.4.6 Morphological Study

Scanning Electron Microscopy (SEM)

Surface morphology of control and fire retardant treated jute fibers were observed under SEM. Figure 4.29 represents surface morphology of fire retardant treated top, middle and bottom portions jute fiber. Control fiber surface was rough. Fire retardant jute fiber treated with $NH_4H_2PO_4$ had rather smoother surface and smaller diameter compared to the control fiber. Due to increase of coating properties with the concentration of $NH_4H_2PO_4$, the treated top, middle and bottom portion of fire retardant treated fibers gradually became smoother. The surface of the fire retardant treatment looks like a decay surface and is observable. This is due to the first decay and finally coating property of the fire retardant chemical on the jute fiber.

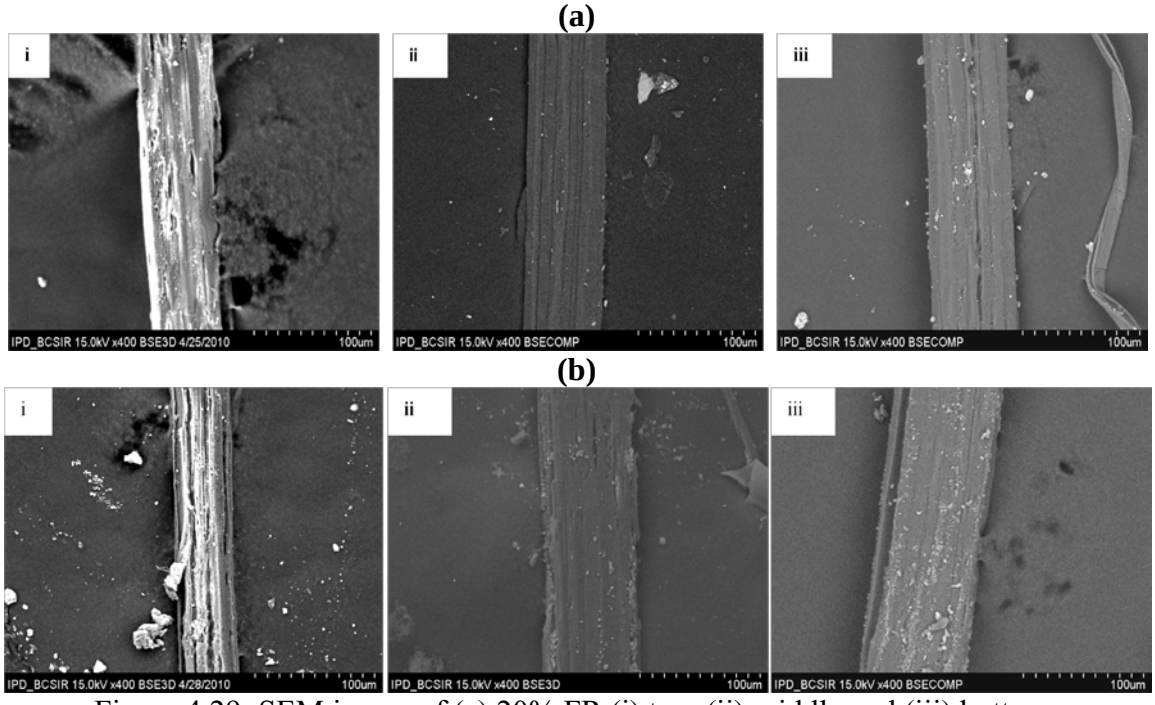

Figure 4.29: SEM image of (a) 20% FR (i) top, (ii) middle and (iii) bottom; (b) 30%FR (i) top, (ii) middle and (iii) bottom portion jute fibers.

Atomic Force Microscopy (AFM)

The AFM images are shown in Figure 4.30. The fiber surface became smoother after fire retardant treatment compared to the control fiber (Figure 4.30) [133]. So the effect of fire retardant treatment was observed in the fiber surface. This is considered as a proof for the surface coverage of the fibers with a coating layer resulting in decreased surface roughness.

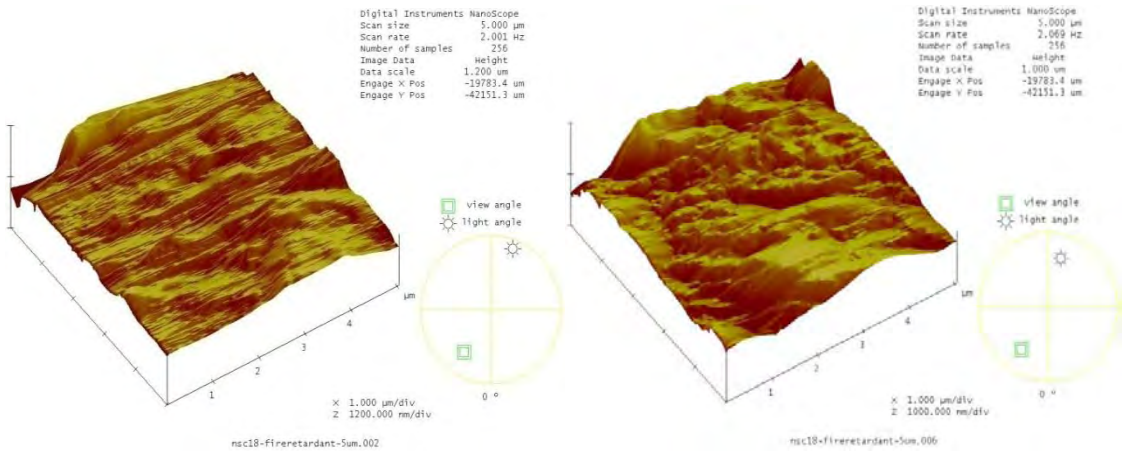

Figure 4.30: Atomic force microscope (AFM) topographic pictures of (a) 30% FR and (b) 20% FR jute fiber.

4.4.7 Thermal Properties

Thermogravimetric Analysis (TGA)

Weight change in different temperature, 10% and 50% weight loss are shown in Table 4.8, which were higher than the control. Residue was also higher compared to the control jute fiber that means flamability of FR treated jute fibers were lower compared to the control jute fiber. The residue at 600°C temperature of FR jute fiber is higher due to volatile material [134] coated by FR treatment that made them non volatile. The mass loss (Figure 4.31 (a)) and derivative mass loss (Figure 4.31 (b)) due the heat was lower compared to the control. The control fiber degraded earlier than the fire retardant treated jute fiber. It means that FR treatment occured in the fiber surface. It can be also concluded that the thermal effect gradually changed (Figure 4.31 (c)) with the fire retardant chemical concentration.

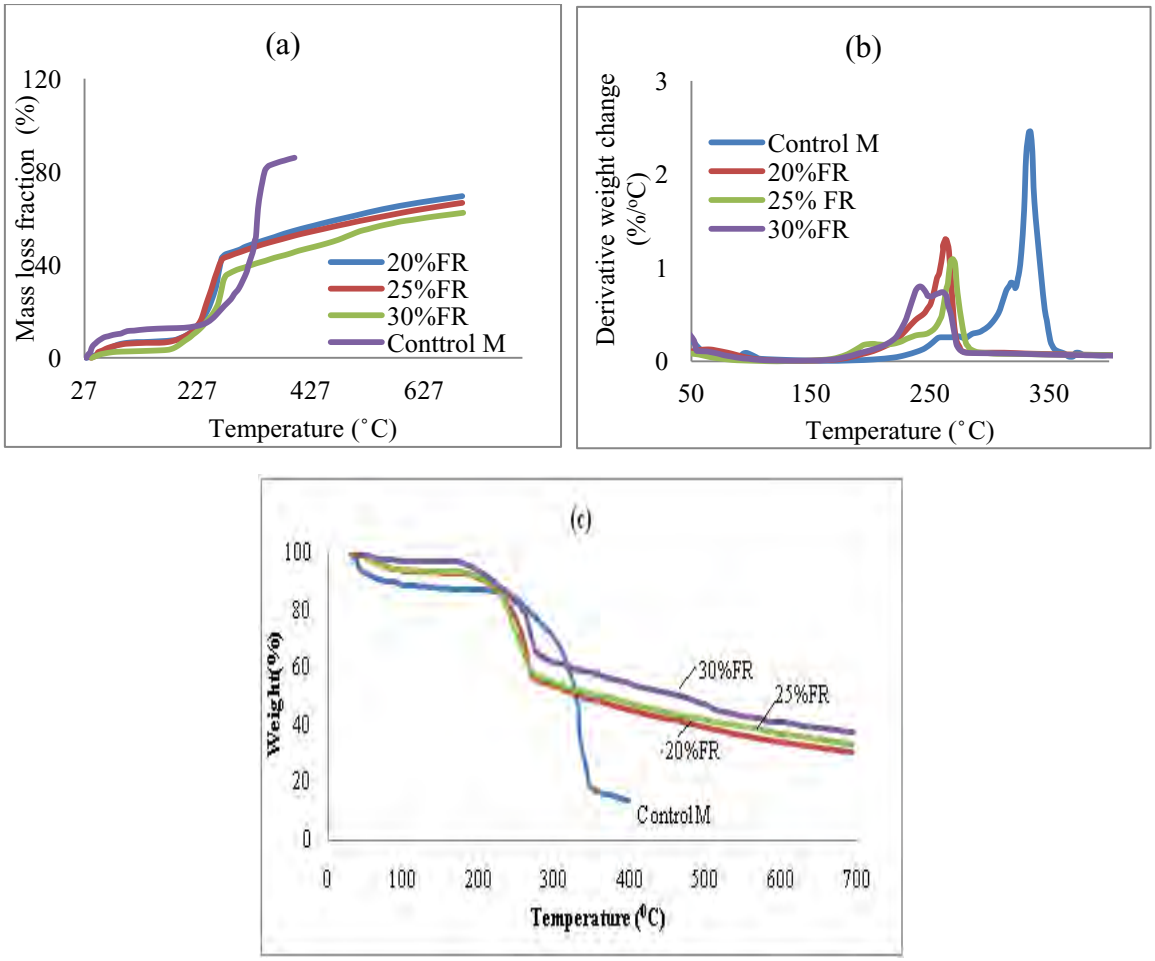

Figure 4.31: (a) Mass loss, (b) DTGA and (c) weight change thermograph of fire retardant jute fiber.

The derivative weight change of the fire retardant treated fiber decreased compared to the control jute fiber due to the fire retardant chemical (NH_4) property. Thus the oxidation resistance increased with the fire retardant chemical concentrations. Due to coating property of the NH_4 salt, which acts as a fire retardant element, the FR treated fiber became thermally stable at higher temperature.

Table 4.8: TGA data of control and FR treated jute fiber.

Sample	Weight change between 50-150°C (%)	Weight change between 150-300°C (%)	Weight change between 300-700°C (%)	Derivative weight change temp (%/°C)	Residual weight (%)	50% Weight loss temp (°C)	10% Weight loss temp (°C)
20%FRM	5.451	39.65	22.24	263.29	30.48	336.35	208.51
25%FRM	4.339	38.84	21.27	262.23	33.53	358.50	208.59
30%FRM	2.028	39.06	19.61	268.61	37.71	464.60	281.00
Control M	5.471	17.83	55.82	332.85	13.96	327.10	76.31

Differential Scanning Calorimetric (DSC) Analysis

Crystallinity and first exothermic peak temperature is a function of concentration of chemical treatment [132]. The 1st endothermic peaks temperature for the fire retardant jute fiber samples decreased with the fire retardant chemical concentration (Tables 4.9 and 4.10).

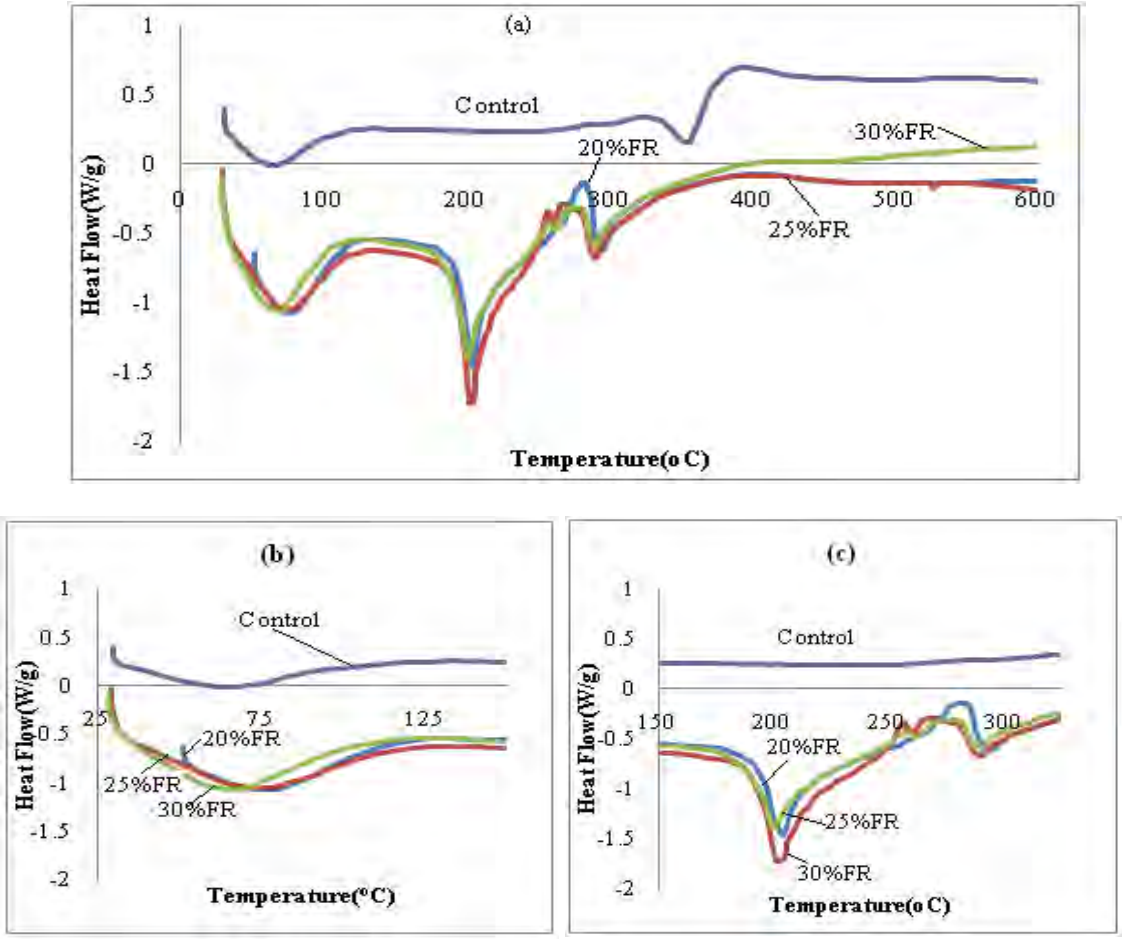

Figure 4.32: DSC thermograph of fire retardant jute fibers.

The exothermic peaks temperature decreased (Figure 4.32 (a)) and this change due to the presence of reactive groups in the fire retardant jute fiber. The appearance of both endo and exothermic peaks could be related to the morphological changes possibly occurred by the de composition of he mi-cellulose and cellulose r espectively. The s lope of t he he at flow increased with the chemical concentration as shown in Figures 4.32 (b) and (c). Due to coating property of the NH_4 salt, which is a fire retardant element, the FR treated fiber heat flow decreased compared to the control jute fiber.

Table 4.9: Peak temperature and nature of peak of FR jute fiber from DSC data.

Sample	1st peak temp (°C)	2nd peak temp (°C)	3rd peak temp (°C)	4th peak temp (°C)	Nature of 1st peak	Nature of 2nd peak	Nature of 3rd peak	Nature of 4th peak
20% FRM	76.53	202.64	282.18	293.64	endo	endo	exo	exo
25% FRM	73.25	203.42	266.71	290.60	endo	endo	exo	exo
30% FRM	66.36	200.87	275.39	189.10	endo	endo	exo	exo
Control M	65.07	353.83	-	396.82	endo	endo	-	exo

Melt onset temperature melt peak and enthalpy changed with the fire retardant chemical as shown in Table 4.10.

Table 4.10: "As received" DSC characterization of control and fire retardant treated jute fiber.

Sample	Melt onset temperature (°C)	Melt peak temperature (°C)	Enthalpy (J/g)	Crystalinity (%)
Control M	331.48	354.78	164.9	Very Low
20%FRM	185.64	200.74	298.9	Very High
25%FRM	190.24	202.59	271.0	High
30%FRM	190.61	203.29	270.9	Low

4.5 Results of WR Jute Fiber

4.5.1 Moisture Content (%)

At room temperature, the moisture content of water retardant jute fiber was lower compared to the control jute fiber. The moisture content varies linearly with the chemical concentration as shown in Figure 4.33. At high moisture conditions, moisture absorption of control jute fiber increased compared to the water retardant treated jute fiber due to acetylating effect of the water retardant chemicals.

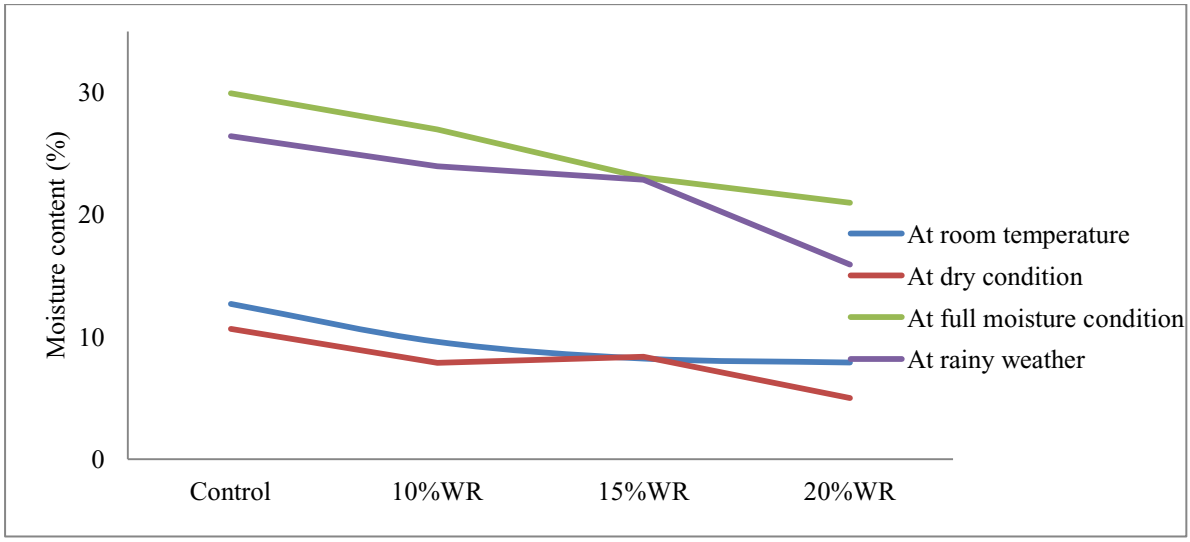

Figure 4.33: Moisture content (%) of water retardant jute fiber.

4.5.2 Tensile Properties

The Tensile test results of water retardant treated and control fibers are mentioned in Appendix 1 [Tables A.21 to A.26]. The tensile strength of different portion control and water retardant (10%WR, 15% WR and 20% WR) jute fibers are shown in Figure 4.34. The tensile strength and Young's modulus of the water retardant jute fiber were lower compared to the control fiber. However strains to failure of control and water retardant jute fiber were similar.

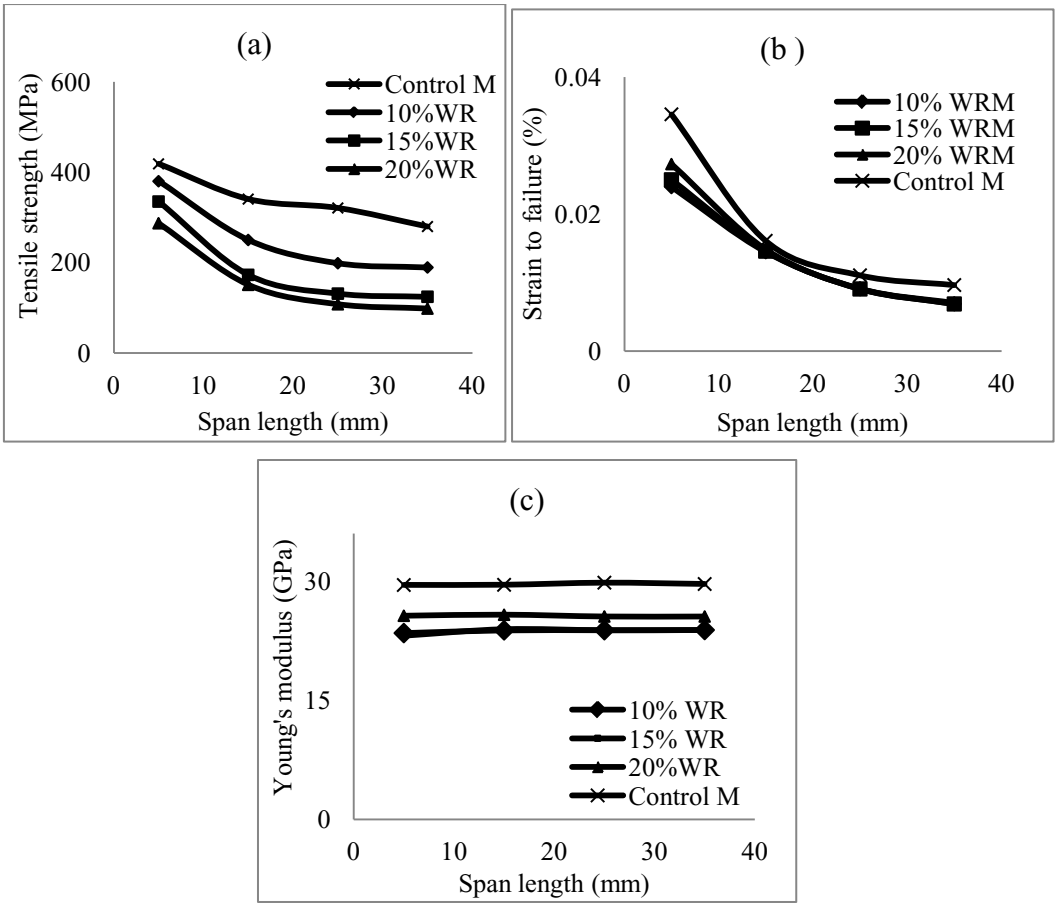

Figure 4.34: (a) Tensile strength (b) strain to failure and (c) Young's modulus of water retardant jute fiber.

4.5.3 FTIR Analysis

The absorption maximum for O-H stretching depends upon concentration, nature of the solvent and temperature [124]. In the water retardant treated jute, the O-H peak became broader with the chemical concentrations as shown in Figure 4.35. The intensity of the WR treated jute fiber decreased compared to the control jute fiber. Higher absorption is observed in the region around 3400 cm^{-1} for the control jute fiber over the water retardant jute fiber since more hydroxyl groups are present. The absorption at the lower band (1300-800 cm^{-1}) is also present may be due to esterification. The esterification occurred due to hydroxyl groups (O-H) of the fiber react with acetyl groups (CH_3CO), therefore rendering the fiber surface more hydrophobic.

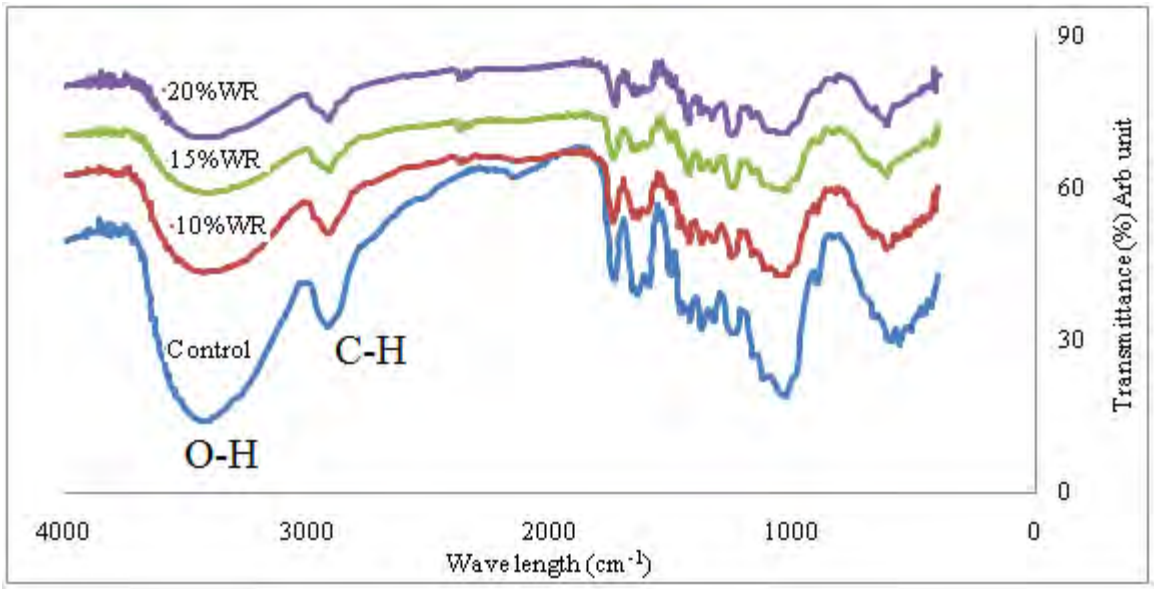

Figure 4.35: ATR- FTIR of WR jute fiber.

4.5.4 XRD Analysis

The XRD spectra of water retardant jute fiber are shown in Figure 3.36. The spectra show that the peak intensity decreased with the water retardant chemical concentration. However the peak position remained same. The crystalinity can not be measured from the peak intensity, because of insufficient peak intensity at 18° and 22°. The existing phase according to plane is not possible to explain due to insufficient peak.

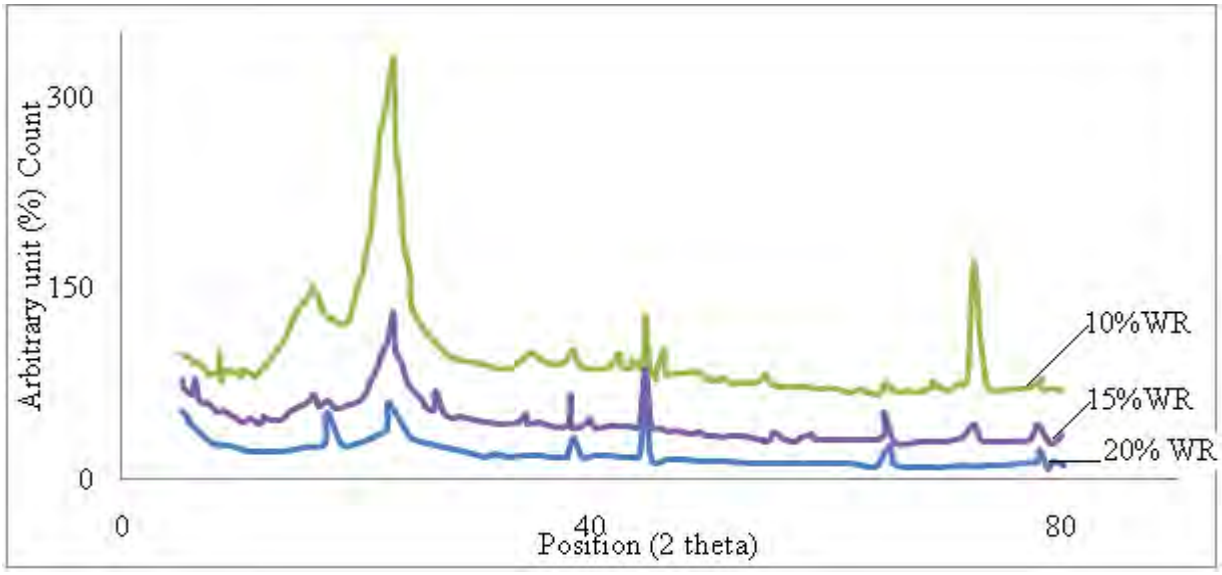

Figure 3.36: XRD pattern of the water retardant jute fiber.

4.5.5 Thermal Properties

Thermo Gravimetric Analysis (TGA)

DTGA thermograph (Figure 4.37 (a)) shows the main decomposition peak for each water retardant sample. With the chemical concentration, the peak height decreased i.e. the chemical concentration existed in the samples. The thermal stability (Figure 4.37 (c)) increased after WR treatment. After 330°C temperature the residue remained higher due to water retardant treatment. That is why derivative weight (Figure 4.37 (a)) decreased compared to the control jute fiber. With the chemical concentration, mass loss **(**Figure 4.37 (b)) due to heat decreased, i.e. they are more stable at high temperature.

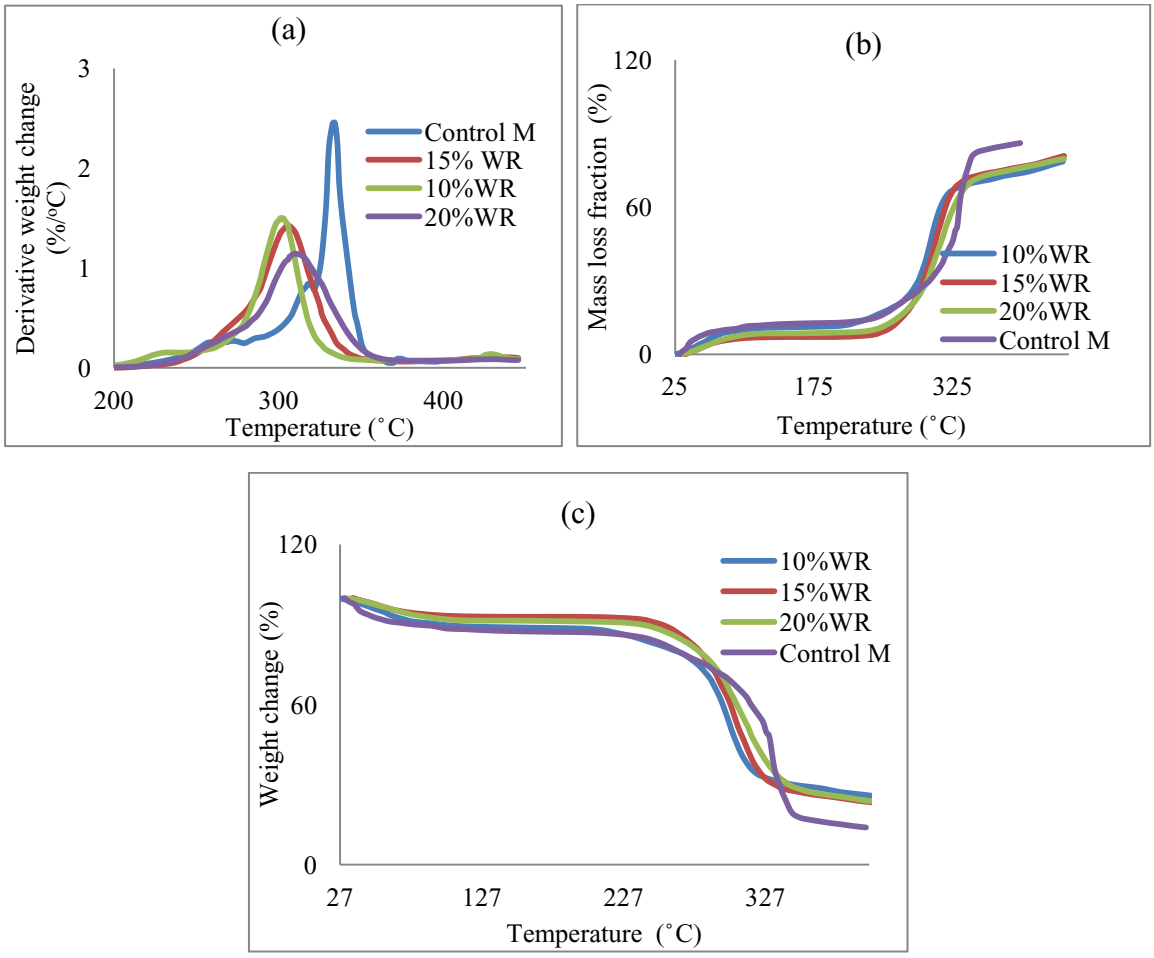

Figure 4.37: (a) DTGA, (b) mass loss and (c) TGA thermograph of water retardant jute fiber.

10% weight loss and 50% weight loss temperature gradually increased with chemical concentration as shown in Table 4.11. The residue of water retardant sample decreased with the chemical concentration. Thus it can be concluded that after WR treatment, the sample became less flammable as well as more water retardable. The derivative weight change of the water retardant treated fiber decreased compared to the control jute fiber due to the water retardant chemical property. Thus the oxidation resistance increased with the water retardant chemical concentrations compared to control jute fiber.

Table 4.11: Weight change due to thermal application on the water retardant treated jute fiber.

Sample	Weight change between 50-150°C (%)	Weight change between 150-300°C (%)	Weight change between 300-700°C (%)	Derivative weight change temp (°C)	10% weight loss temp (°C)	50% weight loss temp (°C)	Residual weight (%)
10%WRM	4.944	33.34	33.95	305.62	97.22	303.46	21.53
15% WRM	7.365	33.34	33.95	301.80	237	308.88	21.26
20% WRM	6.37	23.99	46.95	310.07	254	315.69	20.42
Control M	5.471	17.83	55.82	332.85	76.31	327.10	13.96

Differential Scanning Calorimetric (DSC) Analysis

Differential Scanning Calorimetric (DSC) thermographs obtained from the control and water retardant jute fibers exhibited both endothermic and exothermic transitions (Figure 4.38(a)). The peak-temperatures appeared differently with respect to the sample condition. The rate of the heat flow decreased with the chemical concentration compared to the control as shown in Figures 4.38 (b) and (c). Thus it can be concluded that after WR treatment, the sample became less flammable as well as more water retardant.

Table 4.12: Peak nature and temperature of water retardant jute fiber.

Sample	1st Peak temp (°C)	2nd Peak temp (°C)	3rd Peak temp (°C)	4th Peak temp (°C)	Nature of 1st peak	Nature of 2nd peak	Nature of 3rd peak	Nature of 3rd peak
10%WRM	66.22	293.44	-	521.91	endo	endo	-	exo
15% WRM	68.65	295.07	312.99	502.15	endo	endo	exo	exo
20% WRM	68.65	292.21	307.97	496.42	endo	endo	exo	exo
Control M	65.07	353.83	-	396.82	endo	endo	-	exo

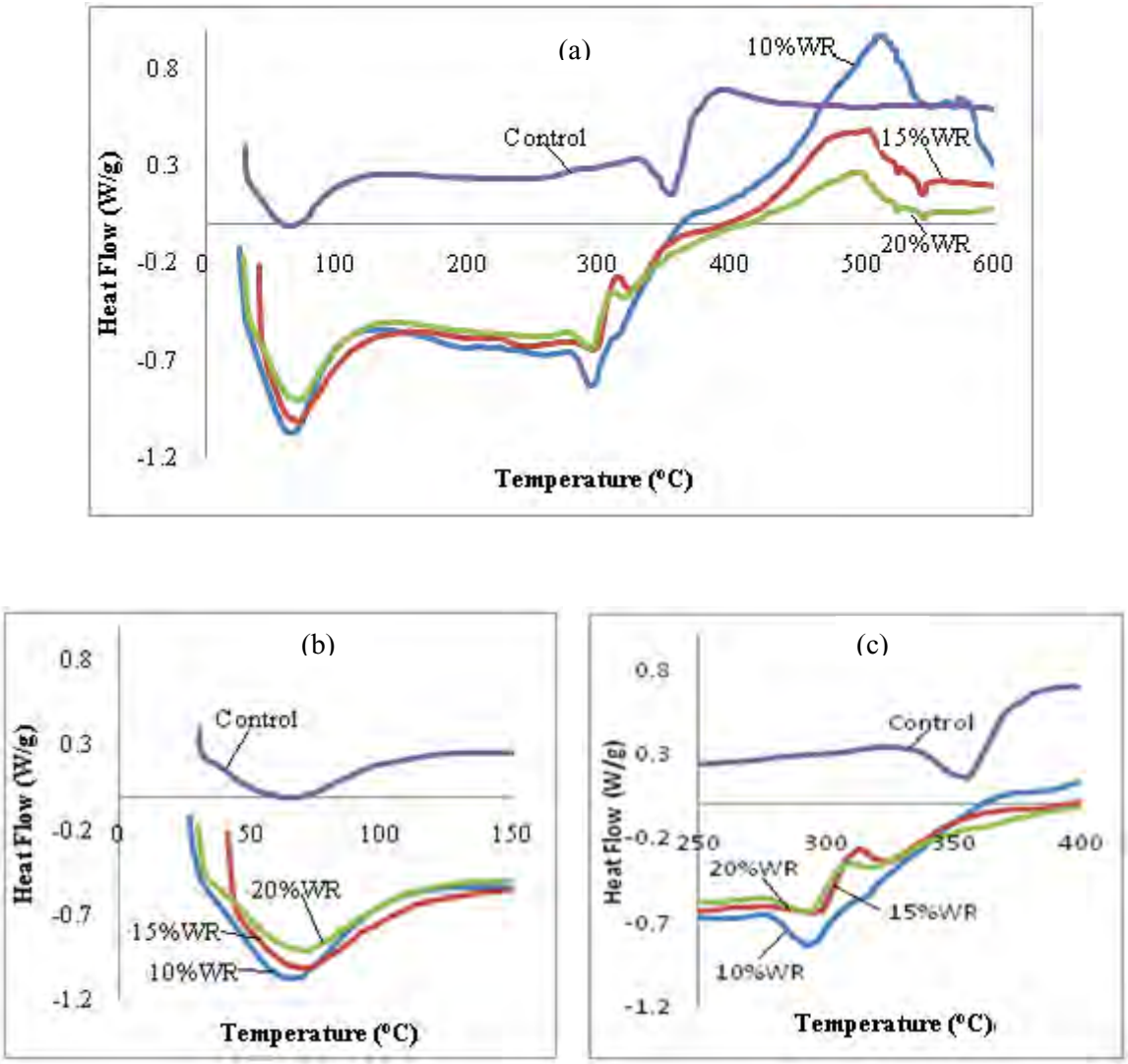

Figure 4.38: DSC thermograph of water retardant jute fiber.

From the DSC data, the crystalinity can be calculated using enthalpy of fusion of 100% crystalline material. But this value is not known. The assumption of the crystalinity can be found from the enthalpy value given in Table 4.13.

Table 4.13: "As received" DSC characterization of control and water retardant treated jute fiber.

Sample	Melt onset temp(°C)	Melt peak temp(°C)	Enthalpy (J/g)	Crystalinity (%)
10% WRM	282.21	296.67	296.67	Very high
15%WRM	276.59	294.43	294.32	High
20% WRM	276.49	293.21	293.32	Low
Control M	190.24	202.59	271.0	Very low

4.5.6 Moisture Absorption Characteristics

The variation in moisture absorption of control and chemically treated jute fiber as a function of time for different WR treatment is shown in Figure 4.39 (a). It is evident that the rate of moisture absorption increased with increase in time. When the WR treated fiber was exposed to moisture, the extra chemical coating was removed in case of higher chemical concentration. That is why the value became negative for higher chemical concentration. Moisture absorption behavior of water retardant jute fiber in water, 10% HCl (Figure 4.39 (b)) and 10% NaCl (Figure 4.39(c)) at room temperature was lower compared to the control jute fiber due to hydroxyl groups (O-H) of the fiber react with acetyl groups (CH_3CO), therefore rendering the fiber surface more hydrophobic[134].

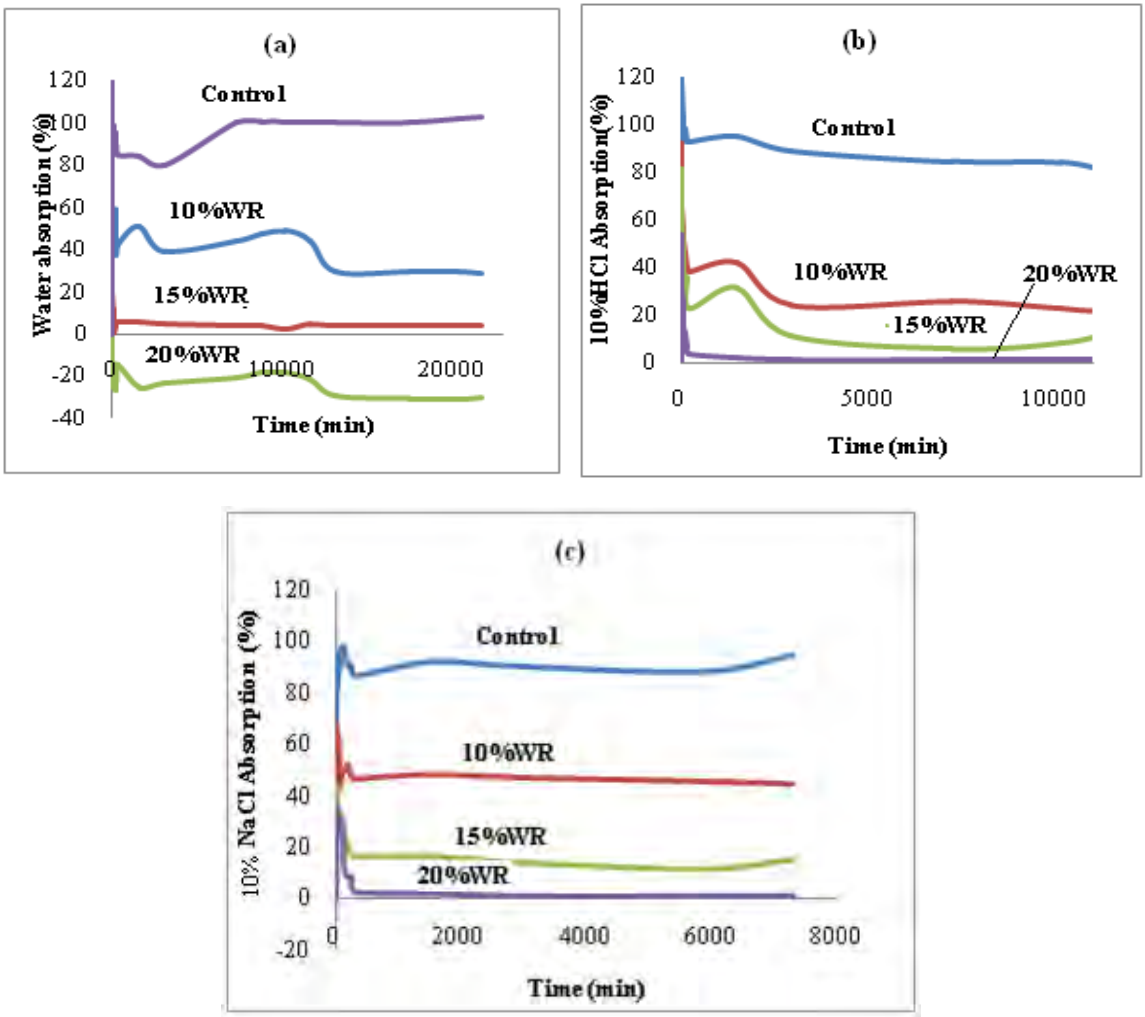

Figure 4.39: Moisture absorption of WR fiber in (a) distilled water, (b) 10%HCl and (c) 10%NaCl.

4.6 Matrix Characterization

4.6.1 Moisture Content (%) of MAgPP Resin

The moisture content of the MAgPP at different conditions is shown in Figure 4.40. At moisture condition, the resin contained more moisture than other conditions. However at hot water vapor condition, they contained low moisture. So moisture should be removed in order to manufacture good quality composites.

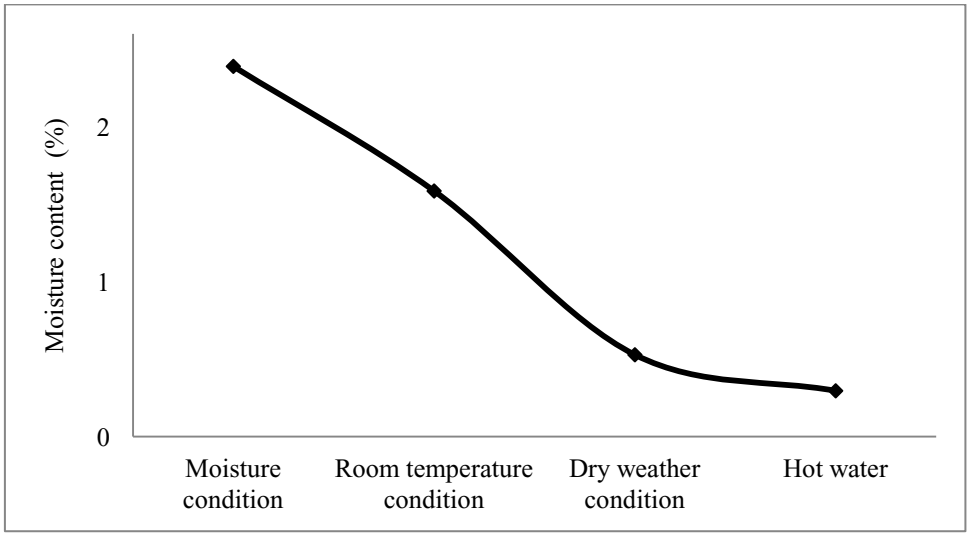

Figure 4.40: Moisture content of MAgPP.

4.6.2 Mechanical Properties

Tensile Properties

The stress strain curves of the 4mm thick MAgPP resin plane sheet are shown in Figure 4.41. The tensile strength, strain to failure and Young's modulus are listed in Table 4.14.

Table 4.14 : Tensile properties of MAgPP matrix.

Sl. No	Max Force (N)	Tensile strength (MPa)	Strain to failure (%)	Young's module (GPa)
1	559.642	24.22693	8.17%	1.183596
2	442.719	19.65701	7.06%	1.235995
3	315.508	17.2725	6.49%	1.11237
Average	439.2897	20.38548	7.24%	1.17732
Std	122.1031	3.53398	0.008521	0.062051

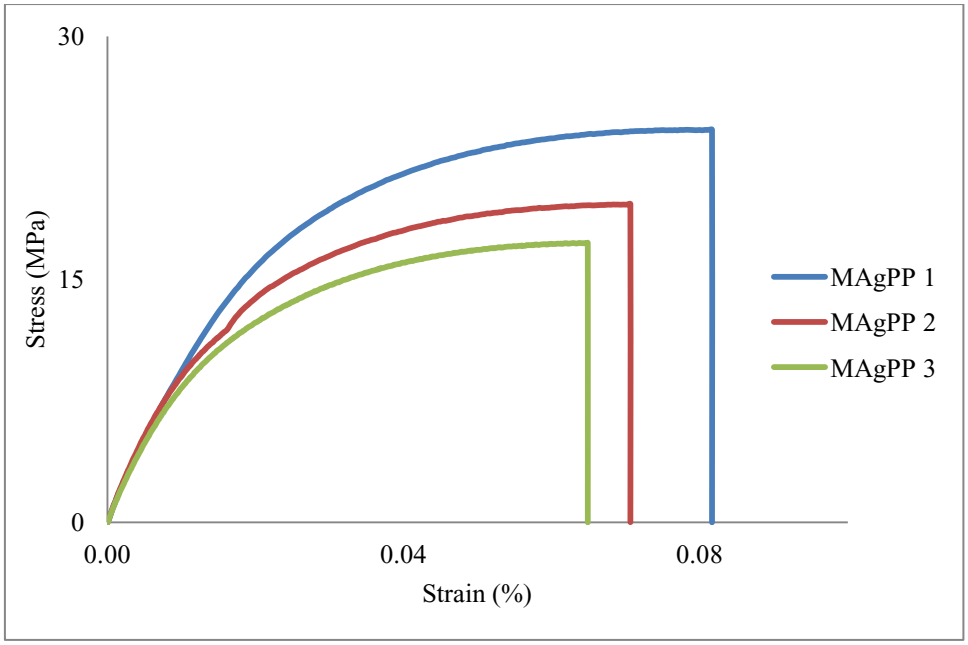

Figure 4.41: Tensile stress strain curve for MAgPP.

Flexural Properties

The flexural stress strain curves are shown in the Figure 4.42. The flexural strength, strain to failure and flexural modulus are listed in the Table 4.15. The flexural strength and strain to failure are 11.62 MPa and 5.56% respectively.

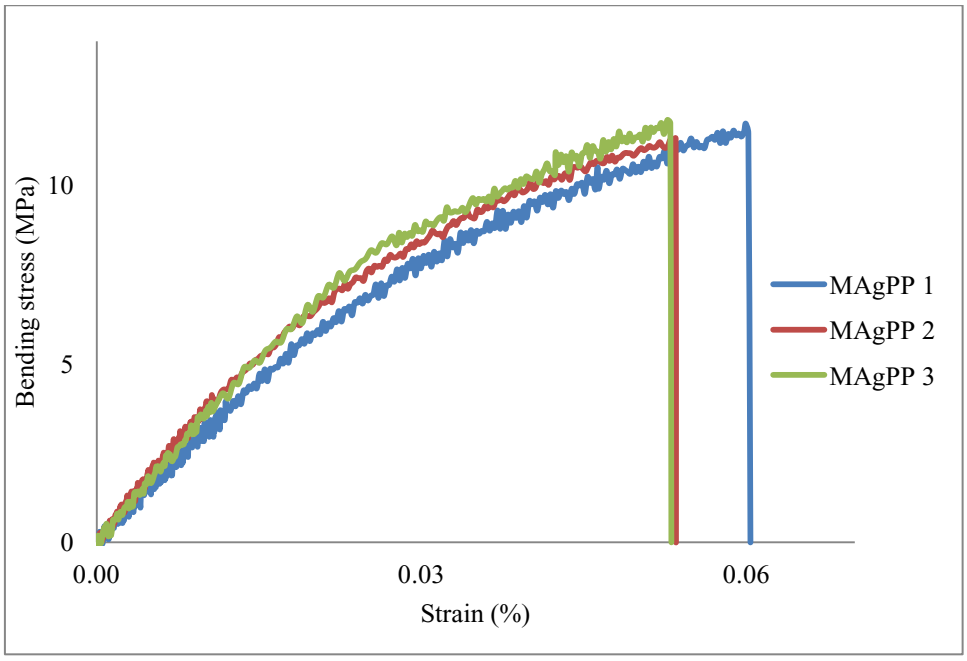

Figure 4.42: Flexural stress strain curve for MAgPP.

Table 4.15: Flexural and impact properties of MAgPP resin.

MAgPP	Flexural modulus (GPa)	Strain to failure (%)	Flexural strength (MPa)	Impact strength (kJ/m^2)
1	0.31	6.04%	11.70	41.17
2	0.39	5.35%	11.36	26.18
3	0.35	5.31%	11.80	60.53
Average	0.35	5.56%	11.62	41.79
Std	0.04	0.004	0.22	14.15

Impact Properties

The impact properties of the MAgPP resin are listed in the Table 4.15. Impact strength of the MAgPP sheet is approximately 41.15 KJ/m^2.

4.6.3 FTIR Spectroscopy Analysis of MAgPP Resin

The FTIR spectrum of the MAgPP is shown in Figure 4.43. The assessments of the FTIR peaks are listed in Table 4.16.

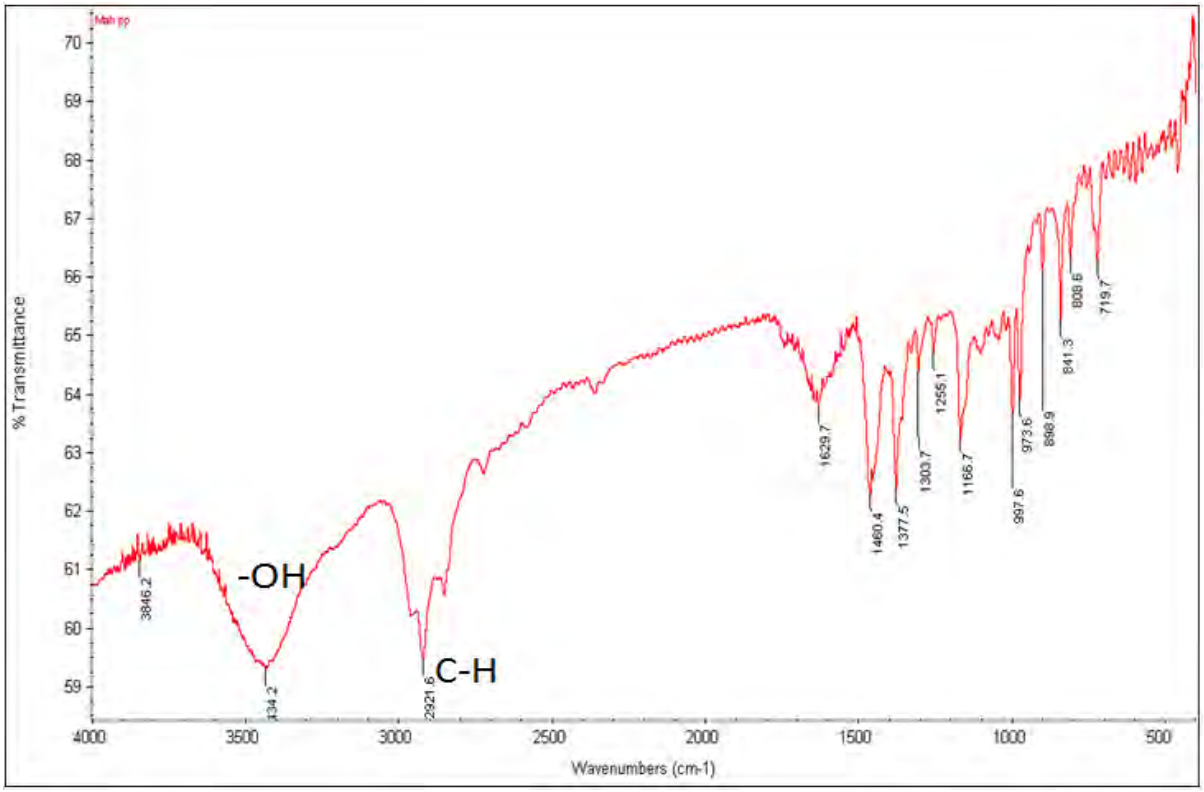

Figure 4.43: ATR- FTIR spectra of MAgPP matrix.

Table 4.16: Spectral data of MAgPP matrix.

Wave number (cm^{-1})	Possible assignment
3400-3500	O-H streching
~2900-2880	Doublet due to C-H vibration of-(CH_3) group
~1463.0	Methyl asymmetric deformation vibration
~1377.8	Methyl symmetric deformation vibration
~1166.9	C-C stretching, CH_3 wagging
~ 997.6	C-C s tretching, C H_2 rocking, C H_3 rocking. A bsorptions are due to the crystalline phase of PP
~ 983.2	C-C stretching, CH_2 rocking, CH_3 rocking. Absorption are due to the amorphous or irregular phase of PP
~898.9	C-C stretching, coupled C-H deformation
~841.1	C-C stretching, CH_2 rocking
~808.3	C-C stretching, coupled C-H deformation

4.6.4 Thermal Properties

Thermo gravimetric Analysis

The TGA and DTGA graphs are given in Figure 4.44. The curve is not so smooth. From the T GA graph it c an be c ertified that the the rmal s tability of the M AgPP is approximately 165 °C. The oxidation resistance abruptly decreased at t he t emperature range of 100-160°C.

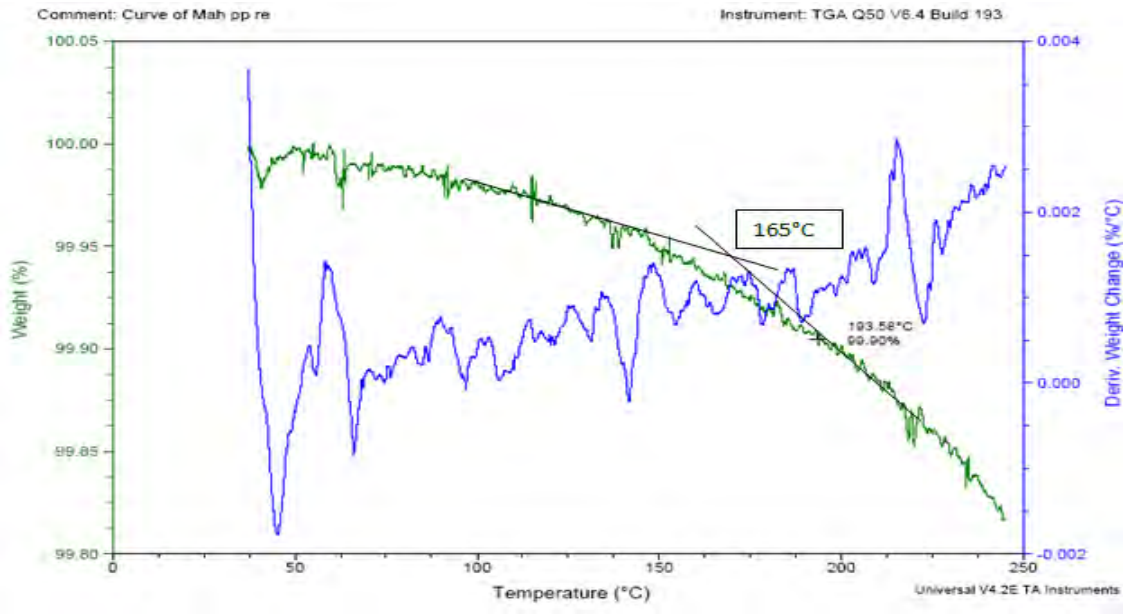

Figure 4.44: TGA graph of MAgPP.

4.6.5 Moisture Absorption Characteristics

The moisture absorption characteristics of MAgPP are shown in Figure 4.45. The moisture absorption characteristic of the matrix is similar in both distilled water and 10% HCl, however different at 10% NaCl. Unwanted peak were observed due to humidity change of the room.

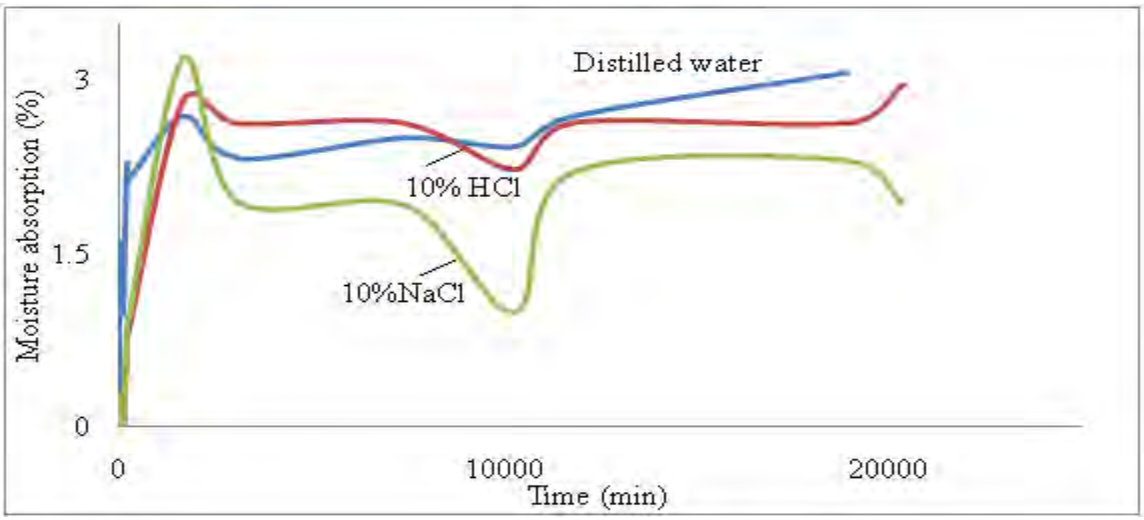

Figure 4.45: Moisture absorption characteristics of MAgPP.

4.6.6 Surface Morphological Study

The surface morphology of MAgPP is shown in Figure 4.46. The surface was smooth so there was no obligation to mark. Some scratch lines are shown in Figure 4.46, which was due to applied pressure in the sample during cutting process.

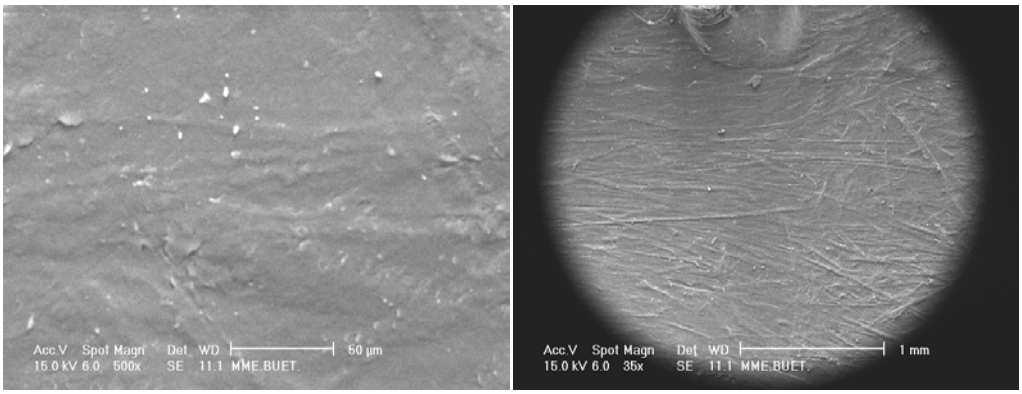

Figure 4.46: Surface morphology of MAgPP.

4.7 Composite Characterization

4.7.1 Mechanical Properties

Tensile Properties

During processing, the fibers tend to orient along the flow direction of matrix causing mechanical properties to vary in different directions [134]. As a result the mechanical properties of the different portion of the composite became different. To eliminate this effect, three samples from each type of composite were tested and the average values were calculated. The stress strain curves for the different fiber weight percentage of control jute composites are shown in Figure 4.47. The Young's modulus, tensile strength and strain to failure increased [134-136] with the fiber weight fraction in the control and treated jute composites as shown in Figure 4.48.

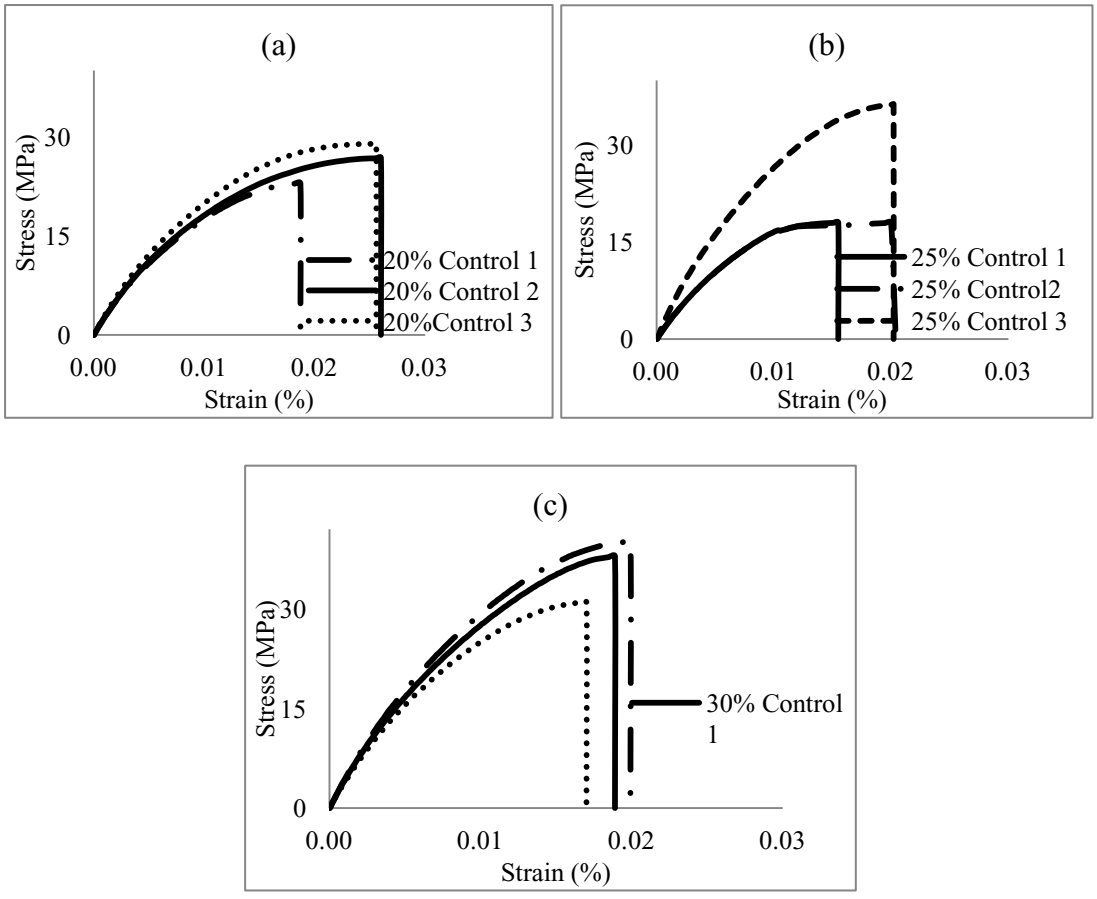

Figure 4.47: Stress-strain curves for transverse loading

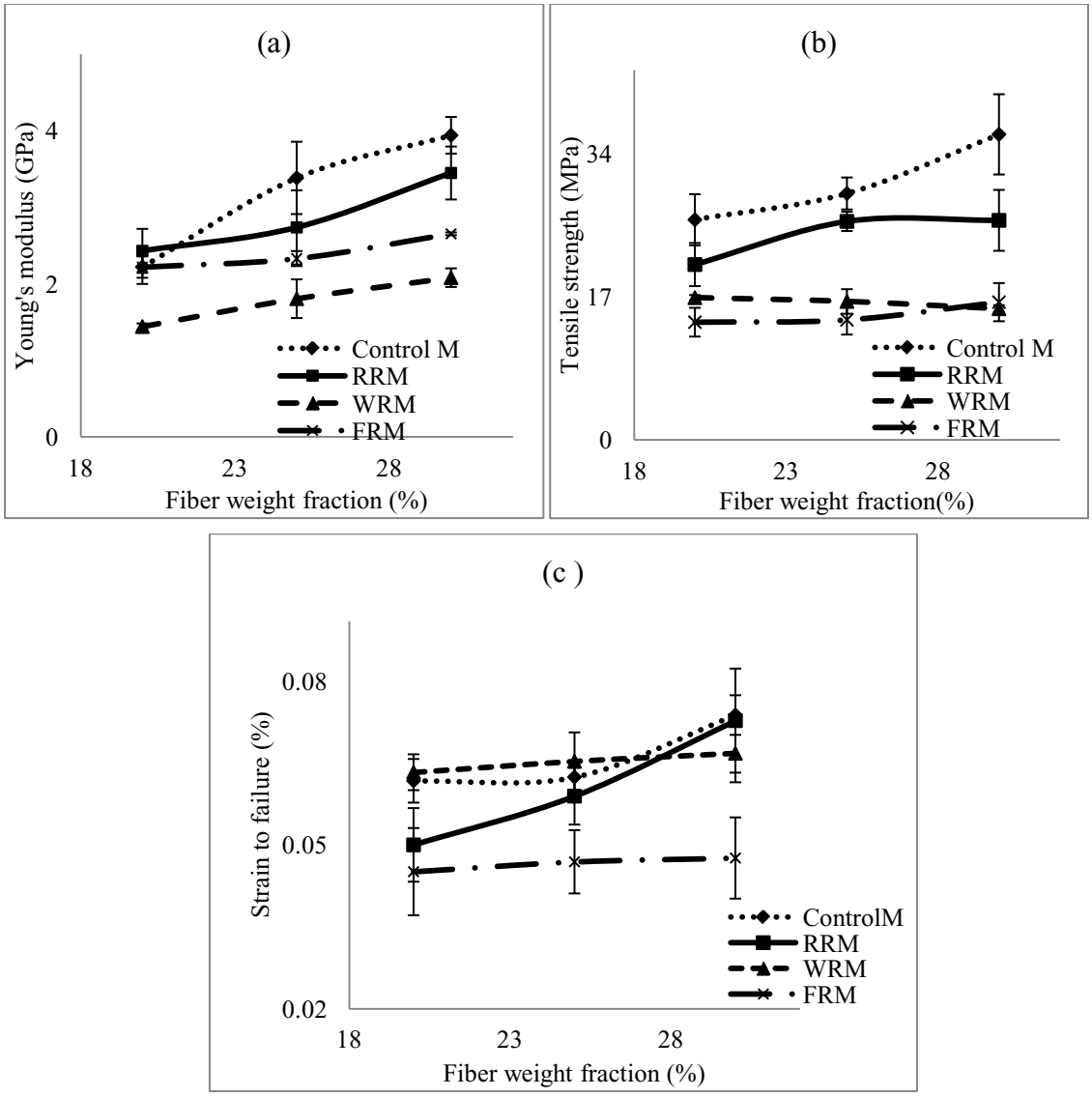

Figure 4.48: Variation of (a) Young's modulus (b) tensile strength and (c) strain to failure against fiber weight fraction of control and treated jute composites.

Young's modulus and tensile strength of control and treated jute composites increased compared to MAgPP. In present work the variation of the Young's modulus (Figure 4.48) increased with fiber loading in accordance with other researchers [136-141]. The Young's modulus increased by 217.74%, 177.41% 113.7% and 67.74% in case of raw, RR, FR and WR respectively compared to matrix.

During tensile loading partially separated microspace are created which obstructs stress propagation between the fiber and matrix [141]. As the fiber loading increases, the degree

of obstruction increases, which consequently increases stiffness. Young's modulus of treated composites decreased compared to the control composite. Similar trends were obtained in case of tensile strength and strain to failure. The decreasing trends may be due to poor adhesion between the fiber and the matrix. However, the values obtained are considerable for low load bearing situation. Poor fiber dispersion results in a loose bundle, embracing an effectively lower aspect ratio with less reinforcing potential than a single fiber. In addition, the bundle itself may be low in strength due to poor adhesion. Both of the above factors reduced the overall strength of the chemically treated composites [142-143]. That is why lower strength (Figure 4.48 (b)) was observed in chemically treated jute fiber composites.

In present work the variation of the tensile strength (Figure 4.48) increased with fiber loading in accordance with other researchers [138-141]. The tensile strength increased by 78.36% and 28.16% for raw and RR jute composites respectively compared to matrix. Removal of he micelluloses and lignin after rot retardant treatment, removed internal constraint and the fibrils became more capable of rearranging themselves in a compact manner. This led to a closer packing of the cellulose chain, which caused improvement in fiber strength and its mechanical properties. This is also responsible for the increase in the crystallinity of the rot retardant treated fiber as supported by XRD analysis.

Theoretical and practical value of tensile strength and the Young's modulus of the control composites are shown in the Table 4.17. To calculate these properties rule of mixture has been used. Practical values were found lower compared to the theoretical values.

Table 4.17: Theoretical and practical values of tensile strength and Young's modulus of control composite.

Weight fraction	Parameter	Theoretical value	Practical value
20%	Strength (MPa)	36.66	26.18
	Young's modulus(GPa)	03.90	02.22
25%	Strength (MPa)	46.61	29.31
	Young's modulus(GPa)	04.95	03.38
30%	Strength (MPa)	56.88	36.35
	Young's modulus(GPa)	06.05	03.94

Flexural Properties

Flexural properties are of great importance for any structural element. Composite materials used in structures are prone to fail in bending and therefore the development of a new composite with improved flexural characteristics is essential [132]. The flexural stress strain curves for the different fiber weight percentage of control composites are shown in Figure 4.49. The Figures reveal that slope and flexural stress increased with fiber weight fraction in control composite. These increments in the mechanical properties were related to the amount of lignin covering the fiber. The author has suggested that higher extension of the hydrogen bonds at fiber–matrix interface gave higher strength and stiffness to the jute MAgPP based composites.

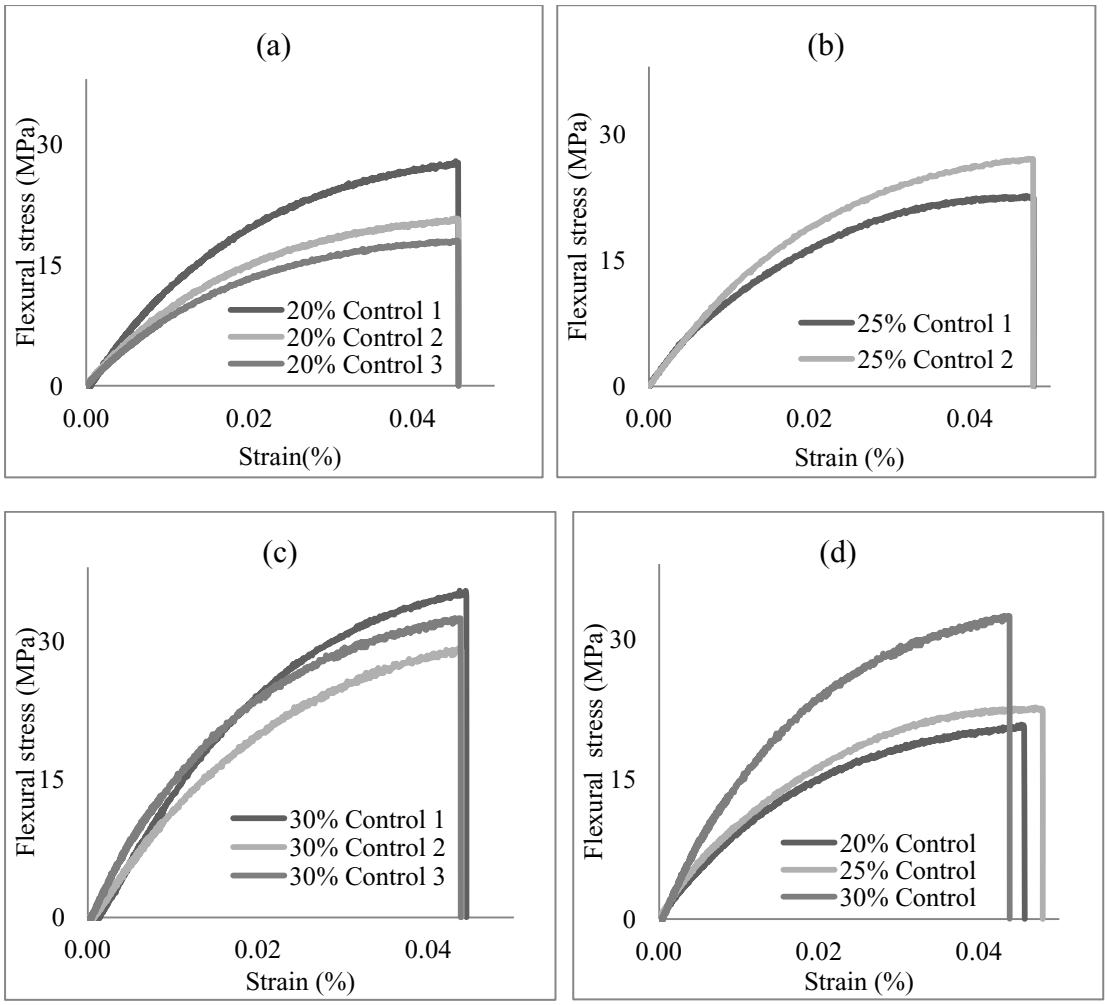

Figure 4.49 : Flexural stress strain curves of (a) 20%, (b) 25%, (c) 30% and (d) different weight percentage control fiber composites.

According to Dhakal [131], the increase in flexural modulus is more pronounced with higher fiber content specimens. The flexural properties of the composites i.e. flexural modulus and strength increased (Figure 4.50) with the fiber weight/volume (%) for control and treated jute fiber compared to MAgPP. After treatment, the flexural modulus and strength decreased more compare to the control composite. It could be due to good mechanical reaction at the interface between the chemically treated jute fiber and matrix results in better load transfer. However, the strain to failure did not follow similar trend.

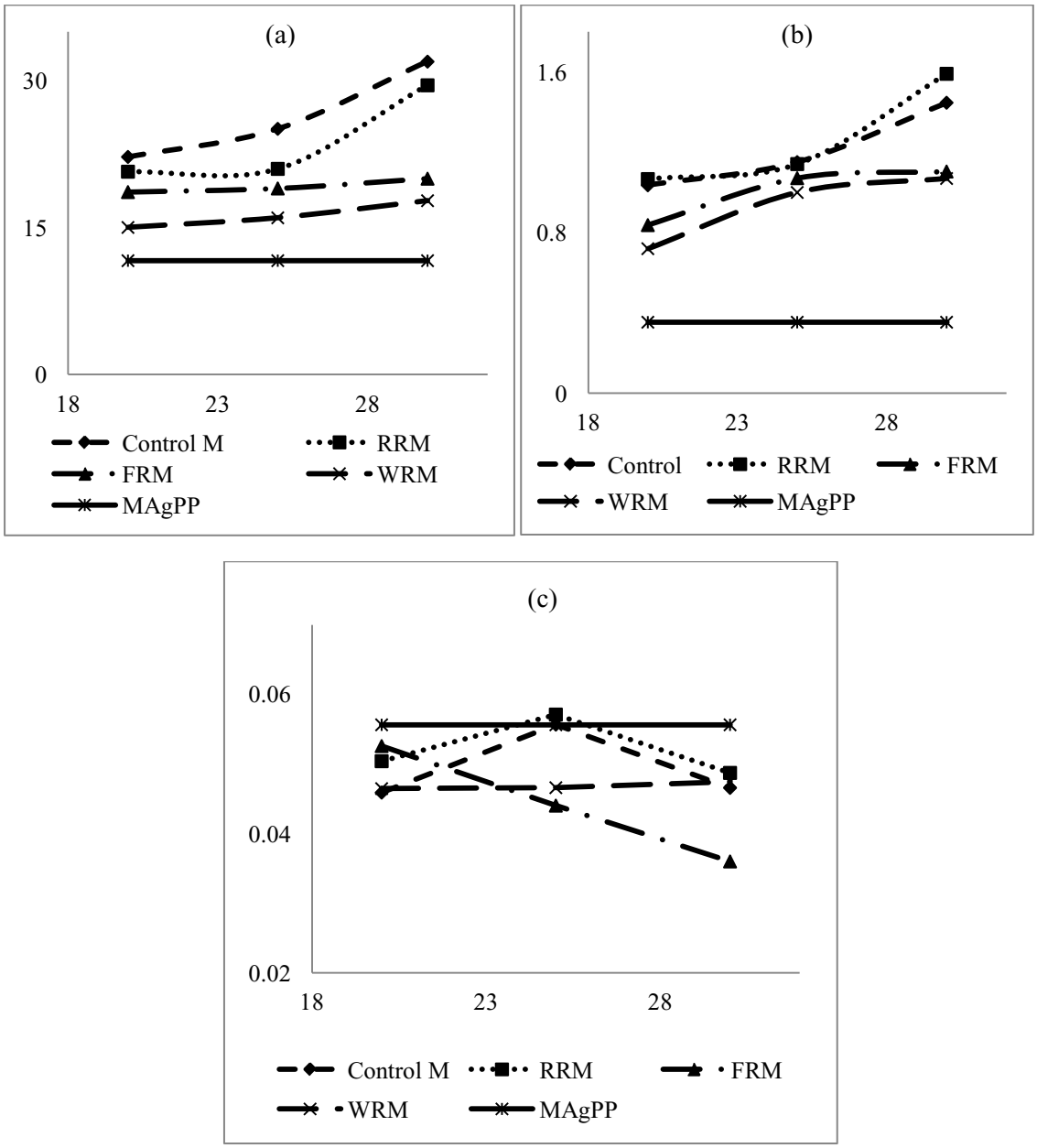

Figure 4.50: Variation of (a) flexural strength (b) modulus and (c) strain to failure against fiber weight fraction of different jute composites.

The flexural strength and modulus of control and chemically treated jute fiber composites are shown in the Figures 4.50 (a) and (b) respectively. The flexural strength increased with fiber loading according to other researchers [136, 141]. It is found that the flexural strength of control, RR, FR and WR jute composite increased approximately 174.85%, 154.03%, 72.05% and 52.60% respectively over the matrix.

According to Figure 4.50 (b) the flexural modulus increased with fiber loading as found by other researchers [136, 141]. The flexural modulus increased by 306.87%, 349.25%, 310.80% and 199.50% in case of raw, RR FR and WR composites respectively compared to the matrix. Since jute fiber is a modulus material, higher fiber concentration demands higher stress for the same deformation. Increased fiber matrix adhesion provides increased stress transfer between them. The flexural strength and modulus obtained in the current research are 31.95 MPa and 1.44GPa for control, 29.53MPa and 1.59GPa for RR, 20MPa, 1.1GPa, 17.74MPa and 1.06GPa for WR respectively.

Impact Properties

The impact energy of the composites increased with the fiber weight fraction (Figure 4.51) [5, 94]. However, after treatment, the energy decreased compared to the control fiber composite and the MAgPP [132]. As far as voids content in natural fiber composites is concern, the fabrication techniques are not yet fully developed and the natural origin of the fiber component necessarily induces an element of variation into the composites; both factors contribute in creation of voids which affects to the overall composite properties. It is evident in this study that as the fiber weight fraction of jute reinforced composite sample increases, the void content also increased. Due to this the influence of the rot, water and fire retardant chemicals on the impact properties is rather limited. The impact properties of the control, RR, FR and WR were decreased by 59.39%, 70.00%, 79.41% and 82.90% over the matrix.

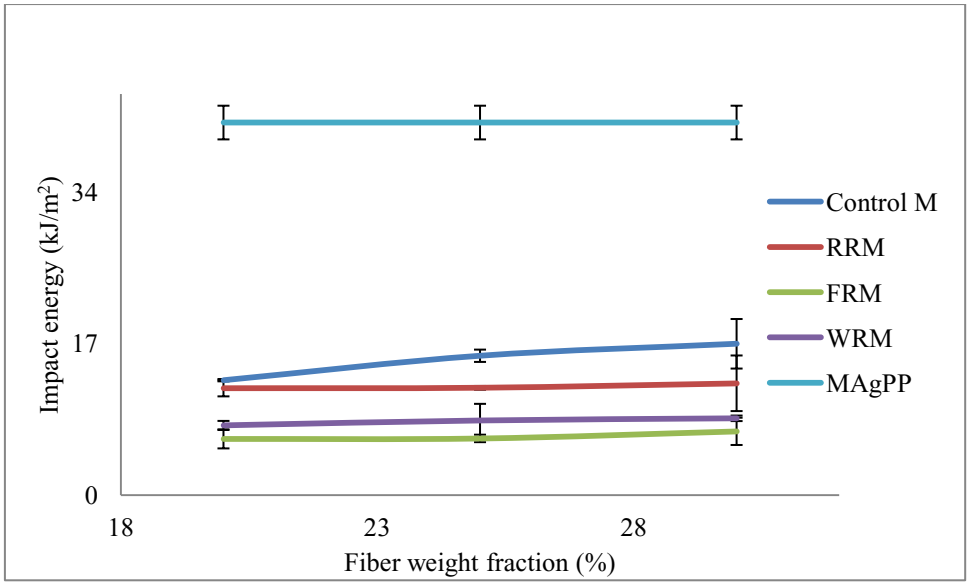

Figure 4.51: Variation of impact strength with fiber weight fraction of different composites.

The impact energy is slightly increased with the fiber loading according to other researchers [94, 145]. However the impact properties of the control and treated jute composites were decreased over the matrix. The improved impact strength of control jute composite can be explained by better toughness of the matrix itself [146].

The impact strength of the fiber reinforced polymer composites depends on the nature of the fiber, polymer and the fiber-matrix interfacial bonding [147]. It has been reported that higher fiber content increases the probability of fiber agglomeration which results in region of stress concentration requiring less energy for crack propagation [148]. As presented in the Figure 4.51 impact strength of all composites increase with fiber loading. These results suggest that the fiber was capable of absorbing energy because of strong interfacial bonding between the fiber and matrix. Another factor of impact failure of composite is fiber pull out. With increase in fiber loading, bigger force is required to pull out the fibers. This consequently increases the impact strength. The impact strength of the jute polyphene composites found in the previous research was 32-85 J/m [149].

4.7.1 Morphological Study

With the increase of the fiber weight fraction, the fiber content in the surface of control composites (Figure 4.52) increased. Similar results were obtained in case of chemically

treated (FR and RR) jute fiber composites (Figures 4.53 and 4.54). During processing, the fibers tend to orient along the flow direction of resin causing mechanical properties to vary in different directions [134]. The fiber direction was controlled by resin or matrix as shown in the surface morphology Figures 4.52 to 4.55.

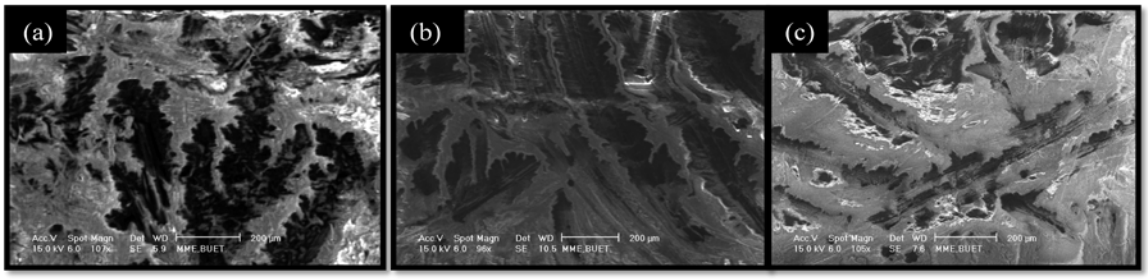

Figure 4.52: Surface morphology of (a) 20%, (b) 25%, and (c) 30% control jute composites.

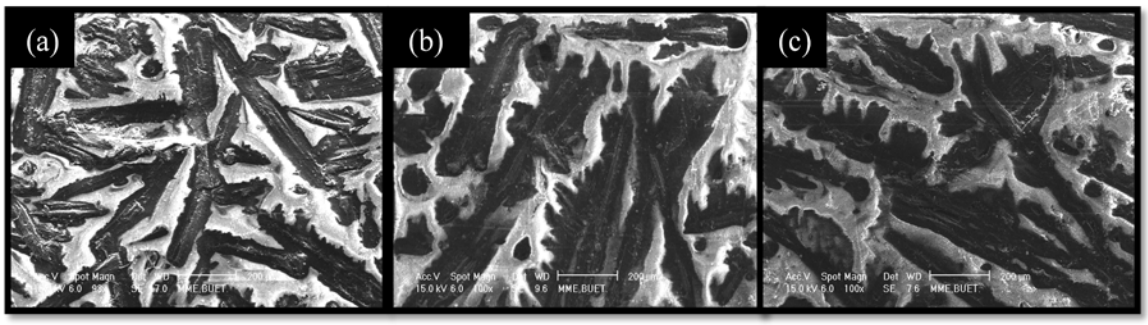

Figure 4.53: Surface morphology of (a) 20%, (b) 25% and (c) 30% FR treated jute composites.

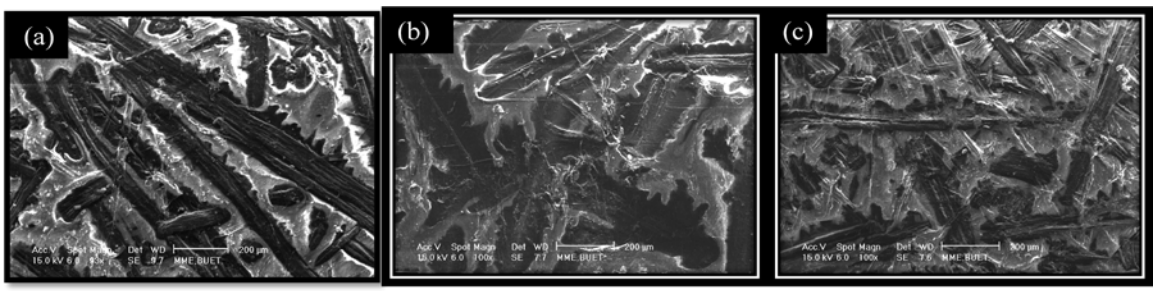

Figure 4.54: Surface morphology of (a) 20%, (b) 25% and (c) 30% RR treated jute composites.

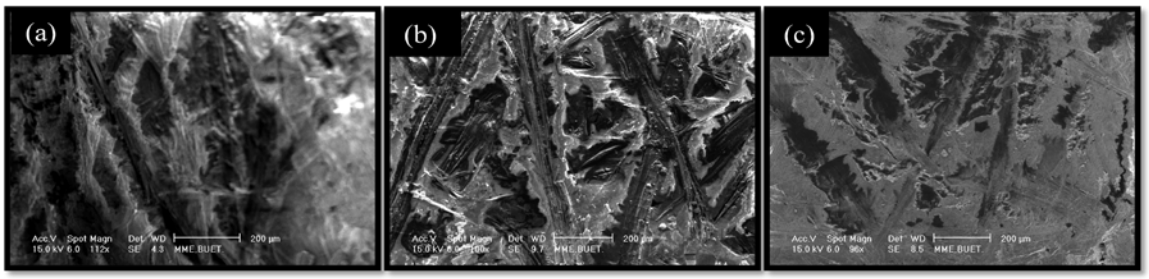

Figure 4.55: Surface morphology of (a) 20%, (b) 25% and (c) 30% WR treated jute composite.

The major limitations of using natural fibers as reinforcements in such matrices include poor interfacial adhesion between polar-hydrophilic fiber and nonpolar- hydrophobic matrix and difficulties in mixing due to poor wetting of the fiber with the matrix. This in turn would lead to composite with weak interface [135].

But in case of water retardant (WR) jute fiber composite, the fiber content did not clearly increase with the fiber weight fraction (Figure 4.55). In case of water retardant (WR) jute composite, the resin is highlighted compared to the other jute fiber composites. In some portion of the composite, only resin was present. From the surface morphology of the WR jute fiber composite, it can be concluded that the fibers of the water retardant were not well bonded with the resin MAgPP. Thus some void was found in the WR jute fiber composite. The mechanical properties of the WR jute fiber composite were affected due to void. In case of RR, FR and control fiber composite, the resin was properly mixed with the treated and control fiber.

4.7.3 Fracture Surface of the Composite

Fracture surface of the composites are shown in Figures 4.56 to 4.60. Those Figures reveal that the resin or matrix behaved as fiber. The resin pulled out from its position, elongated and finally broke down which is shown as like as fiber pull out.

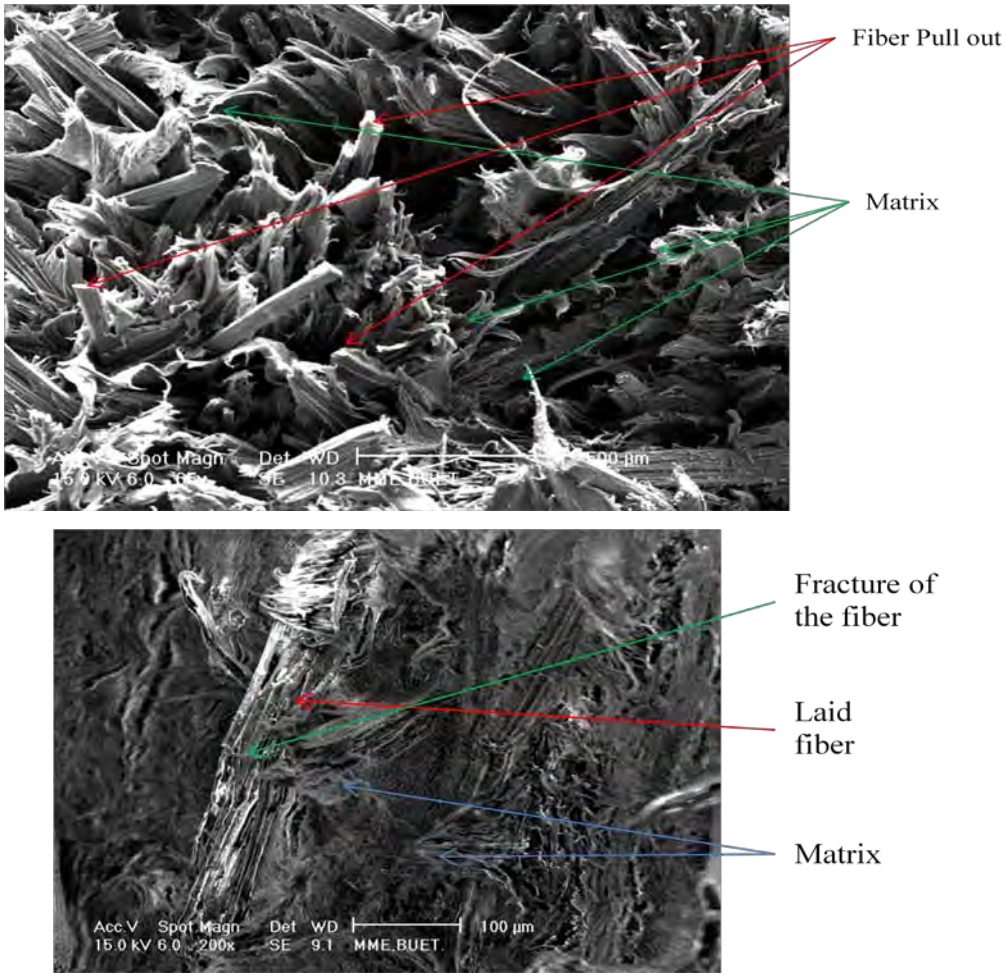

Figure 4.56: Fracture surface of control jute composite.

When fiber was positioned along the tensile test direction, the fiber as well as matrix was taking the load. However, when fiber was in the 90^0 position to the tensile direction, the fiber was taking the load due to high strength of fiber. That is why the matrix pulled out around the laid fiber along the tensile test direction.

In case of 30% FR jute composite (Figure 4.57(b)), the fiber mainly bear the load because of better bonding between the fiber and matrix. Mainly better bonding occurred as shown in the fracture surface. The adhesion between MAgPP and FR jute fiber is good, as broken jute fiber can be seen with no gap between the MAgPP matrix and jute fiber surfaces.

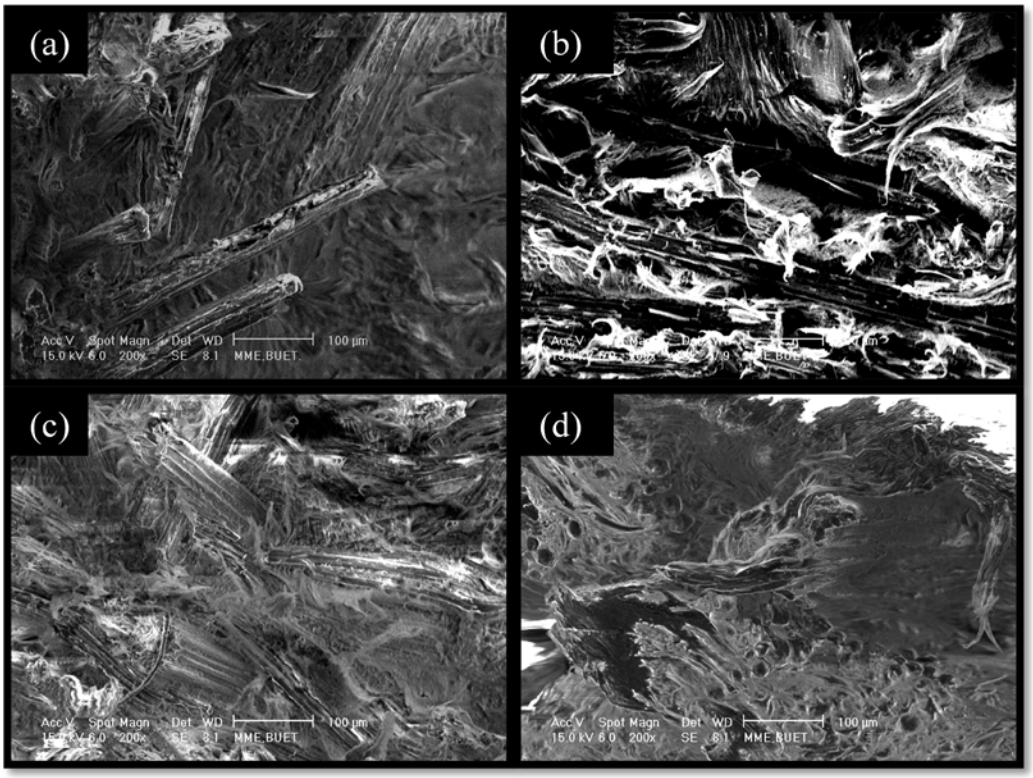

Figure 4.57: Fracture surfaces of the 30% (a) control, (b) FR, (c) RR and (d) WR jute composites.

In the 30% RR composite, sufficient fiber pull out occurred as shown in Figure 4.57 (c). The rot retardant jute fiber easily detach from the MAgPP matrix due to poor interfacial adhesion. When adhesion is not so good, there are voids around the jute fiber and places where jute has pulled out.

In case of 30% WR (Figure 4.57 (d)), less fiber and matrix pull out occurred. As a result, mechanical properties became poor. Some small and large types of voids were also present in the WR jute composites.

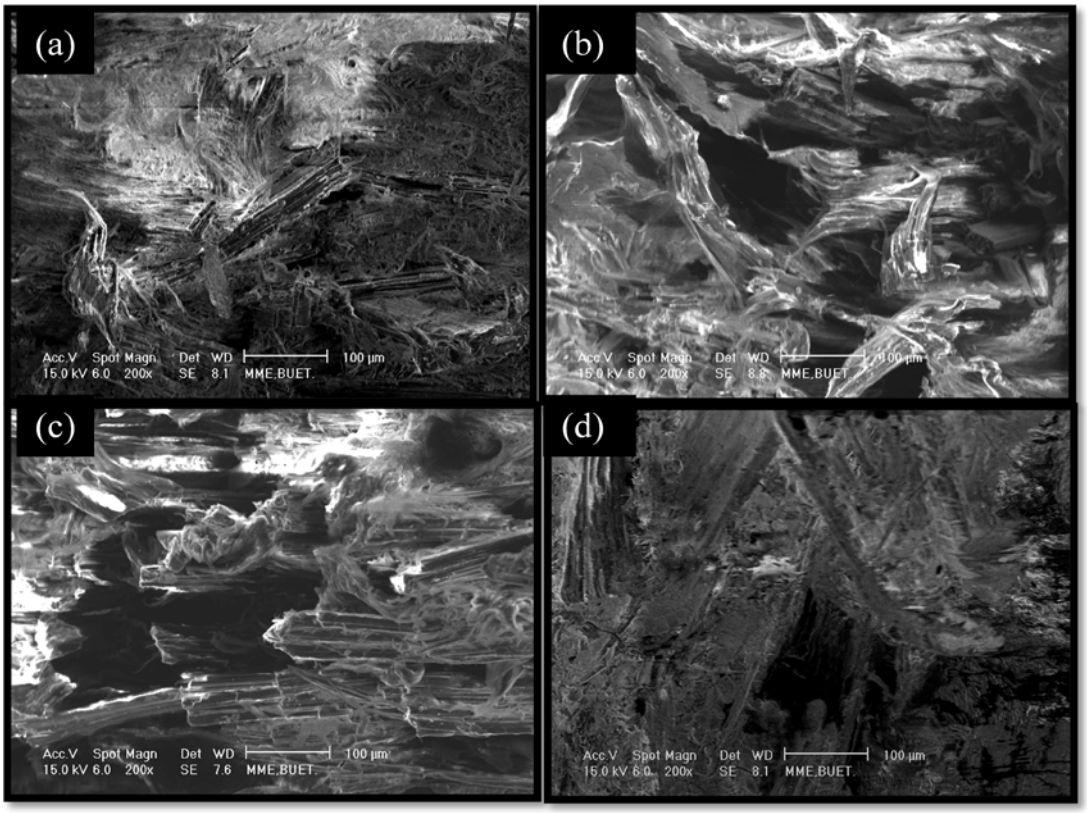

Figure 4.58: Fracture surfaces of 25% (a) control, (b) FR, (c) RR and (d) WR jute composites.

In case of 25% control fiber composite (Figure 4.58 (a)), the amount of jute fiber found was less compared to the 30% control fiber composite. In this case, fibers pulled out occurred as shown in Figure 4.58.

Generally, it is more difficult to differentiate jute fiber from the MAgPP matrix in case of 25% FR jute composite. This may suggest that the jute fibers are coated, probably by the matrix, and that the failure most commonly occurs in the matrix [117]. In case of 25% FR (Figure 4.58 (b)), the fracture surfaces were quite similar to 30% FR jute composite. In this case, the matrix pulled out. The bonding between the fiber and matrix was quite better. As a result the fiber was almost everywhere covered by the matrix. However the fiber pull out was not sufficient.

In case of 25% RR jute composite (Figure 4.58 (c)), the fiber pull out occurred as like as 30% RR jute composite.

In case of 25% WR jute composite (Figure 4.58 (d)), the fiber pull out was not observed. The amount of fiber present was less compared to control and RR jute composites. Void was also present in the composite.

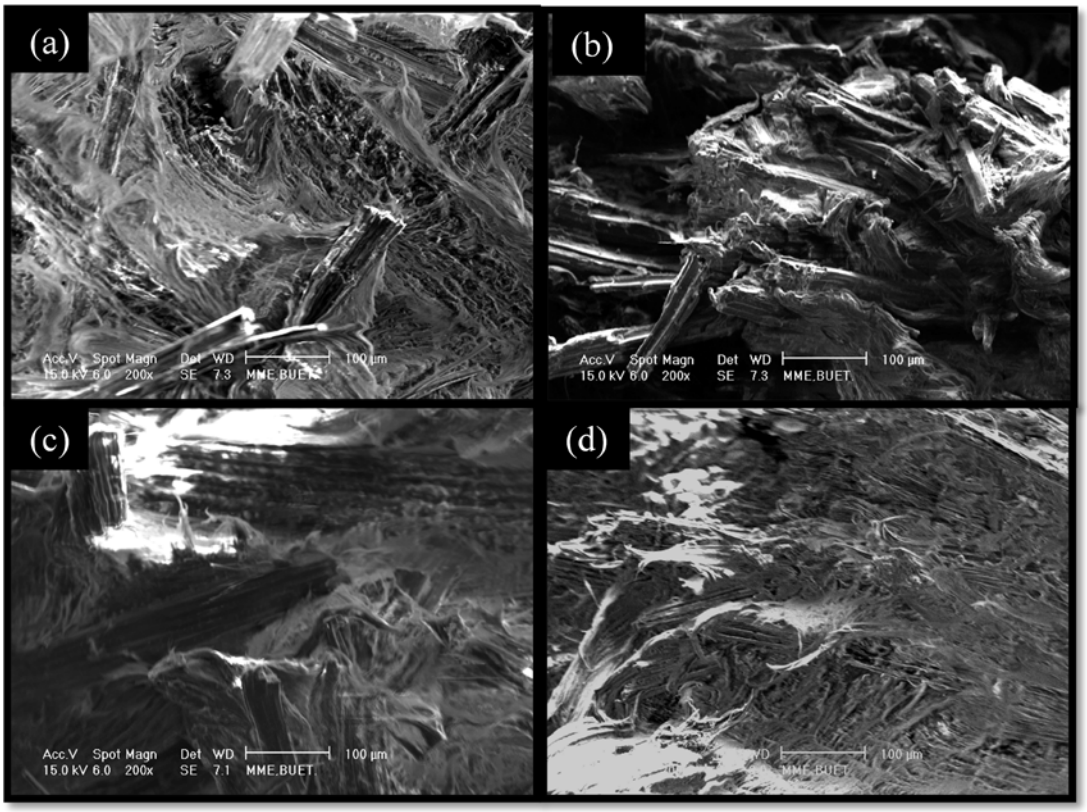

Figure 4.59: Fracture surfaces of 20% (a) control, (b) FR, (c) RR and (d) WR jute composites.

In case of 20% control, RR and FR jute composite, sufficient amount of fiber pull out were observed as shown in Figures 4.59 (a), (b) and (c) respectively.

In case of 20% WR jute composite (Figures 4.59 (d)), fiber pull out was not observed. However the matrix pulls out occurred in the fracture line.

4.7.4 Fourier Transform Infra Red Study

The FTIR observations of WR jute composites (Figure 4.60) reveal that with increase in fiber weight fraction, the transmittance value increased. The O-H peak became sharper with increasing fiber weight fraction.

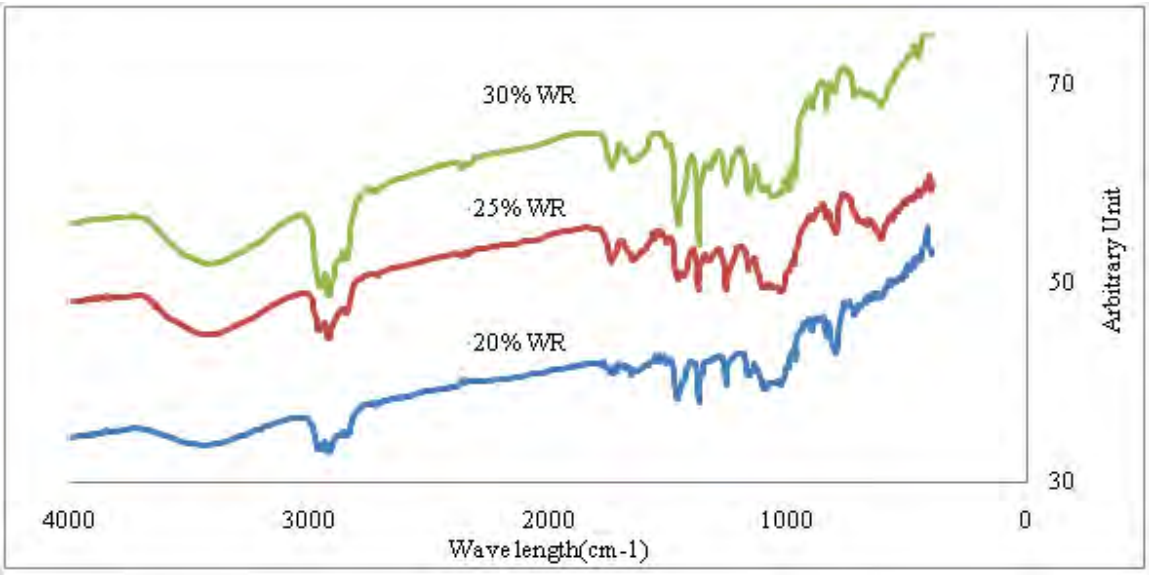

Figure 4.60: FTIR spectrum of WR jute composite corresponding to fiber weight fraction.

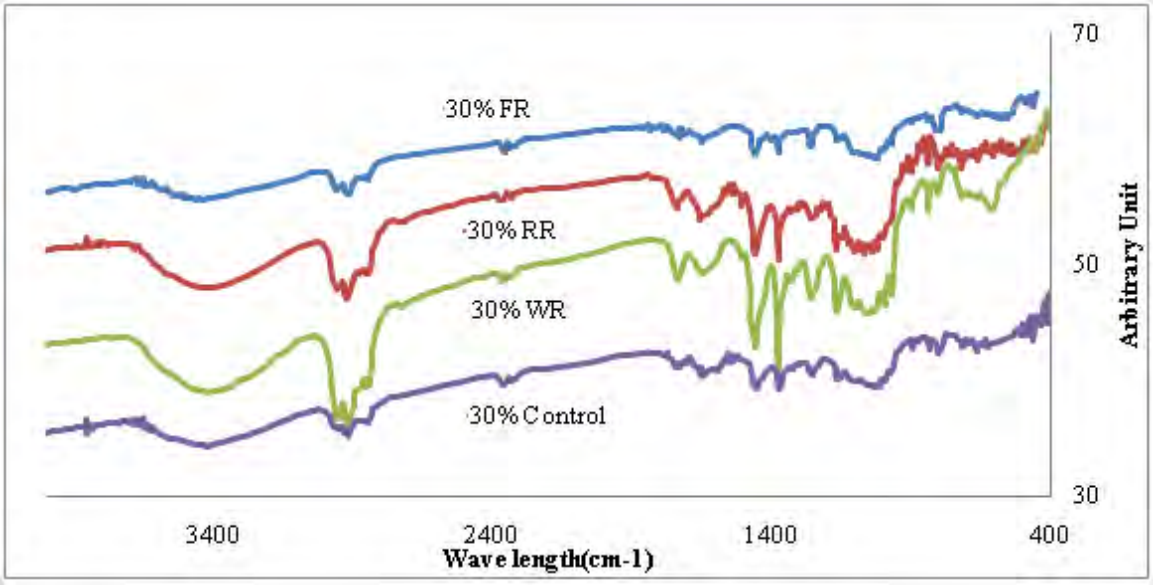

Figure 4.61: FTIR spectrum of different composites.

The FTIR spectrum of the different treated and control jute composites are shown in Figure 4.61. The OH peak of the RR and WR was sharper compared to control and FR jute composites. Each graph of the composite follow the MAgPP trends at lower wave length (1000-400cm^{-1}).

4.7.5 Moisture Absorption Characteristics

All natural fibers have a tendency to absorb moisture and possess low wettability by hydrophobic resins due to presence of hydrophilic hydroxyl groups of cellulose, hemicellulose and lignin. Hemicellulose is mainly responsible for the moisture absorption in

composites. Non crystalline cellulose and lignin also play an important role in moisture uptake process. Moisture diffusion in polymeric composites has shown to be governed by three different mechanisms [11, 12].

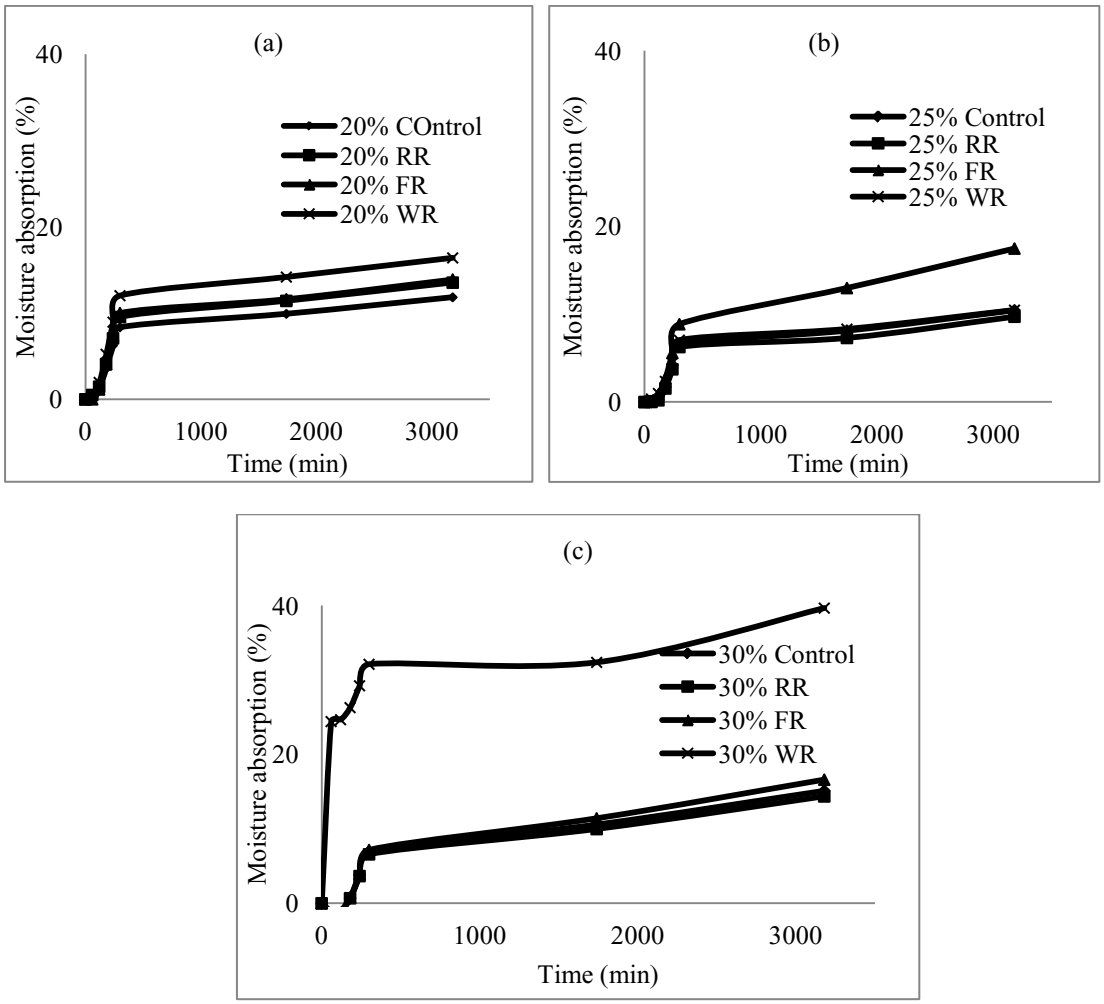

Figure 4.62: Moisture absorption characteristics of the (a) 20%, (b) 25% and (c) 30% treated and control jute composites.

The first involves diffusion of water molecules inside the micro gaps between polymer chains. The second involves capillary transport into the gaps and flaws at the interfaces between fiber and the matrix [137]. The moisture absorption characteristics of the control and treated jute composites are shown in Figure 4.62. The moisture absorption Figure reveal that the 20% WR (Figure 4.62 (a)) absorbed much water compared to other composites due to the void present in the composite. Similar result obtained in the case of

25% FR (Figure 4.62 (b)) and 30% WR (Figure 4.62 (c)) jute composite due to void present in corresponding composite. The SEM evidence supports this explanation.
At room temperature moisture uptake increased with fiber weight fraction (Figure 4.62) due to increased voids and cellulose content [118, 137]. The water absorption pattern of these composites at room temperature is found to follow Fickian behavior, whereas at the elevated temperature the absorption behavior is non-Fickian. Water uptake behavior is radically altered at elevated temperatures due to significant moisture induced degradation.

Swelling of fibers continues till the cell walls are saturated with water. After the saturation point, moisture exists as free water in the void structure leading to composite defects such as delamination and void formation. Absorbed moisture weakens the interfacial bonding, accelerates the delamination and hence decreases the tensile properties especially tensile strength. Absorbed moisture in composites causes hydrolytic degradation of resin, fibers interface during service [136].

Chapter 5

Conclusion and Recommendation for Future Work

5.1 Conclusion

In the present study, tensile testing of single raw and chemically treated jute fibers was carried out by varying span length. Surface morphology was observed by using scanning electronic microscope (SEM). Structural properties (crystalinity) were measured by X-ray diffraction analysis. Thermal properties were measured by differential scanning calorimetry (DSC) and thermo gravimetric analysis (TGA). Compositional analysis was carried out by Fourier Transform Infra Red (FTIR) spectrophotometer. Water uptake at different conditions was carried out for raw and chemically treated jute fibers. Subsequently, discontinuous random fiber orientated composites were manufactured and mechanical properties were determined. Based on the experimental results, the following can be concluded.

- The tensile strength and strain to failure decreased with increase in the span length. This is due to the presence of more flaws in longer span length fibers that makes the probability of failure larger. The Young's modulus increased with span length. This is because no extensometer could be used in the test set up and machine displacement was used for the modulus determination. So at longer span lengths, the relative effect of slippage in the clamps was smaller. Similar results obtained for raw and chemically treated top, middle and bottom portions jute fibers.
- The tensile properties (tensile strength, strain to failure and Young's modulus) of top, middle and bottom portions gradually changed with the span length. After correction, the strain to failure and Young's modulus became independent of the span length. The middle portion of the control fiber was found better according to strength, modulus and strain to failure data. However after rot retardant treatment, whole portion of the jute fiber showed nearly similar strength. So for this treatment, fiber can be collected from any portion of jute plant.

- The present study also reveals that accurate results of jute and chemically treated jute fibers can be successfully found by using newly developed technique. It is observed that with an increase in span length, machine displacement (alpha, •) also decreased. Among the rot retardant, fire retardant and water retardant fibers, rot retardant jute fiber had the highest Young's modulus values.
- Thermogravimetric analysis (TGA) was used to monitor the fiber decomposition as a function of increasing temperature. TGA results showed that the incorporation of chemically treated fiber increased the thermal stability of the fire retardant treated jute fiber. While the rot retardant coating did not show any improvement when compared with control fiber, the FR and WR coating showed significant difference in the thermograph. The decomposition of the fiber was significantly reduced which can be seen by the weight loss reduction even at 800 degrees. It can be concluded that the FR coating has a direct effect on the flame.
- Atomic force microscope was used to show that the surface roughness of fiber decreased with the rot and fire retardant chemical concentration. This was considered a proof for the surface coverage of the fibers with a rot retardant and fire retardant chemical layers.
- It was also seen that the crystallinity index of the jute fibers increased with rot retardant treatment. The increase in crystallinity obtained by rot retardant treatment of the jute fibers is thought to be the main contributing factor for the increase in fiber strength. Similar result has been obtained in case of fire retardant treated jute fiber.
- The percentage moisture uptake by RR jute fiber in pure water, 10% HCl and 10% NaCl as a function of time at room temperature evident that the moisture uptake behavior is quite different in water, acidic and saline environments supporting different diffusion processes. The equilibrium time was considerably longer in water and acidic environments compared to that in saline atmosphere. The observed trend in moisture uptake is acid > water > salt. Thus, substantially low moisture absorption tendency of RR/MAgPP in 10% NaCl supports its utility in marine applications.
- FTIR results showed the O-H bonds hifted as leftward in case of RR and rightward for WR and FR with increase in the chemical contents.
- Incorporation of modified jute fibers in polymer composites showed better interfacial bond between fiber and thermo plastic resin.

- Fiber reinforced MAgPP composites showed an improvement in tensile and flexural properties compared to MAgPP.

5.2 Recommendation for Future Work

In the present work, chemically treated and control fibers were characterized for polymer composite. The following recommendations are set out for future work.

- The cellulose and lignin content of the fiber and composite should be measured because the strength of the fiber and composite depend on those components.
- Chemical constituent of the rot retardant (Cu and CO_3) and fire retardant (NH_4) should be measured to observe the degree of rotting and flammability in the fiber and composite respectively.
- Weathering behavior of the rot and water retardant fiber and composite should be evaluated. Method of water retardant should be improved by chemical treatment.
- Surface tension of the rot and water retardant fiber should be measured to observe the water and other liquid adhesion and contact angle. Atomic force microscopy also should be carried out to observe the value of roughness in the fiber and composite surface. X-ray Photon spectroscopy (XPS) should be conducted on all treated fiber and composite to observe the surface properties.
- DSC and XRD analysis should be wider for application basis. To measure the density of the fiber, gass pycnometer should be used instead of only pycnometer.
- Composition of MAgPP needs to be known with accuracy. Proper mixing of MAgPP with fibers is required to get uniform mechanical properties. Different fabrication techniques can be used. In case of MAgPP polymer matrix composites processing, mold releasing agent is good enough, Teflon mould release agent or other sorts of chemical may produce good results. Without proper mold releasing agent, processing will be very difficult.
- Higher percentage of fiber could be incorporated through modern machine. To get better composite using chop fiber, the extruder machine may be used. Hybrid approach could be done for enhancing the mechanical properties and dimensional stability of the composite. Foaming could be incorporate to get light weight composites.

- The composite should be made by using other portion (top and bottom) of jute fiber to observe the effect on composite properties. All types of chemical treatment should be conducted on the fabric and after that their composite should be prepared by using different matrix.
- Moisture absorption characteristics (other environment conditions) of the composite and fiber should be checked out. Electrical property, friction and sliding wear property and durability of composite should be tested.

Bibliography

[1] E.T.N. Bisanda, and M.P. Ansell, "Properties of sisal - CNSL composites", Journal of Materials Science, Vol-27, pp: 1690 - 1700. 1992.

[2] M. S. Sreekala, M.G. Kumaran and S. Thomas, "Oil palm fibres: Morphology, Chemical composition, surface modification, and mechanical properties", Journal of Applied Polymer Science, Vol-66, pp: 821 – 835. 1997.

[3] L. Hegbom and B. Ultne, "Microscopy studies of some non-wood raw materials for the pulp and paper industry", Chemical and Process Engineering for Development – A challenge for the 21st century. 1990.

[4] L. Y. Mwaikambo, and M.P. Ansell, "The effect of chemical treatment on the properties of hemp, sisal, jute and kapok fibres for composite reinforcement", 2nd International Wood and Natural Fibre Composites Symposium June in Kassel/Germany Department of Materials Science and Engineering University of Bath, Bath BA2 7AY, UK,. pp:28-29. 1999.

[5] S. Biswas, Q. Ahsan, I. Verpoest and M. Hasan, "Effect of span length on the tensile properties of natural fibers", paper ID -116 accepted to be published to the International Conference on Advanced materials processing Technology by International Islamic University, Malaysia (IIUM), 2009.

[6] S. Shahinur, M. Kabir, N. Sultana, and Z. Hossain, "Report on Status of pulp and paper in Bangladesh", Bangladesh Jute Research Institute, pp: 1-12, April 2007.

[7] S. Sultana, "Studies on the effect of additives on the physic-Mechanical Properties of Jute Reinforced Composites". M. phil Thesis, Department Of Chemistry, Bangladesh University Of Engineering and Technology Dhaka, Bangladesh, July 2005.

[8] P. S. Murherjee, and K. G. Satyanarayana, "Structure properties of some vegetable fibers, part 1". Sisal fibre. Journal of Materials Science, Vol-19, pp: 3925-34. 1984.

[9] A. Bismarck, I.A. Askargorta, and, "Surface Characterization of Flax, Hemp and Cellulose Fibers; Surface Properties and the Water Uptake Behavior Polymer Composites", October 2002, Journal of Springerlink, Vol- 23, No- 5, pp: 872-894.

[10] P.O. Olesen and D.V. Plakett, "Perspectives on the Performance of Natural Plant Fibers"., Plant Fibre Laboratory, Royal Veterinary and Agricultural University., Copenhagen, Denmark Natural Fibres Performance Forum. pp: 1-7. 27 – 28 MAY 1999. http://www.ienica.net/fibersseminar/olesen.pdf .

[11] Rating report of Janata Jute Mills Ltd (JJML) Credit Rating Agency of Bangladesh, 28th February 2010 to 31 December 2010. mavinahmed@crab.com.bd and alamin@crab.com.bd .

[12] Taratola Road, Kolkata-700088, India, Workshop in International Jute Study Group.

[13] D. M. Baker, M. Edwards and C.G. Jarman, "The rot proofing of jute – a review". Tropical Science. T ropical pr oduct i nstitute, 56/ 62 G ray's Inn Road, London W CIX 8LU.Vol-23(3), pp: 197-204. 1981.

[14] W. G. MacMillan, "Deterioration of jute and other cellulosic materials. Part –I". The causes and mechanism of rotting. Jute Gunny Rev., Vol-8, pp: 753-759. 1956.

[15] A.B. Sen Gupta, "Yellowing of jute and its prevention". Jute Gunny Rev., Vol-6, pp: 453-459. 1954.

[16] S. N. Basu, and S.N. Gosh, "Fungi growing on j ute". Journal of Science Industrial Research, Vol- 9B, pp:151-155. 1950.

[17] S. N. Basu, and S. N. Ghose, "Fungal decomposition of jute fiber and cellulose part III. The decomposition of cellulose as influenced by its physical state and by associated substances". Journal of Textile Institute, Vol-43, T2789. 1952.

[18] H.W. Bustion and S. N. Basu. "Some factor affecting the growth and sporulation of cheatomium globosum and memnonilla echinata". Journal of Genetics Microbial Vol-2, pp:162-172. 1948.

[19] J. P. B hattachariya and S.N. Basu, "Comparative deterioration of j ute and cotton canvases due to microorganisms and weathering". Textile Research Journal, Vol- 33, pp: 868-869. 1963.

[20] W. G, Macmillan, S. N. Basu, and P. N. Pal, "Rot proofing of jute by treatment with soluble copper salt", Journal of Science Industrial Research Vol-16A, pp:135-137. 1957.

[21] C . D oree, T he m ethod of cellulose chemistry. 2 nd edition (Chapman a nd Hall, London) pp: 12. 1974.

[22] M . A li, "Cuprammonium f luidity as an i ndex of damage in lignified fibers", Bangladesh Journal of Science Industrial Research, Vol-9 No.-1-2, pp : 40-46. 1974.

[23] W.G. Macmillan and S.N. Bose, "The detection and estimation of damage in jute fiber part-I., A new microscopical test and the implementation of certain chemical tests", Journal of Textile Institute, Vol-38, pp: 353-367. 1947.

[24] H. Chatterjee, and A.K. Mazumder, "A note on the degradation of jute cellulose on storage". Textile Research Journal, Vol-29, pp: 282-283. 1959.

[25] H. M. Rahman, M.M.A. Bhuiyan, G. Mohiuddin and A.K.M. Mafizullah, "Studies on t he de gradation pa ttern of j ute dur ing r otting". Bangladesh jute r esearch Institute., Bangladesh Journal of Fiber Research, Vol-4(1and 2), pp: 21-26. 1979.

[26] P.L.D. Peill, "Permanent bleaching of lignocellulosic materials in Nature", Vol-158, pp: 554, 1946.

[27] W.G. M ack M illan, "Deterioration of jut e". Part-II., Anti r ot (microbiological) treatment and their application. Jute Gunny Rev.,Vol-8, pp: 831-841. 1956.

[28] S. R. Agarwal, and A. Sreenivasan, "Effect of impregnation of vinyl plastics on r ot resistance of j ute f abrics. I. r adiation i nduced gr afting". Indian J ournal o f Technology, Vol-12, pp: 630-640. 1974.

[29] S.N. Pandey, A. Day and M.D. Mathew , "Thermal Analysis of Chemically Treated Jute F ibers," Jute t echnological r esearch l aboratories, Indian C ouncil of a gricultural research, Calcutta 700 040, India, Textile Research Journal, Vol-63, pp: 143-150. 1993.

[30] Source: W ikipedia, t he f ree e ncyclopedia, http://en.wikipedia.org/wiki/Combustion Date of acess-11th February 2010.

[31] Source: http://en.wikipedia.org/wiki/Fire_retardant., Fire retardant, From Wikipedia, the free encyclopedia. Date of acess-11th February 2010.

[32] Source: http://en.wikipedia.org/wiki/Flame., Flame, From Wikipedia, the free encyclopedia. Date of acess-11th February 2010.

[33] L ittle, W R obert, "Flame pr oofing T extile F ibers". American C hemical S ociety Monograph No. 104, Reinhold, New York. 1947.

[34] S . B uck, G eorge. "Flameproofing A gents". T he E ncyclopedia of Chemistry, b y George L. Clark and G. G. Hawley. Reinhold, New York. 1957.

[35] S. C oppick, "Mechanisms of F lameproofing. C hapter 3 i n Flame p roofing" Textile Fabrics, by Robert W. Little, Reinhold, New York. 1947.

[36] F . R . E irich, I. S aad, a nd J . M . Leonard, "Improvement o f T hermal S tability o f Textile Fibers". Annual progress report by Polytechnic Institute of Brooklyn on C ontract No. N 140(132)57745B, R esearch a nd D evelopment D iv. , U . S . N avy C lothing a nd Textile Office, U. S. Naval Supply Activities. 1957.

[37] M . A . G ottlieb a nd Irvin, "Theory o f Fl ame-Retardant F inishes". Textile R esearch Journal, Vol-26, pp: 156-68. 1956.

[38] A. Gellius, Noctes atticae XV, 1 (reported in reference 113). pp:113-164. 1956.

[39] L. M artin. "A W eather-Resistant F ireproofing T reatment f or C otton Fabrics". U . S . Department of Agriculture Circular, pp: 466. 1938.

[40] H . A . S chuyten, J . W . W eaver a nd R . J . D avid, "Some T heoretical A spects of t he Flameproofing of C ellulose". N o. 9 of Advances i n C hemistry S eries, Fire R etardant Paints, published by American Chemical Society. 1954.

[41] Jr. S chwenker, F . R obert, a nd P . E ugene, "Chemically M odifying C ellulose f or Flame Resistance". Industrial and Engineering Chemistry, Vol-50, pp: 91-6. 1958.

[42] S ource: http://en.wikipedia.org/wiki/Flame_retardant., F lame r etardant., From Wikipedia, the free encyclopedia. Date of access 21th February 2010.

[43] J. E . R amsbottom, "The F ireproofing of F abrics". Department o f S cience and Industry R esearch (Great B ritain). (Includes e arlier ma terial in reports of R amsbottom and Snoad, A. W. in 1925 and 1926) 1947.

[44] L . F . H awley a nd J. W iertelak, "Effect of M ild Heat T reatment on the C hemical Composition of Wood". Industrial and Engineering Chemistry, Vol-23, pp: 184-6. 1931.

[45] K. Katsushiro and Y. Eiichi, "The Decomposition Process of Wood Constituents in the Course of Carbonization. I. The Decomposition of Carbohydrate and Lignin in Mizunara". Journal of Japan Wood Research Society, Vol-3(4), pp: 125-7. 1957.

[46] A. Kuriyama, "Studies on Carbonization Phenomena in Wood. VIIL Pyrolysis of Cellulose and Lignin in Wood". Journal Japan Wood Research Society, Vol-4(1), pp: 30-4. 1958.

[47] W.M. Robert and A. H. White, "Partial Hydrolysis of Wood". Industrial and Engineering Chemistry, Vol-35, pp: 297-301. 1943.

[48] R. L. Mitchell, R. M. Seborg, and M. A. Millett, "Effect of Heat on the Properties and Chemical Composition of Douglas-fir Wood and Its Major Components". Journal Forest Products Research Society, Vol-3(4), pp: 38-42, 72-73. 1953.

[49] B. O. Nekleevich, "Carbonization of Wood". Mem. Inst. Chem. Tech. Acad. Sci., Ukrain S. S. R. Vol-8, pp: 64-66. 1938.

[50] D. F Othmer, and W. S. Fred. "Destructive Distillation of Maple Wood". Industrial and Engineering Chemistry. Vol-33, pp : 188-96. 1941.

[51] V. N. Sergeeva, and A. Vaivads, "Thermographic Study of Pyrolysis of Wood and Its Constituents". Latvijas PSR Zinatnu Akad. Vestis, Vol-9 (Whole No. 86), pp: 103-8. 1954.

[52] T. Haruhiko. "Mechanism of Thermal Decomposition of Coal". International Journal of Coal Research Institute (Japan), Vol-3, pp:43-8. 1952.

[53] C. D. Hurd, The Pyrolysis of Carbon Compounds. Chemical Catalogue Co. (now Reinhold), New York. 1929.

[54] Mutti and Montalti, "A Study of the Possibility of Obtaining Alcohol from Cellulose and from Wood through the Medium of Levoglucosan". Ann. chim. Applicata ., Vol-17, pp: 188-96. 1927.

[55] B. C. Herodotus, Neun Bucher Geschichte (ed. Goldhagen) Vol-II, pp: 172, 180 (reported in reference 113).

[56] D. Hird and D. L. Simms, "Fire Retardant Treatments". Wood Vol-18, pp: 92-5, 134-7, 176-7. 135 Vitruvius. Writings X, 21 (reported in reference 113). 1953.
[57] M. W. Sandholzer, Flameproofing of Textiles. National Bureau of Standards, Circular C455. 1946.

[58] J. Franke and others. "Report of Committee on the Uses of Wood in Building Construction". National Fire Protective Association Proceedings, pp: 106-7. 1915.

[59] R. Schlegel, V. Chemie, and G. M. B. H. Berlin, "Investigation of the Scientific Basis of the Fireproofing of Wood". Mathematical Formulation of the Mass Law in the Fire Protection of Wood. Korrosion u. Metallschutz Vol-10, pp: 195-6. 1934.

[60] J. L . G ay-Lussac, “Note on t he P roperties of S alts f or Making Fabrics Incombustible”. Ann. Chim., Vol- (2)18, pp: 211-17. 1821.

[61] S. R . S engupta, “ Bromination of j ute f abrics”, I ndian Jute I ndustrial Research Association., Calcutta, India Clearage, Vol- 22(18), pp:35-8, 1975.

[62] L. M enachem, f lameproofing l ingocellulosic articles. Chemical a bstract, State of Israel, pp: 59., 8971a.

[63] R . A. D avis, U .S F ire r etardency of l ignocellulosic m aterials b y phosphorilating chlorinated or brominated lignocellulosics, pp:71., 92852W

[64] W. Little, Robert, Flame p roofing T extile Fibers. American Chemical S ociety, Monograph No. 104, Reinhold, New York. 1947.

[65] M. A. Tyuganova, Z.A. Rogovin and Kryazhv., “Fire resistance cellulose materials”., chemical abstract., Vol-78, pp: 5639k.

[66] F. Jr. Schwenker and P. Robert Eugene, and flame resistance derivation, U.S. patent reference 2 990 232 June 27. 1961. www.freepatentsonline.com/2990232.html

[67] M . A . H ossain, A .S. M ia, a nd M .A. S alam, “ Effect of ammonium br omide a nd phosphoric a cid on j ute f or f ire r esistance”. Bangladesh Journal of J ute a nd F iber Research, Vol–V, No-1&2, pp: 40-44, December 1980.

[68] G . C amino, N . G rassie, I. C . M cNeill, “Influence of t he fire r etardant, a mmonium polyphosphate, on t he thermal de gradation of poly(methyl m ethyl acrylate).”, Chemistry Department, University of Glasgow, Glasgow G12 8QQ, Scotland., Journal of Polymer Science: Polymer Chemistry Edition, Vol-16, Issue 1, pp : 95 – 106.

[69] J. T aylor a nd F . P ollock, “Effect of V arious C hemicals, M ore P articularly S odium Bicarbonate, on the Ignition of Cellulose, Coal Dust, and Activated Charcoal”. Fuel Vol-28(4), pp: 77-87. 1949.

[70] M . H . G eorge, T . R . T ruax a nd C . A . Harrison, “Experiments i n F ireproofing Wood”. 3r d pr ogress r eport. A merican W ood-Preservers' A ssociation Proceedings, pp: 71-93. 1932.
[71] L . P eter, “Flameproofing A gent”. D ingler's Polytechnic J ournal J ahr., Vol-74(290), pp: 230-5. 1893.

[72] T . K enji, “Pyrolysis a nd C ombustion of C ellulose i n the P resence of Inorganic Salts”. Bulletin Chemical Society., Japan Vol-24, pp: 164-8. 1951.

[73] T. Setsuro, I. Yoshiki, and M. Satoshi. “Physicochemical Studies of Wood”. Journal Chemical Society Japan, Vol-55, pp: 30-52. 1934.

[74] T . R. T ruax, The U se of C hemicals i n F orest Fire C ontrol. Forest P roducts Laboratory mimeographed report. 1939.

[75] F. Versmann and A. Oppenheim, "On the Comparative Value of Certain Salts for Rendering Fibrous Substances Noninflammable", British Association of Advance Science Report, Trans. Sect. Meetings., Vol-29, pp: 86. 1859-60.

[76] P. W. Robert, and M. W. Westgate, "Fire-Resistance and Fire-Retardant Compositions - A Patent Survey". National Paint, Varnish & Lacquer Association, Scientific Section Circular pp: 727. 1948.

[77] A. Kling, and D. Florentine, Genie civil Vol-80, pp: 180. 1922.

[78] F. L. Browne, Theories Of Combustion Of Wood And Its Control December Madison 5, Wisconsin United States Department of Agriculture Forest Service In Cooperation With The University of Wisconsin Forest Products Laboratory Madison. Report no-1236, pp: 2, 5, 7, 9 and 59. 1955.

[79] Source: http://www.cf-chem.com/pages/product15-e.htm Date of access 3rd March 2010.

[80] S. Stevens, HES Extension, College of Human Environmental Sciences, University of Missouri-Columbia

[81] W. Brouwer, "Natural fibre composites in structural components: alternative application for sisal? Seminar, Commond Fund for Commodities- Alternative Applications for Sisal and Henecuen". Rome: Food and Agriculture Organization of the UN (FAO) and the Common Funds for Commodities (CFC). 2000.

[82]. Chemical modification of agro-resources for property enhancement, Paper and Composites from Agro-based resources. CRC Press, Boca Raton, 1996.

[83] J. Comyn, Adhesion Science, RSC Paperbacks, Cambridge, 1997.

[84] C. A. S. Hill and H. P. A. Khalil, Journal of Applied Polymer Science, Vol- 77, pp:1322. 2000.

[85] R. S. Williams, C William. Feist, Water Repellents and Water-Repellent Preservatives for Wood Department of Agriculture, Forest Service, Forest Products Laboratory, General Technical., Report FPL–GTR–109 United States.

[86] S. Malaysiana, R. Wirawan, E.S. Zainudin and S.M. Sapuan, "Mechanical Properties of Natural Fibre Reinforced PVC Composites: A Review" Vol-38(4), pp: 531–535. 2009.

[87] Madison 5, Wisconsin., Department Of Defense., Handbook "Composite Materials Handbook"., Polymer Matrix Composites. Guidelines for Characterization of Structural Materials Mewls Cif Ti11, Vol-1.

[88] Patent 6165920 Issued on December 26, 2000. Estimated Expiration Date: March 31, 2019. http://www.patentstorm.us/patents/6165920/description.html., patent strom., www.patentstorm.us/patents/6165920/description.html

[89] J. A. Brydson, “Plastic Materials” seventh edition. Oxford, Elsevier. Callister, W. D. pp: 744-761. 1997.

[90] M. R. Rahman, M. M. Huque, M. N. Islam and M. Hasan, “Improvement of physico-mechanical pr operties of jut e f iber reinforces pol ypropylene composites b y post-treatment”, Composites: Part A, Vol- 39, pp: 1739–1747. 2008.

[91] http://en.wikipedia.org/wiki/Polypropylene Date of access 3rd march 2010.

[92] K.S. Whiteley, T . G H eggs, H . K och a nd W . I mmel, pol yolefins, In U llmann’s Encyclopedia o f Industrial c hemistry, V ol- a 21 Fifth E dition, V CH publ ishers, E ditors: B. Elvers, S. Hawkins, G. Schulz, 1992.

[93] G. Harutun a nd A. K arian, “ Handbook of pol ypropylene and P olypropylene composites” pp: 32-57.

[94] Md. S aiful Islam, S ilk F iber R einforced P olymer C omposites: F abrication a nd Mechanical P roperties, thesis Bachelor of S cience in Materials a nd Metallurgical Engineering, Bangladesh University of Engineering And Technology. October 2009.

[95] S. Kusmono, “Effects O f C lay M odification A nd C ompatibilizers O n T he Mechanical, M orphological, A nd T hermal P roperties O f P olyamide 6/ Polypropylene Nano composites”, University of Malaysia , 2008

[96] L. Drzal, D. Mohanty, R. Burgueno and M. Misra,. “Bio-based structural composite materials f or hous ing a nd i nfrastructure applications: oppor tunities a nd c hallenges”. Proceedings of t he N SF H ousing R esearch A genda W orkshop, V ol- 2, pp : 129 -140. 2004.

[97] S. I. Mavani, N. M. Mehta and P. H. Parsania, “Synthesis, Fabrication, Mechanical, Electrical and M oisture A bsorption S tudy of Epoxy P olyurethane–Jute a nd E poxy Polyurethane–Jute–Rice/ W heat H usk Composites”, J ournal of A pplied P olymer Science., DOI 10.1002 /app: pp:1228-1233 P ublished onl ine i n W iley Inter S cience (www.interscience.wiley.com), 6 July 2007.

[98] S. H. Aziz, and M.P. Ansel, “The effect of alkalization and fiber alignment on t he mechanical and thermal p roperties of ke naf a nd he mp ba st f iber c omposites: pa rt-I-polyester resin matrix”, Composite Science Technology, Vol-64 pp: 1219-30. 2004.

[99] G. Mehta, L.T Drzal, A.K. Mohanty and M. Misra, “Effect of fiber surface treatment on t he pr operties o f bi ocomposites f rom non woven i ndustrial he mp f iber m ats and unsaturated polyester resin”, Journal of Applied Polymer Science., Vol-99(2), pp: 1055-68. 2005.

[100] D . R ay, B.K. S arkar, a nd N. Bose, “ Impact f atigue be havior of vinylester r esin matrix c omposites r einforced with alkali tr eated jut e f ibers”, Composites Part-A, Vol-33(2), pp: 233-41. 2002.

[101] J. George, M.S. Sreekala and S. Thomas. “A review on i nterface modification and characterization of na tural f iber r einforced pl astic c omposites”, P olymer Engineering Science Vol-41, pp: 1471-85. 2001.

[102] J. Gassan and A. K. Bledzki, "Possibilities of forming the mechanical properties of jute/epoxy composites by alkali treatment of fibers", Composite Science and Technology, Vol-59, pp: 1303-1309, 1999.

[103] A. Mukherjee, P.K. Ganguly, and D.J. Sur, "Structural Mechanics of jute: the effect of hemicelluloses or lignin removal" Journal of Textile Institute., Vol-84, pp: 348. 1993.

[104] J. Gassan, and A. K. Bledzki, "Alkali treatment of jute fibers: relationship between structure and mechanical properties", Journal of Applied Polymer Science, Vol- 71(4), pp: 6230-9. 1999.

[105] N. Sgriccia, M.C. Hawley and M. Misra, "Characterization of natural fiber surfaces and natural fiber composites" Received 8 January 2007; revised 30 June 2008; accepted 14 July 2008. Available online 24 July 2008.

[106] S. Jafrin, F. A. Dilruba, M. K. Uddin, I. Gomes and M. E. Islam "Uses of natural fruit (diospyros embrypteris pers) as a rot-proofing agent", Daffodil International University Journal of Science And Technology, Vol- 4(1), January 2009 .

[107] I. Vogel (Third Edition). A Text-Book of Quantitative Inorganic analysis Including Elementary instrumental analysis: The English Language Book Society and Longmans, Green & Co. Ltd. pp: 358, 1961.

[108] ASTM Standard D-570. Standard test methods for water absorption plastics. Annual book of ASTM standard; 2002.

[109] LABORATORY TEST MANUAL FOR 16 CFR Part 1610 : Standard for the Flammability of Clothing Textiles, United States Consumer Product Safety Commission October 2008.

[110] K. Srikulkit, C. Iamsamai, S. T. Dubas, "Development of Flame Retardant Polyphosphoric Acid Coating Based on the Polyelectrolyte Multilayers Technique" Journal of Metals, Materials and Minerals., Vol-16(2) pp:41-45. 2006.

[111] L. Roger. Blaine, "Determination of Polymer Crystallinity by DSC" Ph.D Thesis. TA Instruments, 109 Lukens Drive, New Castle DE 19720, USA., pp: 1 TA123-3 TA123

[112] Elin Persson., Laboratory Assignment Processing & Sample Preparation., LTH Department of Polymer and Materials chemistry, Polymer Physics., Teaching assistant., Elin Persson, pp:12-15.2010.

[113] B. R. Guduri and S. C. C. George, Lawrance and R. D. Anandjiwala, "The Effect of Water Absorption on Mechanical Properties of Hemp Fibre/Polyolefin's Composites".

[114] A. Pietak, S. Korte, E. Tan, A. Downard, M. P. Staiger, "Atomic force microscopy characterization of the surface wettability of natural fibers", Science Direct, Applied Surface Science, Vol- 253, pp:3627-3635, 2007.

[115] ASTM Standard D 638-01. Standard test methods for tensile properties of plastics. Annual book of ASTM standard; 2002.

[116] ASTM Standard D 6110-97. Standard test methods for determining the charpy impact resistance of notched specimens of plastics. Annual book of ASTM standard; 2002

[117] ASTM Standard D 790-00. Standard test methods for flexural properties of unreinforced and reinforced plastics and electrical insulating materials. Annual book of ASTM standard; 2002

[118] A. K. Bledzki, and J. Gassan,. "Composites reinforced with cellulose based fibres". Progress of Polymer Science, Vol- 24(2), pp: 221-74. 1999.

[119] S. N. Pandey and A. Day, and M. D. Mathew, "Thermal Analysis of Chemically Treated Jute Fibers". Textile Research Journal, Vol-63, pp: 143. 1993.

[120] I. K. Varma, S.R. Anantha Krishnan and S. Krishnamoorthy "Effect of Chemical Treatment on Density and Crystallinity of Jute Fibers", Textile Research Journal, Vol- 59, pp: 368 http://trj.sagepub.com 1989.

[121] J. R. Barone, "Polyethylene/keratin fiber composites with varying polyethylene crystallinity", Vol-36, pp:1518–1524., Science Direct., Composite Part-A, Applied science and manufacturing., www.elsevier.com/locate/compositesa. 2005.

[122] R. Bodîrlău and C.A. Teacă, "Fourier Transform Infrared Spectroscopy And Thermal Analysis Of Lignocellulose Fillers Treated With Organic Anhydrides", Rom. Journal of. Physics, Vol- 54, No- 1–2, pp: 93–104, Bucharest, 2009.

[123] A. K. Mubarak, F. Mina and L. T. Drzal, "Influence Of Silane Coupling Agents Of Different Functionalities On The Performance Of Jute-Polycarbonate Composite". 3rd International Wood and Natural Fibre Composites Symposium September, Kassel/Germany pp:19-20, 2000.

[124] Y.R. Sharma, Elementary Organic Spectroscopy. S. Chand & Company Ltd. 2000.

[125] P. U. Agarwa and N. Kawai " Self-Absorption Phenomenon In Near-Infrared Fourier Transform Raman Spectroscopy Of Cellulosic And Lignocellulosic Materials" Applied Spectroscopy, Vol-59, No-3, pp: 102-5. 2005.

[126] M. J. John and R. D. Anandjiwalal, "Recent Developments in Chemical Modification and Characterization of Natural Fiber-Reinforced Composites". Polymer Composites. Vol-195, pp : 187-207. 2008.

[127] Chapter 7. XRD (Chapter 8 Campbell & White, Alexander "X-ray Diffraction Methods in Polymer Science").

[128] Sławomir Borysiak, Beata Doczekalska , "Research into the Mercerization Process of BeechWood Using the Waxs Method", Fibres & Textiles in Eastern Europe, January / December / B, Vol- 16, No- 6 (71) pp: 101-103. 2008.

[129] L. A. Pothan, F. Simon, S. Spange, and S. Thomas, XPS Studies of Chemically Modified Banana Fibers, American Chemical Society, Biomacromolecules, Vol -7 (3), pp: 892–898, 2006.

[130] J. Gassan, V. S. Gutowski, "Effect of corona discharge and UV treatment on the properties of jute-fiber epoxy composites". Composite Science and Technology, Vol- 60, pp : 2857-2863, 2000.

[131] H.N. Dhakal , Z.Y. Zhang, M.O.W. Richardson "Effect of water absorption on the mechanical properties of he mp fibre reinforced unsaturated polyester composites". Composites Science and Technology, Vol- xxx, pp: xxx–xxx.2006.

[132] B. Suresha, B .N. Ravi Kumar, M. Venkataramareddy T . Jayaraju "A Role of micro/nano fillers on mechanical and tribological properties of polyamide66/polypropylene composites", Materials and Design, Vol-31, pp: 1993–2000. 2010. www.elsevier.com/locate/matdes

[132] I. Bashir, I Alaloush, A.L. Raqibah and M. Ibrahim, "Evaluation of Three Methods for the Measurement of Crystallinity of PET Resins, Preforms, and Bottles", Polymer Engineering and Science, Vol- 40, No- 11 pp: 2442-2455, November 2060.

[133] Q. Ahsan, University of Cincinnati, 2009.

[134] Maya Jacob John, Rajesh D . Anandjiwala, "Recent Developments in Chemical Modification and Characterization of Natural Fiber-Reinforced Composites". Published online in Wiley Inter Science (www.interscience.wiley.com).VVC 2 007 Society of Plastics Engineers.

[135] S. V. Prasad, C Pavithran, P.K. Rohatgi. "Alkali treatment of coir fibers for coir–polyester composites", Journal of Material Science, Vol-18, pp : 1443-1454. 1983.

[136] H.S. Yang, H.J. Kim, J. Son, H.J. Park, B.J. Lee and T.S. Hwang . " Rice –husk flour filled polypropylene composite: mechanical morphological study". Composite structure, Vol-63, pp: 305-12. 2004.

[137] M . M . Thwe and K . Liao, "Effects of environmental aging on the mechanical properties of bamboo-glass fiber reinforced polymer matrix hybrid composites". Composite A. Vol-33, pp: 43-52. 2002.

[138] A . K . Rana, A . Mandal and S . Bandyopadhyay, "Short fiber reinforced polypropylene composite: effect of compatibiliser, impact modifier and fiber loading ". Composite Science Technology. Vol-63, pp: 801-806. 2003

[139] F. Vilaseca, J. A. Mendez, A. Pelach, M. Lop, N. Canigueral and J. Girones et al. "Composite materials derived from biodegradable starch polymer and jute strands". Process of Biochemistry. Vol-42, pp: 329-34. 2007

[140] M.S. Jamil, I. Ahmed and I. Abdullah. "Effect of rice husk filler on the mechanical and thermal properties of liquid natural rubbercompatibilizedhigh density

polypropylene/natural rubber blends". Journal of Polymer Research. Vol-13, pp: 315-21. 2006.

[141] S. Joseph, M. S.Oommen, P. Koshy, S.A. Thomas, "A comparison of mechanical properties od phe nol f ormaldehyde c omposite r einforced w ith ba nana f iber a nd g lass fiber".Composite Science Technology, Vol-62, pp:1857-68. 2002.

[142] N. Chand and P. K. Rohatgi, "Adhesion of sisal fibre-polyester system", Polymer Communications, Vol-27, pp: 157–160. 1986.

[143] L. Ponsonnet, K. Reybier, N. Jaffrezic, V. Comte, C. Lagneau, M. Lissac and C. Martelet, "Relationship be tween s urface pr operties (roughness, w ettability) of titanium and titanium alloys and cell behavior". Vol-27, pp: 151–169. 1968.

[144] Vincent Busigny, Pierre Cartigny, Pascal Philippot and Marc Javoy "Ammonium quantification in muscovite by infrared spectroscopy". Chemical Geology, Vol- 198, pp: 21–31. 2003.

[145] Jayaraman K, "Manufacturing sisal polypropylene composite with minimum fiber degradation." Composite Science Technologyk. Vol-63, pp: 367-74. 2003

[146] K ristiina O ksman, C raig C lemons, " Mechanical P roperties P olypropylene-Wood and Morphology of Impact M odified Flour C omposites" Journal of A pplied P olymer Science, Vol- 67, pp: 1503-1513, 1998.

[147] Joseph P .V., M athew G , J oseph K , a nd T homas S .A. " Dynamic m echanical properties of short sisal fiber reinforced polypropylene composites", Composite A, Vol-34, pp: 275-90. 2003.

[148] Karmakar A, Chauhan S. S. Modak J.M. and Chanda M, "Mechanical properties of wood f iber r einforced polypropylene c omposite", C omposite A , V ol-38, pp: 227-33. 2007.

[149] Mishra S., Naik J.B., Patil Y.P., "The compitibilizing effect of maleic anhydride on swelling a nd m echanical pr operties of pl ant f iber r einforced nov olac com posites", Composite Science Technology, Vol-60, pp: 1729-35. 2000.

Appendix 1

Table A.1: Tensile properties of raw jute middle portion.

Span length	Diameter (mm)	Tensile strength (Mpa)	Uncorrected Young's modulus (GPa)	Uncorrected strain to failure (%)	Corrected Young's modulus (GPa)	Corrected strain to failure (%)
5 mm	64.33±13.23	405.60±143.36	9.59±4.29	3.59%±0.0058	26.29±9.58	0.93%± 0.0025
15 mm	67.13±12.77	311.73± 74.09	18.13±6.89	1.97%±0.0089	26.39±10.96	0.93%±0.0061
25 mm	67.12±13.12	264.60±88.66	19.64±5.63	1.45%±0.0041	26.32±7.80	0.93%±0.0033
35 mm	66.76±12.95	248.62± 130.17	20.91±6.52	1.03%±0.0044	26.98±8.69	0.92%±0.0049

Table A.2: Comparison between uncorrected and corrected tensile properties of raw jute fiber middle portion.

Span length	Young's modulus (GPa)	Strain to failure(%)	Corrected Young's modulus (GPa)	Corrected strain to failure (%)
5 mm	9.59±4.29	3.59%±0.0058	26.29±9.58	0.93%± 0.0025
15 mm	18.13±6.89	1.97%±0.0089	26.39±10.96	0.93%±0.0061
25 mm	19.64±5.63	1.45%±0.0041	26.32±7.80	0.93%±0.0033
35 mm	20.91±6.52	1.03%±0.0044	26.98±8.69	0.92%±0.0049

Table A.3: Corrected tensile properties of 4% RR middle portion.

Span length	Diameter (µm)	Tensile strength (MPa)	Corrected Young's modulus (GPa)	Strain to failure (%)
5 mm	99.10±20.11	228.06±60.83	26.29±9.58	0.74%±0.0069
15 mm	89.78±15.51	183.70±53.41	22.68±4.32	0.74%±0.0025
25 mm	84.60±14.55	159.76±65.40	22.45±4.97	0.74%±0.0022
35 mm	78.39±12.20	147.25±59.19	22.60±4.78	0.74%±0.0024

Table A.4: Corrected tensile properties of 8% RR miidle portion.

Span length	Diameter (µm)	Tensile Strength (MPa)	Corrected Young's Modulus (GPa)	Strain to failure (%)
5 mm	70.06±12.82	270.58±64.12	26.29±9.58	0.75%±0.0022
15 mm	93.18±15.27	222.88±31.78	23.96±3.67	0.75%±0.0026
25 mm	78.95±13.41	198.58±63.740	23.84±2.20	0.75%±0.0017
35 mm	80.55±13.49	193.31±72.41	23.86±4.62	0.75%±0.0023

Table A.5: Corrected tensile properties of 20% RR miidle portion.

Span length	Diameter (µm)	Tensile strength (MPa)	Corrected Young's modulus (GPa)	Strain to failure (%)
5 mm	82.76±15.91	332.64±139.01	26.29±9.58	0.76%±0.0040
15 mm	90.41±17.45	258.49±90.22	25.92±7.71	0.76%±0.0018
25 mm	83.32±16.06	221.55±135.66	25.88±3.33	0.76%±0.0049
35 mm	92.61±14.87	217.51±76.55	25.47±7.88	0.76%±0.0036

Table A.6: Corrected tensile properties of raw jute fiber top portion.

Span length	Diameter (µm)	Tensile strength (MPa)	Corrected Young's modulus (GPa)	Strain to failure (%)
5 mm	79.50±12.98	195.15±113.48	15.90±5.65	0.64%±0.0011
15 mm	75.31±14.95	162.86±66.77	15.90±5.15	0.65%±0.0027
25 mm	69.80±11.30	140.00±46.12	15.86±3.77	0.65%±0.0014
35 mm	80.01±11.98	129.21±48.46	15.25±5.26	0.65%±0.0018

Table A.7: Corrected tensile properties of 4%RR of top portion.

Span length	Diameter (µm)	Tensile strength (MPa)	Corrected Young's modulus (GPa)	Strain to failure (%)
5 mm	58.41±10.86	222.99±33.13	22.46±12.67	0.75%±0.0046
15 mm	59.39±11.59	191.49±94.90	22.35±14.19	0.75%±0.0025
25 mm	48.39±7.45	168.72±78.96	22.20±8.21	0.75%±0.0006
35 mm	52.45±8.89	155.05±63.00	22.26±8.56	0.76%±0.0005

Table A.8: Corrected tensile properties of 8%RR of top portion.

Span length	Diameter (µm)	Tensile strength (MPa)	Corrected Young's modulus (GPa)	Strain to failure (%)
5 mm	68.96±12.34	245.87±69.71	20.21±10.53	0.72%±0.0005
15 mm	74.18±12.13	213.76±89.00	21.41±6.741	0.74%±0.0015
25 mm	74.28±10.03	183.30±79.99	21.85±11.04	0.74%±0.0022
35 mm	84.88±13.58	169.34±44.78	22.00±10.85	0.73%±0.0017

Table A.9: Corrected tensile properties of 20%RR of top portion**.**

Span length	Diameter (µm)	Tensile strength (MPa)	Young's modulus (GPa)	Strain to failure (%)
5 mm	76.94±12.64	294.04±108.77	22.79±8.68	0.73%±0.0039
15 mm	77.77±12.30	243.23±77.21	22.71±11.67	0.73%±0.0029
25 mm	66.52±10.22	212.06±92.16	22.29±8.61	0.73%±0.0019
35 mm	73.53±11.75	201.39±105.92	22.03±6.12	0.73%±0.0025

Table A.10: Corrected tensile properties of raw bottom portion.

Span length	Diameter (µm)	Tensile strength (MPa)	Corrected Young's modulus (GPa)	Strain to failure (%)
5 mm	62.88±9.89	214.62±92.47	17.44865±6.47	0.66%±0.0019
15 mm	69.46±10.80	151.54±36.58	17.44723±5.55	0.66%±0.0025
25 mm	85.66±15.35	107.66±66.19	17.45768±6.31	0.66%±0.0033
35 mm	82.87±12.97	84.17±61.43	17.62376±2.36	0.66%±0.0030

Table A.11: Corrected tensile properties of 4%RR bottom portion.

Span length	Diameter (µm)	Tensile strength (MPa)	Corrected Young's modulus (GPa)	Strain to failure (%)
5 mm	69.89±12.95	251.32±118.74	19.78±14.00	0.74%±0.0048
15 mm	63.66±10.15	190.10±82.04	19.83±10.09	0.74%±0.0032
25 mm	78.65±13.96	156.60±91.85	19.90±6.30	0.74%±0.0026
35 mm	62.93±9.36	153.76±26.62	19.90±6.30	0.74%±0.0021

Table A.12: Corrected tensile properties of 8%RR of bottom portion.

Span length	Diameter (µm)	Tensile strength (MPa)	Corrected Young's modulus (GPa)	Strain to failure (%)
5 mm	64.33±10.71	270.80±175.68	20.09±22.41	0.75%±0.0026
15 mm	66.85±9.72	212.56±124.75	20.35±4.27	0.75%±0.0031
25 mm	70.86±14.32	184.08±117.443	20.43±7.03	0.75%±0.0017
35 mm	64.39±10.03	174.69±73.816	20.45±0.89	0.75%±0.0034

Table A.13: Corrected tensile properties of 20%RR of bottom portion.

Span length	Diameter (µm)	Tensile strength (MPa)	Corrected Young's modulus (GPa)	Strain to failure (%)
5 mm	87.02±14.09	310.73±74.02	22.06±4.42	0.76%±0.0045
15 mm	78.86±11.98	229.52±43.56	22.42±9.03	0.76%±0.0024
25 mm	78.34±10.67	210.34±57.27	22.62±9.07	0.76%±0.0024
35 mm	74.02±10.92	192.70±108.98	22.64±8.05	0.76%±0.0031

Table A.14: Corrected tensile properties of raw and rot retardant middle portion jute fiber.

Fiber types	Average tensile stress (MPa)	Average Young's modulus (GPa)	Average strain (%)
Control M	279.71~418.39	29.63	0.93%
4% RRM	171.79~363.17	22.67	0.74%
8% RRM	171.34~300.90	23.70	0.75%
20% RRM	104.33~246.89	25.66	0.76%

Table A.15: Corrected tensile properties of raw and rot retardant top portion jute fiber.

Fiber types	Average tensile stress (MPa)	Average Young's modulus (GPa)	Average strain (%)
Control T	93.81~212.59	15.73	0.65%
4% RRT	127.45~222.99	22.32	0.51%
8% RRT	136.97~245.87	21.37	0.51%
20% RRT	162.99~277.77	22.46	0.56%

Table A.16: Corrected tensile properties of raw and rot retardant bottom portion jute fiber.

Fiber types	Average tensile stress (MPa)	Average Young's modulus (GPa)	Average strain (%)
Control C	84.17~272.36	17.49	0.66%
4% RRC	164.77~341.51	20.24	0.74%
8% RRC	129.86~278.37	20.32	0.75%
20% RRC	121.02~299.47	22.44	0.76%

Table A.17: Uncorrected Young's modulus of RR top, middle and bottom portions.

	Uncorrected Young's modulus(GPa)				Uncorrected strain to failure (%)			
Span length	5	15	25	35	5	15	25	35
4%RRT	6.65	14.39	16.19	16.97	2.50%	1.46%	0.91%	0.69%
8%RRT	6.01	14.16	16.03	17.00	2.73%	1.48%	0.91%	0.70%
20%RRT	7.25	15.24	17.18	17.60	3.29%	1.60%	1.07%	0.92%
Control T	6.18	13.31	15.16	15.56	3.46%	1.61%	1.11%	0.96%
4%RRM	4.50	14.57	16.70	18.02	2.47%	1.66%	1.26%	0.83%
8%RRM	4.81	14.02	15.67	16.81	3.15%	1.79%	1.27%	0.95%
20%RRM	7.40	14.71	16.97	17.59	3.23%	1.77%	1.30%	0.93%
Control M	9.59	18.13	19.64	20.91	3.59%	1.97%	1.45%	1.03%
4% RRC	5.95	16.10	18.22	19.42	2.78%	1.58%	1.20%	0.75%
8%RRC	6.84	16.78	19.35	20.54	3.17%	1.54%	0.98%	0.82%
20%RRC	7.83	18.17	21.35	21.65	3.24%	1.44%	1.03%	0.95%
Control C	5.62	13.02	14.50	15.06	2.47%	1.29%	0.79%	0.60%

Table A.18: Tensile strength of RR top, middle and bottom portions.

Tensile strength (MPa)				
Span length	**5**	**15**	**25**	**35**
4%RRB	341.51	242.73	183.79	164.77
8%RRB	278.37	212.56	145.38	129.86
20%RRB	299.47	195.19	136.71	121.02
Control B	272.36	180.84	118.40	84.17
4%RRM	363.17	256.36	217.12	171.79
8%RRM	300.90	226.19	198.53	171.34
20%RRM	246.89	172.82	131.31	104.33
Control M	418.39	340.50	324.79	279.71
4% RRT	222.99	176.96	142.89	127.45
8%RRT	245.87	195.84	160.09	136.97
20%RRT	277.77	220.06	185.16	162.99
Control T	212.59	152.86	117.26	93.81

Table A.19: Corrected Young's modulus and strain to failure of RR top, middle and bottom portions.

Corrected Young's modulus (GPa)						Corrected strain to failure (%)				
Span length	**5**	**15**	**25**	**35**	**Avg**	**5**	**15**	**25**	**35**	**Avg**
4%RRT	22.46	22.35	22.20	22.26	22.32	0.75%	0.75%	0.75%	0.76%	0.75%
8%RRT	20.21	21.41	21.85	22.00	21.37	0.72%	0.74%	0.74%	0.73%	0.73%
20%RRT	22.79	22.71	22.29	22.03	22.46	0.73%	0.73%	0.73%	0.73%	0.73%
Control T	15.90	15.90	15.86	15.25	15.73	0.64%	0.65%	0.65%	0.65%	0.65%
4% RRM	22.94	22.68	22.45	22.60	22.67	0.74%	0.74%	0.74%	0.74%	0.74%
8% RRM	23.15	23.96	23.84	23.86	23.70	0.75%	0.75%	0.75%	0.75%	0.75%
20% RRM	25.37	25.92	25.88	25.47	25.66	0.76%	0.76%	0.76%	0.76%	0.76%
Control M	26.29	26.39	26.32	26.98	26.49	0.93%	0.93%	0.93%	0.92%	0.93%
4%RRB	19.78	19.83	19.90	21.47	20.24	0.74%	0.74%	0.74%	0.74%	0.74%
8%RRB	20.09	20.32	20.43	20.45	20.32	0.75%	0.75%	0.75%	0.75%	0.75%
20%RRB	22.06	22.42	22.62	22.64	22.44	0.76%	0.76%	0.76%	0.76%	0.76%
Control B	17.44	17.44	17.45	17.62	17.49	0.66%	0.66%	0.66%	0.66%	0.66%

Table A.20: Corrected strain to failure of RR top, middle and bottom portions.

Corrected strain to failure (%)					
Span length	**5**	**15**	**25**	**35**	**Avg**
4%RRT	0.75%	0.75%	0.75%	0.76%	0.75%
8%RRT	0.72%	0.74%	0.74%	0.73%	0.73%
20%RRT	0.73%	0.73%	0.73%	0.73%	0.73%
Control T	0.64%	0.65%	0.65%	0.65%	0.65%
4%RRM	0.74%	0.74%	0.74%	0.74%	0.74%
8%RRM	0.75%	0.75%	0.75%	0.75%	0.75%
20%RRM	0.76%	0.76%	0.76%	0.76%	0.76%
Control M	0.93%	0.93%	0.93%	0.92%	0.93%
4%RRB	0.74%	0.74%	0.74%	0.74%	0.74%
8%RRB	0.75%	0.75%	0.75%	0.75%	0.75%
20%RRB	0.76%	0.76%	0.76%	0.76%	0.76%
Control B	0.66%	0.66%	0.66%	0.66%	0.66%

Table A.21: Tensile properties of middle portion FR top jute fiber.

Fiber types	Average tensile stress (MPa)	Average Young's modulus (GPa)	Average strain (%)
Control T	93.81~212.59	15.73553	0.65%
20% FRT	79.19~158.06	19.56942	0.51%
30% FRT	66.01~146.09	17.58434	0.45%

Table A.22: Corrected tensile properties of control and FR middle portion Jute Fiber.

Fiber types	Average tensile stress (MPa)	Average Young's modulus (GPa)	Average strain (%)
Control M	279.71~418.39	29.63733	0.93%
20% FRM	144.84~267.55	25.77	0.68%
30% FRM	109.47~207.31	25.62	0.62%

Table A.23: Tensile properties of middle portion FR bottom jute fiber.

Fiber types	Average tensile stress (MPa)	Average Young's modulus (GPa)	Average strain (%)
Control B	84.17~272.36	17.49433	0.66%
20% FRB	128.42~260.93	19.4605	0.72%
30% FRB	136.42~275.61	19.55978	0.73%

Table A.24: Uncorrected Young's modulus and strain to failure of FR treated jute fiber.

	Uncorrected Young's modulus (GPa)				Uncorrected strain to failure (%)			
Span length	**5**	**15**	**25**	**35**	**5**	**15**	**25**	**35**
Control T	6.18	13.31	15.16	15.56	3.46%	1.61%	1.11%	0.96%
20%FRT	6.27	14.98	17.16	18.32	1.45%	0.75%	0.51%	0.44%
30%FRT	5.50	13.53	15.90	16.93	2.17%	1.05%	0.74%	0.55%
Control M	9.59	18.13	19.64	20.91	3.59%	1.97%	1.45%	1.03%
20%FRM	7.84	15.45	17.019	17.87	2.10%	1.45%	1.00%	0.92%
30%FRM	5.81	13.36	15.37	16.07	1.86%	1.08%	0.62%	0.51%
Control B	5.62	13.02	14.50	15.06	2.47%	1.29%	0.79%	0.60%
20%FRB	6.72	13.25	14.93	15.69	2.29%	1.27%	0.78%	0.62%
30%FRB	6.21	13.67	15.25	16.03	1.98%	1.27%	0.79%	0.66%

Table A.25: Corrected Young's modulus of FR top, middle and bottom portions.

Corrected Young's modulus (GPa)						Corrected strain to failure (%)				
Span length	**5**	**15**	**25**	**35**	**Avg**	**5**	**15**	**25**	**35**	**Avg**
Control T	15.90	15.90	15.86	15.25	15.73	0.64%	0.65%	0.65%	0.65%	0.65%
20%FRT	19.71	19.02	19.88	19.65	19.56	0.51%	0.51%	0.51%	0.51%	0.51%
30%FRT	17.56	17.67	17.88	17.22	17.58	0.45%	0.45%	0.45%	0.45%	0.45%
Control M	26.29	26.39	26.32	26.98	26.49	0.93%	0.93%	0.93%	0.92%	0.93%
20%FRM	22.30	22.26	22.31	22.27	22.29	0.68%	0.68%	0.68%	0.68%	0.68%
30%FRM	19.13	19.42	19.12	19.12	19.20	0.63%	0.62%	0.63%	0.63%	0.62%
Control B	17.44	17.44	17.45	17.62	17.49	0.66%	0.66%	0.66%	0.66%	0.66%
20%FRB	19.18	19.39	19.54	19.72	19.46	0.72%	0.72%	0.72%	0.72%	0.72%
30%FRB	19.77	19.02	19.51	19.92	19.55	0.73%	0.73%	0.73%	0.73%	0.73%

Table A.26 : Tensile strength of FR top, middle and bottom portions.

Tensile strength (MPa)				
Span length	**5**	**15**	**25**	**35**
Control T	212.59	152.86	117.26	93.81
20%FRT	158.06	121.90	95.81	79.19
30%FRT	146.09	114.32	84.30	66.014
Control M	405.60	311.73	264.60	248.62
20%FRM	267.55	174.22	151.85	144.84
30%FRM	207.31	145.78	116.58	109.47
Control	214.62	151.54	107.66	84.17
20%FRB	260.93	186.49	145.74	128.42
30%FRB	275.61	197.57	152.81	136.42

Table A.27: Corrected tensile properties of control and WR middle portion jute fiber.

Fiber types	**Average tensile stress (MPa)**	**Average Young's modulus (GPa)**	**Average strain (%)**
Control M	279.71~418.39	29.64	0.93%
10% WRM	189~390.50	23.7481	0.87%
15% WRM	124.74~345.79	23.7036	0.89%
20% WRM	98.23~297.78	25.64	0.90%

Table A.28: XRD data analysis for RR treated jute fiber.

Sample	**Area**	**Peak at**	**Width**	**Height**
Control M	53679.66	15.1232	13.57545	1825.49
20%RRM	63202.1	15.3653	15.21915	1808.94
20%RRT	49618.27	15.0605	13.32367	1820.26
20%RRC	59034.96	15.4752	16.33373	1809.98
4%RRM	49618.27	15.0605	13.32367	1820.26

Table A.29: XRD data analysis for FR treated jute fiber.

Sample	**Area**	**Peak at**	**Width**	**Height**
20%FRM	42616.18	17.0666	9.25629	1805.54
25%FRM	44013.91	16.5897	9.61609	1815.7
30%FRM	38400.92	16.3063	8.86011	1818.07
Control M	53679.66	15.1232	13.57545	1825.49

APPENDEX 2

List of Publications:

1. **Water retardant jute fiber characterization for composite,** Sweety Shahinur, Qumrul Ahsan, Mahbub Hasan, Md. Kamal Uddin, Dr. Dilip Kumar Saha, National Conference on Physics for Development (10-11 February 2011) ID-Poster No-26: pp-67.

2. **Effect of rot proof treatment on the physical and mechanical properties of jute fiber**, Sweety Shahinur, Quamrul Ahsan , A.K.Mahabobuzaman, International Conference on Magnetism and Advanced Materials (ICMAM-2010) 03-07 March 2010, Dhaka, Bangladesh , ID-NC-19 :pp-85.

3. **Effect of rot proof treatment on the physical and mechanical properties of jute fiber**, Sweety Shahinur, Quamrul Ahsan, A.K.Mahabobuzaman, International Conference on Magnetism and Advanced Materials (ICMAM-2010) 03-07 March 2010, Dhaka, Bangladesh, Conference proceeding : pp-238-241.

4. **Characterization of $CuSO_4$ (rot proof) treated jute fiber**, Sweety Shahinur, Qumrul Ahsan, Mahbub Hasan and Samina Jafrin, 3rd Intl. Conference on Structure, Processing and Properties of Materials, (SPPM2010) 24 -26 February 2010, Dhaka Sheraton Hotel and BUET, Dhaka, proceedings ID- E32.

5. **Modification and characterization of rot retardant jute fiber,** Sweety Shahinur, Qumrul Ahsan$_2$, Samina Jafrin, A.K.Mahabobuzaman, International Conference on Recent Advances in Physics 2010, March 27-29, 2010, Dhaka, Bangladesh ID - POS28-19:pp-85

6. **Effects of Chemical Retardant Treatment on Physico-Mechanical Properties of Jute Fiber Reinforced MAgPP Green Composites**, International Symposium On Green Manufracturing Composites -2011.Seoul National University. Sweety Shahinur, Mahbub Hasan and Qumrul Ahsan

7. **Effects of rot and water retardant treatment on the properties of jute fiber MAgPP composites.** International seminar on strengthening of collaboration for jute, kenaf and allied fibers research and development. 8-9 June, 2011. Sweety Shahinur, Mahbub Hasan, Qumrul Ahsan. pp:74.

8. **Thermal Behavior of Water Retardant Treated Jute Fibers**. International Conference on Mechanical Engineering (ICME-2011) Sweety Shahinur, Mahbub Hasan, Qumrul Ahsan, Shamina Jafrin, Dilip Kumar Saha.